TELECOMMUNICATIONS

English Edition of

ЭЛЕКТРОСВЯЗЬ

No.4 April 1961

Published by the American Institute of Electrical Engineers
with the aid of a grant from the National Science Foundation

Translated and Produced by Royer and Roger, Inc.

AMERICAN INSTITUTE OF ELECTRICAL ENGINEERS

Established 1884

345 East 47th Street
New York 17, New York

Warren H. Chase, President
N.S. Hibshman, Executive Secretary
C.E. Dean, Technical Vice President, Communications
W.F. Denkhaus, Director of Publications
L.G. Abraham, Chairman, Communications Division

The English edition of TELECOMMUNICATIONS is published by the American Institute of Electrical Engineers with the aid of a grant from the National Science Foundation. © 1961 by American Institute of Electrical Engineers. Also published under the same arrangements are the Russian electronic journals RADIO ENGINEERING AND ELECTRONIC PHYSICS and RADIO ENGINEERING.

TELECOMMUNICATIONS

(ЭЛЕКТРОСВЯЗЬ)

Publication of the
A.S. Popov Technical Society of Radio Engineering and Telecommunications

Translated and Produced
by
Royer and Roger, Inc.

Translation Editor: Jack Warren, Columbia University

AIEE REVIEW COMMITTEE FOR TELECOMMUNICATIONS
H.F. May
Bell Telephone Laboratories, Inc.
Chairman

A.G. Cooley
A.D. Fowler
A.E. Frost
F.G. Hollins
A.E. Joel
W. Miller
L.L. Robinett
R.B. Shanck
D.L. Solomon
F.W. Smith
G. Worthen

Subscriptions to Telecommunications should be sent to AIEE
Special Subscription Department
41 East 28th Street
New York 16, New York

1961 Subscription rates:

	$	£
Individuals	14.25	5
Libraries, institutes, govt. agencies	28.50	10

12 issues per annum comprising approximately 1100 pages

ANALYSIS OF OPEN-LOOP SYSTEMS WITH PULSE-AMPLITUDE MODULATION

Ya. Z. Tsypkin

Systems with Class I pulse-amplitude modulation are examined. It is shown that in studying transient and steady-state processes in such systems it is possible to use the well-known results of the investigations of conventional pulse systems with Class II pulse-amplitude modulation obtained on the basis of the discrete Laplace transform

An open-loop system with Class I pulse-amplitude modulation (PAM) can be represented in the form of a series-connected switch and a continuous circuit (Fig. 1)

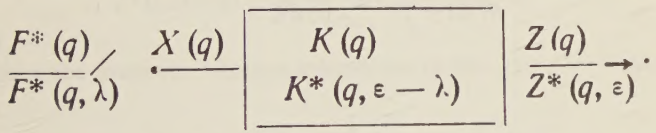

Figure 1

The key is closed periodically, at a given time, in such a manner that a series of pulses act on the continuous circuit with their peaks changing in accordance with the shape of the input signal during the interval of pulse duration (Fig. 2).

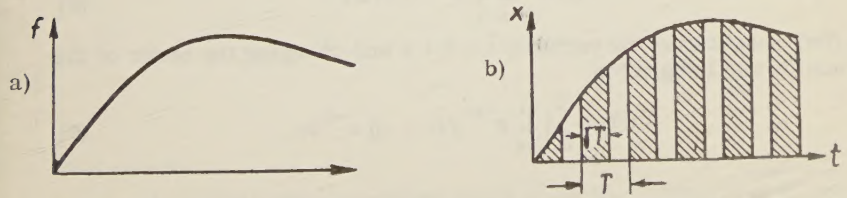

Figure 2

In investigating and calculating similar systems in the works of Farmanfarma [1] and Tou [2], special transforms were introduced (P—transform, τ—transform)[1] which are essentially Laplace transforms of a modulated series of pulses (Fig. 2b).

In the present article it is shown that the study of systems with class I PAM or, as they are otherwise designated, systems with a switch, can be reduced to the study of conventional open-loop pulse systems — systems with Class II PAM, the theory of which has been amply developed [3, 4]. The mathematical method for investigating an open-loop pulse system — the discrete Laplace transform — makes it possible to carry out this investigation by the most simple means.

Let us designate the operating period of the key by T, and the duration of the closing of the key by γT. The output value of the system will be expressed as

$$Z(p) = K_1(p) X(p), \tag{1}$$

where X(p) — is the expression for the modulated series of pulses, and $K_1(p)$ — is the transfer function of a continuous circuit. In relative values this equation is written in the form

$$Z(q) = K(q) X(q). \tag{2}$$

Here, q = pT and

$$K(q) = \frac{1}{T} K_1\left(\frac{q}{T}\right). \tag{3}$$

Let us find the expression X(q). By definition

$$X(q) = \int_0^\infty e^{-qt} x(\bar{t})\, d\bar{t}, \tag{4}$$

where

$$x(\bar{t}) = \begin{cases} f(\bar{t}) & \text{for } n \leqslant \bar{t} \leqslant n+\gamma \\ 0 & \text{for } n+\gamma \leqslant \bar{t} \leqslant n+1 \end{cases} \tag{5}$$

and $\bar{t} = t/T$.

Equation (4), after substituting $x(\bar{t})$ from (5), can be rewritten as

$$X(q) = \sum_{n=0}^{\infty} \int_n^{n+\gamma} e^{-q\bar{t}} f(\bar{t})\, d\bar{t} \tag{6}$$

or, after substituting the variable $\bar{t} = n + \epsilon$ and changing the order of the summation and integration

$$X(q) = \int_0^\gamma \left[\sum_{n=0}^{\infty} e^{-qn} f(n+\varepsilon)\right] e^{-q\varepsilon} d\varepsilon. \tag{7}$$

---

[1] See Jury's book, Chapter 9 (Ref. 3).

But f[n + ϵ] = f[n, ϵ] is a matrix function, and

$$\sum_{n=0}^{\infty} e^{-qn} f[n, \varepsilon] = F^*(q, \varepsilon) \tag{8}$$

determines the discrete transformation of this matrix function [4]. Thus, the expression for a modulated series of pulses may be represented in the form[2]

$$X(q) = \int_0^{\Upsilon} F^*(q, \varepsilon)\, e^{-q\varepsilon} d\varepsilon. \tag{9}$$

Consequently, from Equation (2) and considering Equation (9), we obtain the equation for the investigated system (1) in terms of the general Laplace transform.

$$Z(q) = K(q) \int_0^{\Upsilon} F^*(q, \varepsilon)\, e^{-q\varepsilon} d\varepsilon. \tag{10}$$

The use of this equation requires operations on transforms which are functions of q and e^q. In many cases this presents a complicated problem and special tables have to be prepared [1, 2].

In order to avoid these difficulties and to show that these systems can be examined on the basis of the theory of conventional pulse systems [4], let us proceed from a general Laplace transform to a discrete one. Reference [4] shows that

$$Z^*(q, \varepsilon) = \overline{D}\left\{Z(q)\right\} = \sum_{r=-\infty}^{\infty} Z(q + 2\pi jm)\, e^{(q+2\pi jm)\varepsilon}. \tag{11}$$

Using the discrete Laplace transform in Eq. (10), we obtain

$$Z^*(q, \varepsilon) = \overline{D}\left\{K(q) \int_0^{\Upsilon} F^*(q, \lambda)\, e^{-q\lambda}\, d\lambda\right\}. \tag{12}$$

By changing the order of integration and using a $\overline{D}$ — transform, we get

$$Z^*(q, \varepsilon) = \int_0^{\Upsilon} F^*(q, \lambda)\, \overline{D}\left\{K(q)\, e^{-q\lambda}\right\} d\lambda. \tag{13}$$

---

[2]It can be shown that this expression determines the P and τ transforms (used in References [1 and 2]) using the discrete Laplace transform.

But in accordance with the theorem of multiplication by $e^{-q\lambda}$ [3]

$$\overline{D}\left\{K(q)\,e^{-q,\lambda}\right\} = K_0(q, \varepsilon - \lambda) = \begin{cases} K(q, \varepsilon - \lambda) & \lambda \leqslant \varepsilon \\ e^{-q} \cdot K(q, 1 + \varepsilon - \lambda) & 1 \geqslant \lambda \geqslant \varepsilon \end{cases} \tag{14}$$

where

$$K^*(q, \varepsilon) = \overline{D}\left\{K(q)\right\}. \tag{15}$$

Consequently, the final equation of an open system with Class I pulse-amplitude modulation expressed in terms of a discrete Laplace transform is written

$$Z^*(q, \varepsilon) = \int_0^{\gamma} K_0^*(q, \varepsilon - \lambda)\, F^*(q, \lambda)\, d\lambda \tag{16}$$

or, in more detail, taking into account expression (14),

$$Z^*(q, \varepsilon) = \int_0^{\varepsilon} K^*(q, \varepsilon - \lambda)\, F^*(q, \lambda)\, d\lambda + e^{-q} \int_{\varepsilon}^{\gamma} K^*(q, 1 + \varepsilon - \lambda)\, F^*(q, \lambda)\, d\lambda \tag{17}$$

at $\epsilon \leqslant \gamma$,

and

$$Z^*(q, \varepsilon) = \int_0^{i} K^*(q, \varepsilon - \lambda)\, F^*(q, \lambda)\, d\lambda \tag{18}$$

at $1 \geqslant \epsilon \geqslant \gamma$.

Thus, knowing F(q) and K(q), from formulas of the type of Equation (8) or (11), we may obtain F* (q, ϵ) and K* (q, ϵ). Substituting these terms into Equations (17) and (18), we obtain an expression for the output value in terms of a discrete Laplace transform.

Let us examine some special cases of the equations obtained for a Class I PAM system.

1. For sufficiently small values of γ (Fig. 3a) when the integrand can be considered constant, Equation (18) yields

$$Z^*(q, \varepsilon) = \gamma\, K^*(q, \varepsilon)\, F^*(q, 0). \tag{19}$$

Equation (19) is the equation for a simple open-loop pulse system. This result should have been expected since for sufficiently small values of γ the shape of the pulses can be disregarded, and they may be considered instantaneous with a sufficient degree of accuracy.

2. At $\gamma = 1$ (Figure 3b)

---

[3] See Reference (4), p 184, where the theorem of multiplication by $e^{-q\lambda}$ is given.

$$Z^*(q,\varepsilon) = \int_0^1 K^*(q,\varepsilon-\lambda)\,F^*(q,\lambda)\,d\lambda. \tag{20}$$

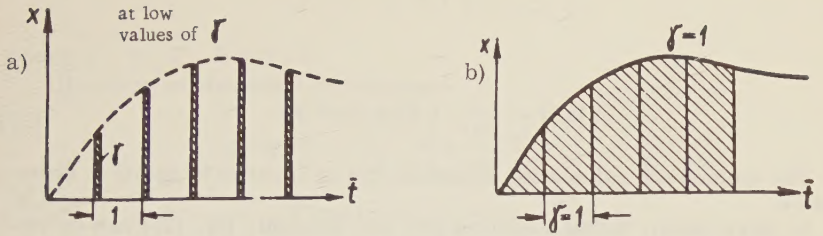

Figure 3

By using in this equation the inverse $\overline{D}$ - transformation [4],

$$\overline{D}^{-1}\left\{Z^*(q,\varepsilon)\right\} = \int_0^1 Z^*(q,\varepsilon)\,e^{-q\varepsilon}\,d\varepsilon = Z(q) \tag{21}$$

we obtain an equation for a continuous system

$$Z(q) = K(q)\,F(q). \tag{22}$$

It can therefore be concluded that for a system with Class I PAM the limiting cases will be an impulse system and a continuous system.

The equation for an open-loop system with Class I PAM can be interpreted in the following manner. The integrand

$$\overline{Z}_0^*(q,\varepsilon-\lambda) = K_0^*(q,\varepsilon-\lambda)\,X^*(q,\lambda) \tag{23}$$

represents an equation for an open-loop, conventional pulse system where the pulse element reacts to the discrete values of the input value at the instant $\overline{t} = n + \lambda$ [4].

Thus, in accordance with Equation (16)

$$Z^*(q,\varepsilon) = \int_0^1 \overline{Z}_0^*(q,\varepsilon-\lambda)\,d\lambda. \tag{24}$$

Inverting Eq. (24)[4], we obtain

$$z[n,\varepsilon] = \int_0^1 \overline{z}_0[n,\varepsilon-\lambda]\,d\lambda, \tag{25}$$

where

---

[4]The parameter-integration theorem was used here. See Ref. [4], p. 130, Theorem 10.

$$\overline{z}[n, \varepsilon - \lambda] = \begin{cases} z_0[n, \varepsilon - \lambda] & \text{when } \varepsilon \geqslant \lambda \\ z_0[n-1, 1+\varepsilon-\lambda] & \text{when } \varepsilon \leqslant \lambda \end{cases} \tag{26}$$

and

$$z_0[n, \varepsilon] = \frac{1}{2\pi j} \int_{c-j\pi}^{c+j\pi} \overline{Z}_0^*(q, \varepsilon)\, e^{qn}\, dq. \tag{27}$$

The method for calculating Equation (27) is covered in detail in reference [4].

In more detail, taking Equation (26) into account, Eq. (25) can be rewritten as two equations:

$$z[n, \varepsilon] = \int_0^{\varepsilon} z_0[n, \varepsilon - \lambda]\, d\lambda + \int_{\varepsilon}^{\gamma} z_0[n-1, 1+\varepsilon-\lambda]\, d\lambda \tag{28}$$

at $\epsilon \leqslant \gamma$,

$$z[n, \varepsilon] = \int_0^{\gamma} z_0[n, \varepsilon - \lambda]\, d\lambda, \tag{29}$$

at $\epsilon \geqslant \gamma$.

Thus, in order to determine the equations and processes of an open system with Class I PAM, it is necessary to integrate Equation (27) from 0 to γ, , for conventional open-loop systems after substitution of ϵ - λ for λ for 0.

This deviation makes it possible to use the well-known results obtained for open-loop pulse systems for the analysis of open-loop systems with Class I PAM.

As an example, let us examine a system with Class I PAM whose transfer function for a continuous circuit is equal to

$$K_1(p) = \frac{k}{p + \alpha_1}. \tag{30}$$

Let us assume that an exponential effect is applied to the input of the system

$$f_1(t) = e^{-\beta_1 t}. \tag{31}$$

The expression for this effect in terms of a general Laplace transform is equal to

$$F_1(p) = \frac{1}{p + \beta_1}. \tag{32}$$

Proceeding to the dimensionless quantity q = pT, we obtain:

$$K(q) = \frac{1}{T} K_1\left(\frac{q}{T}\right) = \frac{k}{q+\alpha}, \tag{33}$$

$$F(q) = \frac{1}{T} F_1\left(\frac{q}{T}\right) = \frac{1}{q+\beta}, \tag{34}$$

where $\alpha = \alpha_1 T$; $\beta = \beta_1 T$.

By these expressions we obtain:

$$K^*(q, \varepsilon) = D\left\{\frac{1}{q+\alpha}\right\} = \frac{k\, e^q}{e^q - e^{-\alpha}} e^{-\alpha\varepsilon}, \tag{35}$$

$$F^*(q, \varepsilon) = D\left\{\frac{1}{q+\beta}\right\} = \frac{e^q}{e^q - e^{-\beta}} e^{-\beta\varepsilon}. \tag{36}$$

Accordingly, the equation for a conventional pulse system (23) can now be rewritten:

$$\overline{Z}_0^*(q, \varepsilon - \lambda) = k \frac{e^{2q}}{(e^q - e^{-\alpha})(e^q - e^{-\beta})} e^{-\alpha\varepsilon} e^{(\alpha-\beta)\lambda}. \tag{37}$$

Reverting to the transforms from the inversion, we obtain

$$z_0[n, \varepsilon - \lambda] = \frac{k}{e^{-\alpha} - e^{-\beta}} (e^{-\alpha(n+1)} - e^{-\beta(n+1)}) e^{-\alpha\varepsilon} e^{(\alpha-\beta)\lambda}. \tag{38}$$

Substituting this value into Equations (28) and (29), after integration and elementary transformation we finally obtain

$$z[n, \varepsilon] = k \frac{e^{-\alpha\varepsilon}}{(e^{-\alpha} - e^{-\beta})(\alpha - \beta)} \left[(e^{(\alpha-\beta)\gamma} - 1) e^{-\alpha(n+1)} - \right.$$
$$\left. - \left[(e^{-\alpha} - e^{-\beta}) e^{(\alpha-\beta)\varepsilon} + (e^{(\alpha-\beta)\gamma} - e^{(\alpha-\beta)}) e^{-\alpha} \right] e^{-\beta n} \right] \tag{39}$$
$(\varepsilon < \gamma)$

and

$$z[n, \varepsilon] = k \frac{e^{(\alpha-\beta)\gamma} - 1}{(e^{-\alpha} - e^{-\beta})(\alpha - \beta)} (e^{-\alpha(n+1)} - e^{-\beta(n+1)}) e^{-\alpha\varepsilon}. \tag{40}$$
$(\varepsilon \geqslant \gamma)$

When γ is small, from Equation (40) we obtain

$$z[n, \varepsilon] = k\gamma \frac{e^{-\alpha\varepsilon}}{(e^{-\alpha} - e^{-\beta})} (e^{-\alpha(n+1)} - e^{-\beta(n+1)}), \tag{41}$$

which corresponds to the process in an impulse system.

When $\gamma = 1$, from Equation (39) we obtain

$$z[n, \varepsilon] = k \frac{1}{\alpha - \beta} (e^{-\alpha(n+\varepsilon)} - e^{-\beta(n+\varepsilon)}), \tag{42}$$

which, at $n + \epsilon = \bar{t}$, corresponds to the process in a continuous system.

REFERENCES

1. Farmanfarma. Analysis of linear samples — data systems with finite pulse width. Open loop. "Communications and Electronics" 1957, No. 28.
2. Tou. Analysis of samples — data control system with finite sampling duration. "Proc. of National Electronics Conference," 1957, v. 13.
3. Jury. "Sampled — data control systems." Willey, 1959.
4. Ya. Z. Tsypkin. Theory of Pulse Systems. Fizmatgiz, 1958.

Received September 14, 1960

NOISE PROOFNESS IN INTEGRAL RECEPTION OF SIGNALS UNDER THE INFLUENCE OF FLUCTUATING AND SINUSOIDAL NOISE

N. L. Teplov

A comparison is carried out of noise proofness of integral and conventional narrow-band reception of pulse signals under the influence of fluctuating and sinusoidal noise[1].

INTRODUCTION

As a rule, methods of integral reception are compared with methods of conventional narrow-band reception. Such a comparison is a natural one because integration (averaging), as a physical process, is equivalent to filtration (smoothing out).

Narrow-band reception is usually understood to mean the reception of signals with the most adequate passbands which correspond to maximum

---

[1] The evaluation of noise proofness in the indicated methods of reception for other forms of noise is given in a separate article.

noise proofness of reception. The values of the indicated bands are not the same for different forms of noise. For example, in the case of fluctuating noise, the most suitable bands for the reception of single pulses are the so-called optimum frequency bands [1].

A characteristic feature of conventional narrow-band reception (referred to hereafter simple as narrow-band reception) is that the filtering of the signal and noise is accomplished by means of filters with fixed connections. Accordingly, the selectivity of the latter is determined by their static resonant characteristics and passbands.

The most suitable values for the filter bands, as indicated above, correspond to the conditions (and consequently, the most suitable values for the filter passbands) for identical forms of noise are found to be different during the reception of single pulses (following one after another with large gaps in between, for example, as in radar) as compared with the reception of a continuous series of pulses (for example, in radio telegraphy). In the first case, mutual overlap of the pulses due to transients in the filters practically never takes place. Whereas, in the reception of a continuous series of pulses, the appearance of each pulse takes place in the presence of residual oscillations in the filters from preceding pulses. As a rule, the most suitable frequency bands in the latter case are found to be wider ones: they must, as a compromise, satisfy two contradictory requirements — the assurance of the highest possible increase in signal over noise in the filter, and minimum interaction between adjacent pulses.

Thus, for conventional narrow-band reception the conditions for reception with minimum probability of error are found to be different (do not coincide) for different forms of noise, and depend also on the pulse-repitition period in the total sequence.

Let us now examine the features of integral signal reception.

It is understood that by integral reception we mean reception with accumulation of the signal and noise only during the interval of signal duration. Integration in this sense can, in practice, be realized in filters (circuits) with very narrow bands,[2] switched on and off in phase with the rise and fall of each signal pulse.[3] Switching filters (circuits) with very-narrow frequency bands shall hereafter be referred to as integrating filters.

We may formulate the following distinctive features of the integral reception method:

1. The effect of noise on the integrating circuit takes place only in the interval of signal duration (in contrast to reception on narrow-band filters with fixed connections in which the voltages and currents are generated continuously by the noise during its full operating period).

---

[2] By very narrow-band filters we mean those in which the time for the establishment of steady-state conditions is known to be greater than the duration of a single signal pulse.

[3] In radiotelegraphic apparatus known at this time, the switching on and off of the integrating filters in phase with the limits of the unit pulses is achieved by means of forced quenching of the residual oscillations in the filters at the end of each pulse; in this way, null conditions are established in the integrating circuits at the beginning of each following pulse.

2. During integral reception, the mutual superimposition of adjacent pulses, caused by the long duration of transients in the narrow-band filters, is eliminated; this is achieved through artificial (forced) quenching of the residual oscillations in the integrating circuits at the end of each pulse separately.

The above-indicated features of integral reception lead to a new quantitative correlation of signal and noise which is different from the analagous correlation for conventional narrow-band reception. The qualitative difference of integral signal reception from conventional narrow-band reception stems from the fact that its frequency selectivity is determined not by the static characteristics as in narrow-band reception, but by the dynamic resonant characteristics and bandwidth of the integrating circuits.

The overall advantage of integral reception methods is their greater noise proofness. At the same time, the conditions for highest noise proofness for various types of noise are satisfied simultaneously (mutually compatible); whereas with conventional narrow-band reception, the maximum attenuation of different types of noise is attained without identical conditions for the various noise signals (especially with different values for the filter bandwidths.)

We shall also note that noise proofness of integral signal reception does not depend on the pulse repetition rate of the sequency (since with integral reception the interaction between pulses is eliminated).

The noise proofness of integral reception of pulse signals is evaluated below, with integration of signal and noise in the radio frequency channel of the receiver (to the detector stage).

Figure 1 shows a block diagram of the receiver with integration to the detector; the integrating circuit is designated as the integrator for simplicity.

A corresponding block diagram for a narrow-band receiver is given in Figure 2.

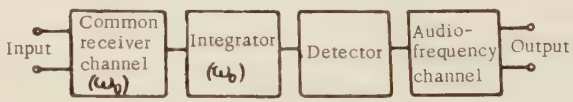

Figure 1

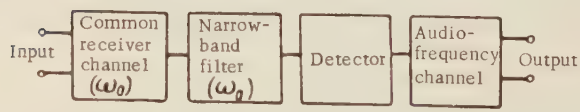

Figure 2

The whole radio frequency channel (up to the detector), which also includes the integrator or the narrow-band filter, is tuned to the signal frequency $\omega_c = \omega_0$.

In the general case, we shall represent the signal in the form of a series of radio-frequency pulses with rectangular wave-shape

$$A(t) = a \sin \omega_0 t \quad \text{when } 0 \leqslant t \leqslant \tau \tag{1}$$

where a and τ are the amplitude and duration of the unit pulses.

It is further assumed that the signal is not noticeably distorted in the common (relatively wide bandwidth) channel of the receiver.

The pulse repetition rate of the series may be varied.

NOISE PROOFNESS OF INTEGRAL AND NARROW-BAND RECEPTION UNDER THE INFLUENCE OF FLUCTUATING NOISE

Integral Reception. Fluctuating noise at the integrator input is represented by the oscillation

$$B(t) = b(t) \sin [\omega_0 t + \theta(t)], \tag{2}$$

where b(t) and $\theta(t)$ are the random amplitude and phase.

The quadratic for the effective value (intensity) of the fluctuating noise (2) is equal to

$$\overline{[B(t)]^2} = \sigma^2 = \nu_0^2 \Delta f_{\text{eff}}, \tag{3}$$

where Δf_{eff} is the effective frequency band of the receiver channel at the integrator input; ν_0^2 — is the noise intensity in a 1-cps band (specific noise intensity).

The oscillation (2) may be divided into the components

$$B(t) = x(t) \sin \omega_0 t + y(t) \cos \omega_0 t, \tag{4}$$

where

$$\left.\begin{aligned} x(t) &= b(t) \cos \theta(t) \\ y(t) &= b(t) \sin \theta(t) \end{aligned}\right\}. \tag{5}$$

The probabilities of the amplitudes x(t) and y(t) are normally distributed with an average value equal to zero,

$$\overline{x(t)} = \overline{y(t)} = 0 \tag{6}$$

and dispersion equal to

$$\overline{[x(t)]^2} = \overline{[y(t)]^2} = \sigma^2 = \nu_0^2 \Delta f_{\text{eff}} \tag{7}$$

The oscillation (4) is also represented by the vector diagram in Figure 3.

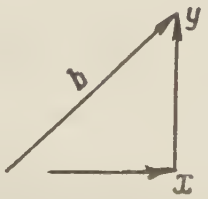

Figure 3

Let us determine the intensity of the fluctuating noise at the integrator output.

In accordance with the expression (4), the fluctuating noise at the integrator output is a sum obtained by integrating the oscillations of amplitudes x(t) and y(t). The amplitudes of these oscillations after their integration in the interval of signal duration τ is equal to:

$$\left.\begin{aligned} x_\tau &= \int_0^\tau x(t)\,dt \\ y_\tau &= \int_0^\tau y(t)\,dt \end{aligned}\right\}. \tag{8}$$

The resulting amplitude of the fluctuating noise at the integrator output is equal to the geometric sum of the amplitudes (8) [See formula (4) and Figure 3].

$$b_\tau = \sqrt{x_\tau^2 + y_\tau^2}. \tag{9}$$

The amplitudes of the oscillations x_T and y_T are random values with normal distribution (as are the instantaneous values of the amplitudes x and y). The intensity (dispersion) of the fluctuations of the amplitudes x_T and y_T are shown to be equal to [3]

$$\overline{x_\tau^2} = \overline{y_\tau^2} = \overline{\left[\int_0^\tau x(t)\,dt\right]^2} = \overline{\left[\int_0^\tau y(t)\,dt\right]^2} = \sigma^2 \frac{\tau}{\Delta f_{\text{eff}}} = v_0^2 \tau. \tag{10}$$

The mean quadratic value of the amplitude of the fluctuating noise at the integrator output is determined in accordance with Formulas (9) and (10)

$$\overline{b_\tau^2} = \overline{x_\tau^2} + \overline{y_\tau^2} = 2v_0^2 \tau. \tag{11}$$

The dispersion of the fluctuating noise (the quadratic of its effective value) at the integrator output is equal to

$$\overline{[B(t)]_\tau^2} = \frac{\overline{b_\tau^2}}{2} = v_0^2 \tau. \tag{12}$$

The amplitude of the signal at the integrator output is equal to

$$a_\tau = \int_0^\tau a\,dt = a\tau. \tag{13}$$

Let us take the power ratio between the signal and noise at the integrator output [which, quantitatively, is equal to the ratio of the quadratics of the signal (13) and noise (11) amplitudes]

$$h_\tau^2 = \frac{a_\tau^2}{\overline{b_\tau^2}} = \frac{a^2\tau}{2v_0^2}. \tag{14}$$

The power ratio between signal and noise is usually called the signal-to-noise ratio.

Accordingly, the signal-to-noise ratio at the integrator output is equal to the relationship between the signal energy ($\frac{\alpha^2 T}{2}$) and the specific

noise intensity (ν_0^2), and does not depend on the frequency band of the receiver channel up to the integrator.

The signal-to-noise (14) corresponds to the maximum noise proofness of signal pulse reception. On the strength of this ratio, (14) may be considered the limiting value.

Thus, integral reception assures maximum noise proofness in pulse signal reception under the influence of fluctuating noise.

Narrow-Band Reception. The maximum signal-to-noise ratio for fluctuating noise in conventional narrow-band reception is realized with so-called optimal frequency bands of the filters.

Depending on the shape of the resonance curve of the filter, the values for optimal frequency bands under the action of single pulses are found within the limits

$$\Delta f_{\text{eff opt}} = \frac{0.7 - 1.4}{\tau}, \tag{15}$$

where τ is the pulse duration of a signal of rectangular waveform.

The optimal frequency bands correspond to the following maximum signal-to-noise ratio

$$h^2_{\text{opt}} = 0.82 \frac{a^2 \tau}{2\nu_0^2}. \tag{16}$$

The relationship (16) holds true for any filter with an optimal frequency band. This position is illustrated below by examples corresponding to two extreme cases: 1) the case of a single oscillatory circuit, and 2) the case of an ideal filter.

The amplitude of a signal at the output of a single resonant circuit (src) with radio pulses of rectangular waveform acting on its input is established according to the law

$$a(t)_{\text{out}} = a\left(1 - e^{-2\Delta f_{\text{eff}} t}\right),$$

where Δf_{eff} is the effective frequency band, related to the circuit attenuation factor by $\Delta f_{\text{eff}} = \frac{\alpha}{2}$; the transmission factor of the circuit at resonant frequency is taken conditionally as equal to unity.

The maximum value of signal amplitude at the circuit output, at the instant $t = \tau$, is

$$a_{\text{out max}} = a\left(1 - e^{-2\Delta f_{\text{eff}} \tau}\right).$$

The signal-to-noise ratio at the circuit output when $t = \tau$ is equal to

$$h^2_{\text{src}} = \frac{a^2 \left(1 - e^{-2\Delta f_{\text{eff}} \tau}\right)^2}{2\nu_0^2 \Delta f_{\text{eff}}} = \frac{a^2 \tau}{2\nu_0^2} \frac{\left(1 - e^{-2\Delta f_{\text{eff}} \tau}\right)^2}{\Delta f_{\text{eff}} \tau}. \tag{17}$$

The maximum value of the ratio (17) corresponds to the optimal frequency band for the circuit which is determined from the conditions:

$$\frac{d}{d(\Delta f_{\text{eff}})}\left[\frac{(1-e^{-2\Delta f_{\text{eff}}\tau})^2}{\Delta f_{\text{eff}}\tau}\right]_{\Delta f_{\text{eff}}\ \Delta f_{\text{eff opt}}}=0.$$

By taking the derivative, we obtain the equation

$$1-e^{-2\Delta f_{\text{eff opt}}\tau}(1-4\Delta f_{\text{eff opt}}\tau)=0,$$

the solution of which gives

$$\Delta f_{\text{eff opt}}=\frac{0.65}{\tau}. \tag{18}$$

Substituting the value for the optimal frequency band in the expression (17), we have

$$h^2_{\text{opt src}}=0.815\frac{a^2\tau}{2\sigma_0^2}. \tag{19}$$

The maximum value of signal amplitude at the output of an ideal filter is equal to [1]

$$a_{\text{out max}}=\frac{2}{\pi}a\,\text{Si}\left(\frac{\pi}{2}\Delta f\tau\right),$$

where Δf is the filter passband: Si is the symbol for the integral sine.

The signal-to-noise ratio is equal to

$$h^2_F=\frac{\left[\frac{2}{\pi}a\,\text{Si}\left(\frac{\pi}{2}\Delta f\tau\right)\right]^2}{\sigma_0^2\Delta f}. \tag{20}$$

The optimum frequency band for an ideal filter will have the value [1]

$$\Delta f_{\text{opt}}=\frac{1.37}{\tau}.$$

The substitution of this value for the frequency band in the formula for the ratio (20) gives

$$h^2_{\text{opt F}}=0.825\frac{a^2\tau}{2\sigma_0^2}, \tag{21}$$

which practically coincides with the formula (19) for a single oscillatory circuit.

The relationship of signal-to-noise ratios for integral reception and narrow-band reception with optimal frequency bands is equal to

$$\left(\frac{h_*}{h_{\text{opt}}}\right)^2_{\text{fl}}=1.22. \tag{22}$$

Thus, during the reception of single pulses (followed by long gaps), integral reception and conventional narrow-band reception with optimal frequency bands are practically equivalent.

The advantages of integral reception show up more effectively for a continuous sequence of signal pulses (such as take place in radiotelegraphy).

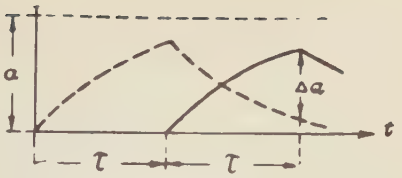

Figure 4

Conventional narrow-band reception with optimal filter frequency bands is characterized by the relatively high duration of transient phenomena. This leads to the superimposition of residual oscillations from the preceding pulse on the incoming pulse (Fig. 4). The indication of each incoming pulse now results not from the absolute value of its level but from the relative difference in level Δa. The optimal frequency band in the case under examination is determined by the conditions for the highest ratio between the difference in level of adjacent pulses and the fluctuating noise intensity.

For example, in the reception of frequency-modulation signals, Δa is the difference voltage in off-and-on keying of messages at the output of the frequency detector (discriminator).

Let us determine the optimal frequency band, taking into consideration the superimposition of pulses, for a single oscillatory circuit

$$\Delta a = a\left(1 - e^{-2\Delta f_{\text{eff}}\tau}\right) - a\left(1 - e^{-2\Delta f_{\text{eff}}\tau}\right) e^{-2\Delta f_{\text{eff}}\tau} = a\left(1 - e^{-2\Delta f_{\text{eff}}\tau}\right)^2.$$

The signal-to-noise ratio in the case under examination will be determined from the relationship

$$h^2 = \frac{\Delta a^2}{2\sigma_0^2 \Delta f_{\text{eff}}} = \frac{a^2\tau}{2\sigma_0^2} \frac{\left(1 - e^{-2\Delta f_{\text{eff}}\tau}\right)^4}{\Delta f_{\text{eff}}\tau}. \tag{23}$$

The maximum signal-to-noise ratio (23) corresponds to the optimal frequency band

$$\Delta f'_{\text{eff opt}} = \frac{1{,}1}{\tau}. \tag{24}$$

Substituting (24) in Formula (23) we obtain

$$h^2_{\text{opt}'} = 0{,}58 \frac{a^2\tau}{2\sigma_0^2}. \tag{25}$$

It can be proved that in receiving a series of pulses the optimal frequency bands will be approximately twice as wide as the optimal frequency bands for single pulses, and the maximum signal-to-noise ratio will be equal to

$$h^2_{\text{opt}'} \approx 0.5 \frac{a^2 \tau}{2 \nu_0^2}. \tag{26}$$

Taking the relationship between (14) and (26), we obtain

$$\left(\frac{h_{\infty}}{h_{\text{opt}'}}\right)^2_{\text{fl}} \approx 2.0. \tag{27}$$

Thus, with integral reception of a continuous series of pulses, the gain in signal-to-noise ratio in comparison with conventional narrow-band reception is shown to be practically double.

The verifications carried out above relate to the reception of a continuous series of pulses of equal amplitude. The gain in noise stability for integral reception was shown to be particularly significant when receiving signal pulses with amplitude variations (in particular, signals subjected to fading). Under these conditions the optimal frequency bands will be even wider and signal-to-noise ratio, smaller.

NOISE PROOFNESS OF INTEGRAL AND NARROW-BAND RECEPTION METHODS UNDER THE INFLUENCE OF SINUSOIDAL NOISE

Integral Reception. We shall write sinusoidal noise in the form of an oscillation

$$E_{\text{n}} = e_{\text{n}} \sin \omega_{\text{n}} t = e_{\text{n}} \sin (\omega_0 + \Delta \omega) t, \tag{28}$$

which is detuned relative to the signal frequency by $\Delta \omega = \omega_{\text{n}} - \omega_0$.

The duration of the sinusoidal noise τ_{n} can be practically any value, but it is necessary to differentiate between the cases:

a) sinusoidal noise of long duration exceeding the signal duration,

τ_{n} [illegible]

b) short-time sinusoidal noise, when

τ_{n} [illegible]

We shall evaluate here the effects of sinusoidal noise of long duration ("non-attenuated" sinusoidal noise). This permits the expression of the frequency-selectivity properties of the integrator in a universally-adopted sense.

Let us rewrite the expression for sinusoidal noise (28) in the form

$$E_{\text{n}} = e_{\text{n}} \cos \Delta \omega t \sin \omega_0 t + e_{\text{n}} \sin \Delta \omega t \cos \omega_0 t = \varphi (\Delta \omega, t) \sin \omega_0 t + \psi (\Delta \omega, t) \cos \omega_0 t \quad \text{for} \quad 0 \leqslant t \leqslant \tau_{\text{n}}. \tag{29}$$

The oscillation (29) corresponds to the vector diagram in Figure 5.

The amplitude of the sinusoidal noise at the integrator output is equal to

$$e_{\text{п}}(\Delta\omega)_{\tau} = \sqrt{\left[\int_0^{\tau} \varphi(\Delta\omega, t)\, dt\right]^2 + \left[\int_0^{\tau} \psi(\Delta\omega, t)\, dt\right]^2} =$$

$$= e_{\text{п}} \sqrt{\left[\int_0^{\tau} \cos \Delta\omega t\, dt\right]^2 + \left[\int_0^{\tau} \sin \Delta\omega t\, dt\right]^2} =$$

$$= e_{\text{п}} \sqrt{\frac{1}{\Delta\omega^2}\left[\sin^2 \Delta\omega\tau + (1 - \cos\Delta\omega\tau)^2\right]} =$$

$$= e_{\text{п}} \sqrt{\frac{2}{\Delta\omega^2}(1 - \cos \Delta\omega\tau)} = e_{\text{п}} \sqrt{\frac{4}{\Delta\omega^2} \sin^2 \frac{\Delta\omega}{2}\tau}.$$

Accordingly,

$$e_{\text{п}}(\Delta\omega)_{\tau} = e_{\text{п}} \frac{\sin \frac{\Delta\omega}{2}\tau}{\frac{\Delta\omega}{2}} = e_{\text{п}}\, \tau \frac{\sin \frac{\Delta\omega}{2}\tau}{\frac{\Delta\omega}{2}\tau}. \tag{30}$$

For $\Delta\omega = 0$ (at signal frequency)

$$e_{\text{п}}(0)_{\tau} = \tau. \tag{31}$$

Thus, the transmission factor for an ideal integrator at resonant frequency is equal to

$$K_0 = \tau.$$

The relationships (30) and (31) determine the equations for the resonance characteristic of the integrator

$$y(\Delta\omega)_{\tau} = \frac{e_{\text{п}}(\Delta\omega)_{\tau}}{e_{\text{п}}(0)_{\tau}} \cdot \frac{\sin \frac{\Delta\omega\tau}{2}}{\frac{\Delta\omega\tau}{2}}, \tag{32}$$

where

$$y(\Delta f)_{\tau} = \frac{e_{\text{п}}(\Delta f)_{\tau}}{e_{\text{п}}(0)_{\tau}} \frac{\sin \pi\Delta f\tau}{\pi\Delta f\tau}, \tag{33}$$

where $\Delta f = \frac{\Delta\omega}{2\pi}$.

The resonance characteristic of the integrator, calculated by Formula (33), is shown in Figure 6.

Let us determine the value for the effective frequency band of the integrator

$$\Delta f_{\text{eff}\,\tau} = \int_{-\infty}^{\infty} y^2(\Delta f)\, d\Delta f = 2\int_0^{\infty} \frac{\sin^2 \pi\Delta f\tau}{(\pi\Delta f\tau)^2}\, d\Delta f = \frac{1}{\tau}. \tag{34}$$

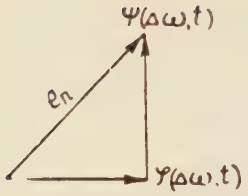

Figure 5

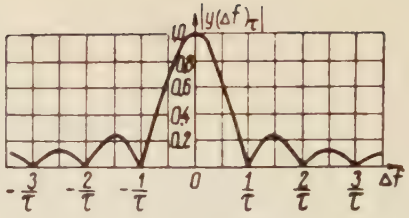

Figure 6

Accordingly, the effective frequency band of the integrator is equal to the inverse value of the integration time (equal to signal duration).

Narrow-Band Reception of Signals. In evaluating the frequency selectivity of narrow-band reception, it is necessary, above all, to keep in mind the limitation of signal duration. Because of this, with a decrease in the filter passband, we shall have, together with the limitation of noise effects, a simultaneous decrease in signal amplitude at the output. A proper criterion for evaluating the actual selectivity of the frequency-selective channel (of the filter) in the case under examination can be the relationship, at its output, between the maximum amplitude of a signal of given duration and the amplitude of the sinusoidal noise in a steady-state condition (as in integral reception, we have examined here the effect of sinusoidal noise of sufficiently large duration, greater than the time required for steady-state conditions in the frequency-selective system). It is assumed that at each given moment only one sinusoidal noise will be effective at one of the frequencies (the case of separate sinusoidal noises).

A complete evaluation of the effects of sinusoidal noise in each concrete case can be carried out if we know all the statistical facts of the sinusoidal noise (in particular, if we know the distribution of the sinusoidal noise by frequency and level). A detailed treatment of the problem of statistical structure of sinusoidal noise (which can be quite different depending on actual operating conditions of a given communications system) is beyond the limitations of the present article. Here, we shall have in mind sinusoidal noise with an equal-probability distribution in frequency and with practically any values of amplitude. In other words, noise at any frequency is assumed to be of equal probability and, on the average, none is predominant over the others in an energy relationship.

Let us introduct the concept of signal-to-noise ratio at a given frequency

$$h'^2 = \frac{a^2}{e_n'^2},$$

where e_n' is the mean statistical value of the sinusoidal noise amplitude at the given frequency.

In accordance with the above, the mean statistical value of the sinusoidal noise amplitude is assumed to be the same at each frequency.

Then, the average, with respect to the full range, power of the sinusoidal noise acting on the receiver with an effective frequency band Δf_{eff} will be equal to (with a 1-ohm resistor)

$$\frac{e_n^2}{2} = \frac{\overline{e_n'^2}}{2} \Delta f_{eff} = \xi_0^2 \Delta f_{eff} \qquad (35)$$

Here $\xi_0^2 = \frac{\overline{e_n^2}}{2}$ is the quadratic for the effective value (for a sufficiently large period of time) of sinusoidal noise acting on the receiver at one of the frequencies.

Let us calculate the signal-to-noise ratio separately for integral and narrow-band reception.

For integral reception we obtain on the basis of Formulas (13), (35) and (30)

$$h_*^2 = \frac{(a\tau)^2}{\overline{e_{II}'^2}\,\tau^2 2\int_0^\infty \frac{\sin^2\frac{\Delta\omega\tau}{2}}{\left(\frac{\Delta\omega\tau}{2}\right)^2} d\,\Delta\omega} = \frac{a^2\tau}{2\xi_0^2}. \tag{36}$$

By comparing Formulas (35) and (3), it is easy to conclude that the determination of maximum excess of signal over the aggregate sinusoidal noise during narrow-band reception can be reduced to the problem, solved above, for sluctuating noise.

Based on this fact, we may write:

$$h_{opt}^2 = 0.82\,\frac{a^2\tau}{2\xi_0^2}, \tag{37}$$

$$h_{opt'}^2 \approx 0.5\,\frac{a^2\tau}{2\xi_0^2}, \tag{38}$$

where h_{opt}^2 and $h_{opt'}^2$ represent the signal-to-noise ratio for sinusoidal noise, which correspond to the optimal frequency bands for the reception of single pulses in a continuous series.

Accordingly,

$$\left(\frac{h_*}{h_{opt}}\right)_{sin}^2 = 1.22 \tag{39}$$

and

$$\left(\frac{h_*}{h_{opt'}}\right)_{sin}^2 \approx 2.0. \tag{40}$$

We shall recall that the results obtained relate to the case where the pulses of the received signal have an equal amplitude. If the pulses in the received series have different amplitudes, then the noise proofness of conventional narrow-band reception, in comparison with the integral-reception method, is decreased to a greater degree.

REFERENCES

1. V.I. Siforov. The Effect of Noise on the Reception of Pulse Signals. Radiotekhnika, No. 1, 1946.

2. V.S. Mel'nikov. Technical Methods for the Development of a Radiotelegraphy Communications System. Collection of Works "60 Years of Radio," 1955.
3. N.L. Teplov. Basic Relationships During the Integration and Filtration of Signals and Fluctuating Noise in the Channels of Radio Receiving Equipment. Collection of Works of NTORiE (A.S. Popov Scientific and Technical Society for Radio Engineering and Telecommunications), No. II, 1958.
4. V.Ya. Korol'. The Integral Method for the Reception of Radiotelegraph Signals. Vestnik Svyazi, No. 5, 1953.
5. The Theory of the Coherent Integrator and Its Application in the Detection of Pulse Signals. Problems of Radar Techniques (Collection of Translations), No. 5(47), 1958.

Received April 27, 1960

CALCULATION OF NON-LINEAR DISTORTION IN WAVEGUIDE TRANSMISSION LINES

Yu. A. Yerukhimovich

An exact solution is given for the problem of any number of inhomogeneities in a waveguide line using the method proposed in reference [1]. A comparison with the approximate solution given in [1] is made. Some results of the exact solution are presented and an example of practical calculation is given.

In [1] as well as in previous works of the author, an approximate solution was given for the problem of long feeders when the number of inhomogeneities, M, is large. In the present article, an exact solution is given for any number M, within the limits of applicability of the method.

We shall consider the results of reference [1] as well-known, and hereafter, for uniformity, we shall use the notation introduced therein.

It should be noted that another method for the solution of this problem was used in reference [2, 3]. However, the results obtained by this method cannot as yet be used in practice for sectionalized waveguides. In accordance with [1], we shall assume that the waveguide (feeder) has M

inhomogeneities distributed at equal distances from each other, and each one of which has the same reflection factor.

CALCULATION OF HARMONIC NOISE IN WAVEGUIDE LINES FOR ANY NUMBER OF INHOMOGENEITIES

The noise power at the qth harmonic at a frequency ω_α, relative to the fundamental, is given by the equation (3) in [1]. Under the conditions stated above, P_q may be written as:

$$P_q = 2\left(q\,\frac{\omega_\alpha}{\Delta\omega}\right)^2 \left\{ r_0^2 r_M^2 I_q^2(\theta) + (r_0^2 + r_M^2) r^2 \sum_{m-1}^{M-1} I_q^2\left(\frac{m}{M}\,\theta\right) + \right.$$
$$\left. + r^4 \sum_{n-1}^{M-2} \sum_{m=n+1}^{M-1} I_q^2\left(\frac{n-m}{M}\,\theta\right) \right\}. \qquad (1)$$

Here $\theta = 2\Delta\omega\,\frac{L}{V_g}$; ω_α is the audio angular frequency of the test-tone modulation, $\Delta\omega$ — is the peak frequency deviation of the multi-channel signal; $L = Ml$ — is the total length of the waveguide; l — is the length of one of its sections; V_g — is the group propagation velocity of the multi-channel signal in the waveguide; r_0, r_M — are, respectively, the reflection factor moduli for the generator and for the load (antenna); r — is the reflection factor modulus for each irregularity; $I_q(z)$ — is a Bessel function of the first kind and qth order.

The summations are replaced in [1] by the corresponding integrals to which they convert with unlimited increase in M. It is assumed that for the final M, its value must be sufficiently large so that the error in the calculations will be small. However, in the work cited, it is not indicated which value of M would be considered acceptable. Neither does it take into account that from the summation in (1), it is possible to separate out terms proportional not only to M^2 or M, but also to lower degrees. A study of Formula (1) showed that the summations it contains may be calculated of any value of M.

For intermediate calculations we shall use the following relationships [5]

$$I_q^2(x) = \sum_{\kappa=0}^{\infty} A_{q,\kappa} \left(\frac{x}{2}\right)^p, \quad p = 2q + 2\kappa, A_{q,\kappa} = (-1)^\kappa \frac{(2q+2\kappa)!}{\kappa!\,(2q+\kappa)\,[(q+\kappa)!]^2};$$

$$\sum_{m=1}^{M} m^p = \frac{M^{p+1}}{p+1} + \frac{M^p}{2} + \frac{pM^{p-1}}{12} - \frac{p(p-1)(p-2)M^{p-3}}{720} + \ldots$$

the final term contains M or M^2.

In order to avoid performing duplicate calculations we shall consider attenuation in the feeders. In accordance with [1], the first summation in Equation (1), taking attenuation into account, may be represented as:

$$S_1 = \sum_{m=1}^{M-1} e^{-4\alpha' m} I_q^2\left(\frac{m}{M}\,\theta\right).$$

Here, α — is the attenuation factor of a wave in a waveguide of unit length.

Let us expand the expression under the summation sign into a series and change the order of summation:

$$S_1 = \sum_{\kappa=0}^{\infty} \sum_{s=0}^{\infty} \sum_{m=1}^{M-1} A_{q,\kappa} \frac{(-4\gamma l)s}{s!} \left(-\frac{\theta}{2M}\right)^p m^{p+s},$$

Let us insert the symbols $\gamma = \frac{\theta}{2M}$ and $\gamma(M-1) = \frac{M-1}{M} \frac{\theta}{2}$. Calculation of the summations with respect to m gives

$$\gamma^{p+s} \sum_{m=1}^{M-1} m^{p+s} = \frac{1}{\gamma} \frac{x^{p+s+1}}{p+s+1} + \frac{x^{p+s}}{2} + \gamma \frac{(p+s)x^{p+s-1}}{12} - \ldots$$

Using the integral and differential forms of the function, we may write

$$\gamma^{p+s} \sum_{m=1}^{M-1} m^{p+s} = \frac{1}{\gamma} \int_0^x y^{p+s}\, dy + \frac{x^{p+s}}{2} + \frac{\gamma}{12} \frac{d}{dx} x^{p+s} - \ldots$$

Let us substitute this relationship in S_1, and take advantage of the feasibility of revers ng the order of the integration and differentiation operations and the summation operations (in an absolutely-converging series). The summations appearing in the resulting expressions are easily calculated by the formulas derived above; as a result we find

$$S_1 = \frac{1}{\gamma} \int_0^{\frac{M-1}{M}\frac{\theta}{2}} e^{-\frac{4\alpha l}{\gamma}x} I_q^2(2x)\, dx + \frac{1}{2} e^{-\frac{4\alpha l}{\gamma}x} I_q^2(2x) +$$

$$+ \frac{\gamma}{12} \frac{d}{dx} e^{-\frac{4\alpha l}{\gamma}x} I_q^2(2x) - \ldots,$$

where $\frac{4\alpha l}{\gamma} = 8\frac{\alpha L}{\theta}$; $\frac{4\alpha l}{\gamma} x = 4\alpha L_M$, $\quad L_M = \frac{M-1}{M} L.$

By substituting $x = \theta_M \frac{y}{2}$ under the integral sign, defining $\theta_M = \frac{M-1}{M}\theta$ (Fig. 1) and using the average value theorem for integration of the product of two functions (as indicated in [1]), we find

$$S_1 = (M-1) \int_0^1 e^{-4L_M y}\, dy \int_0^1 I_q^2(\theta_M x)\, dx + \frac{1}{2} e^{-4\alpha L_M} I_q^2(\theta_M) +$$

$$+ \frac{\theta}{24M} \frac{d}{dx} e^{-4\alpha l x} I_q^2(2x)\Big|_{x=\frac{\theta_M}{2}} - \ldots$$

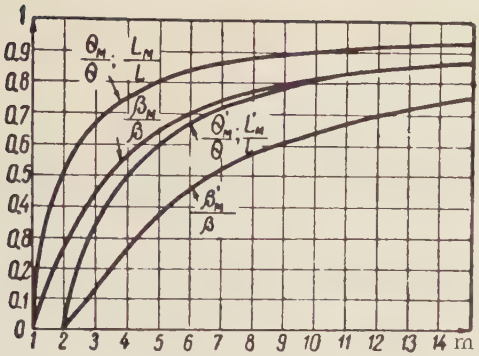

Figure 1

For comparison with the results in the work [1], we shall use the symbols employed there:

$$F_1(\theta) = I_q^2(\theta);\ F_2(\theta) = \int_0^1 I_q^2(\theta x)\,dx;$$

$$F_3(\theta) = \int_0^1 (1-x)\,I_q^2(\theta x)\,dx,$$

and also the quantities $K_1 = e^{-4\alpha L}$ and $K_2 = \frac{1 - e^{-4\alpha L}}{4\alpha L}$. The symbol K_{im} means that in place of the quantity L, in the expression corresponding to K_i we must substitute the quantity L_M. Finally, we shall obtain

$$S_1 \approx (M-1)F_2(\theta_M)\,K_{1M} + 0{,}5\,F_1(\theta_M)\,K_{1M} + \\ + \frac{\theta}{24M}\,\frac{d}{dx}\,e^{-4\alpha l x}\,I_q^2(2x)\Big|_{x=\frac{\theta_M}{2}} \qquad (2)$$

Now we shall find the value of the double summation in (1).

After a simple transformation, S_2 (taking into account the wave attenuation) may be represented in the following form:

$$S_2 = \sum_{n=1}^{M-2}\sum_{s=1}^{M-n-1} e^{-4\alpha' l s}\,I_q^2\left(\frac{s}{M}\,\theta\right).$$

Using the relationships deduced above, we find

$$S_2 = \sum_{\kappa=0}^{\infty}\sum_{\nu=0}^{\infty}\sum_{n=1}^{M-2}\sum_{s=1}^{M-n-1} A_{q,\kappa}\left(\frac{s}{M}\,\frac{\theta}{2}\right)^{p}\frac{(-4\alpha l s)^{\nu}}{\nu!}.$$

Let us determine, first, the summation with respect to s

$$\sum_{s=1}^{M-n-1} s^{p+\nu} = \frac{\mu^{p+\nu+1}}{p+\nu+1} + \frac{\mu^{p+\nu}}{2} + \frac{(p+\nu)}{12}\mu^{p+\nu-1} - \ldots,$$

here $\mu = M - n - 1$.

Further, we shall find the values inside the summations. In calculating the summations with respect to n, we shall use the following auxiliary relationship:

$$\sum_{n=1}^{M-2} n^{p+\nu} = \frac{(M-2)^{p+\nu+1}}{p+\nu+1} + \frac{(M-2)^{p+\nu}}{2} + \frac{(p+\nu)}{12}(M-2)^{p+\nu-1} - \ldots$$

Let us designate $z = \gamma(M-2) = \frac{M-2}{M}\frac{\theta}{2} = \frac{\theta'_M}{2}$. (For the value θ'_M, see Figure 1).

Considering values not greater than the second order of smallness relative to 1/M, we shall have, after determining the sums according to n,

$$S_2 = \sum_{n=0}^{\infty}\sum_{s=0}^{\infty} A_{q,s}\frac{\left(-\frac{4\pi l}{\gamma}\right)^{\nu}}{\nu!}\left\{\frac{z^{p+\nu+2}}{(p+\nu+1)(p+\nu+2)}\frac{1}{\gamma^2} + \right.$$

$$\left. + \frac{1}{\gamma}\frac{z^{p+\nu+1}}{p+\nu+1} + \frac{5}{12}z^{p+\nu} + \frac{\gamma}{12}(p+\nu)z^{p+\nu-1} + \ldots\right\}.$$

In order to simplify this expression, we shall use the following relationship:

$$\frac{z^{p+\nu+2}}{(p+\nu+2)(p+\nu+1)} = \int_0^z (z-y)\,y^{p+\nu}\,dy;\quad \frac{z^{p+\nu+1}}{p+\nu+1} = \int_0^z y^{p+\nu}\,dy;$$

$$(p+\nu)z^{p+\nu-1} = \frac{d}{dz}z^{p+\nu}.$$

After transforming the integrals to fixed limits and using the theorem on the average integral for separating out the dependence of S_2 on the wave attenuation, we have

$$S_2 \approx (M-2)^2 F_3(\theta'_M)\,K'_{2M} + (M-2)F_2(\theta'_M)\,K'_{2M} + \frac{5}{12}F_1(\theta'_M)\,K'_{1M} +$$

$$+ \frac{\theta}{24}\frac{d}{dz}\,e^{-4\pi Lz}\,I_q^2(2z)\Big|_{z=\frac{1}{2}\theta'_M}. \qquad (3)$$

Here, $L'_M = \frac{M-2}{M}L$ (Fig. 1); the symbol «'» for K_{im} means that in the place of L in the explicit form of this function we should substitute L'_M.

Now we shall write the final expression for P_q:

$$P_q = 2\left(q\,\frac{\omega_a}{\Delta\omega}\right)^2 \Big\{ r_0^2 r_M^2\, F_1(\theta)\, K_1 + (M-1)\, r^2 (r_0^2 + r_M^2)\, F_2(\theta_M)\, K_{2M} + \\ + (M-2)\, r^4 F_2(\theta'_M)\, K'_{2M} + \frac{5}{12} r^4 F_1(\theta'_M)\, K'_{1M} + \\ + \frac{1}{2} r^2 (r_0^2 + r_M^2) F_1(\theta_M)\, K_{1M} + (M-2)^2 r^4 F_3(\theta'_M)\, K'_{2M} \Big\}. \tag{4}$$

The functions K_1 and K_2 are shown in Figure 2, in accordance with those given in [1].

The argument of the function $F_n(\theta)$ in reality is found to be dependent on the number of sections in the waveguide. The same applies also to the effective length of the whole waveguide.

An evaluation of the accuracy of the calculation performed by means of (4) may be obtained from the formula

$$\delta\% = \frac{4{,}17}{M}\,\frac{\theta}{\{P_q\}}\left[r^2 (r_0^2 + r_M^2)\,\frac{d}{dx}\, e^{-4\alpha L x}\, I_q^2(2x)\Big|_{x=\frac{\theta_M}{2}} + \right.$$

$$\left. + r^4\,\frac{d}{dx}\, e^{-4\alpha L x}\, I_q^2(2x)\Big|_{x=\frac{\theta'_M}{2}} \right]. \tag{5}$$

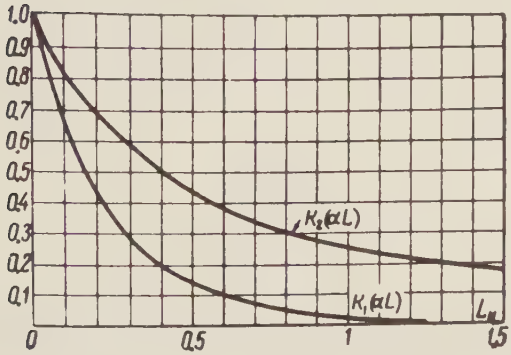

Figure 2

The quantity $\{P_q\}$ designates the expression within brackets in formula (4).

For $M \to \infty$, we have $L_M \to L$; $L'_M \to L$; $\theta_M \to \theta$ and this formula is transformed into (4) from [1] with the following two comments:

1) From Formula (8) in [1], it follows that in order to calculate the attenuation $F_3(\theta)$ in (4), it is necessary to multiply by K_3, which differs from K_2. However, this conclusion is in error. Actually, it follows from [1] Appendix 1) that the function $F_3(\theta)$, with attenuation taken into account, is determined by the expression

$$F_3(\theta) = \int_0^1 \int_x^1 e^{-4\alpha L (y-x)}\, I_q^2 [\theta (y-x)]\, dx\, dy.$$

By a formula derived in this same appendix, it is identically equal to

$$\int_0^1 e^{-4\alpha l x}(1-x) I_q^2(\theta x)\, dx.$$

By applying to this integral the theorem on the mean integral from the product of two functions, we find that in calculating the attenuation $F_3(\theta)$, it is necessary to multiply by

$$\int_0^1 e^{-4\alpha l x}\, dx = K_2.$$

2) From the results of a precise summation of S_1 and S_2, it is clear that in [1], during the substitution of integrals for the summations, a number of terms were not taken into account. This circumstance is the principal shortcoming of the method used in [1] for calculating the sums.

NOISE IN NONLINEAR TRANSITIONS

Of basic interest are the formulas which permit the computation of the relative or absolute value of noise in the nonlinear transitions during the transmission of multichannel messages through the transmission line.

By using the results and data obtained in [1] and in previous works, it is easy to write the general formula analogous to (7) in [1].

For this purpose it is sufficient to note that θ_M not equal to θ, the quantity β should be replaced by the value $\beta_M = (\frac{\theta_M}{\theta})^2 \beta$ and θ'_M by $\beta'_M = (\frac{\theta'_M}{\theta})^2 \beta$, i.e.

$$\beta_M = \left(\frac{M-1}{M}\right)^2 \beta, \tag{6}$$

$$\beta'_M = \left(\frac{M-2}{M}\right)^2 \beta. \tag{7}$$

Now the general expression for the relative noise-power level in nonlinear transitions, analagous to (7) in [1], for the highest frequency of the multichannel signal, may be written as:

$$G_1^2 = \left(\frac{\chi \omega_N^2}{4x^2}\right)\Big\{ r_0^2 r_M^2 F_1(\beta) K_1 + 0{,}5\, r^2 (r_0^2 + r_M^2) F_1(\beta_M) K_{1M} + \\ + 0{,}415\, r^4 F_1(\beta'_M) K'_{1M} + (M-1) r^2 (r_0^2 + r_M^2) F_2(\beta_M) K_{2M} + \\ + (M-2) r^4 F_2(\beta'_M) K'_{2M} + (M-2)^2 r^4 F_3(\beta'_M) K'_{2M} \Big\}, \tag{8}$$

where x — is the utilization factor of the total number of channels ($x \approx 1/4$).

In accordance with [1]

$$F_1(\beta) = \frac{4}{\pi} \int_0^\infty e^{-\beta} \left[e^{\beta \frac{\sin\theta}{\theta}} - 1 - \beta \frac{\sin\theta}{\theta} \right] \cos\theta\, d\theta,$$

$$F_2(\beta) = \frac{4}{\pi} \int_0^{\infty} \int_0^{1} e^{-\beta z^4} \left[e^{\beta z^4 \frac{\sin\theta}{\theta}} - 1 - \beta z^2 \frac{\sin\theta}{\theta} \right] \cos\theta d\theta\, dz,$$

$$F_3(\beta) = \frac{4}{\pi} \int_0^{\infty} \int_0^{1} e^{-\beta z^2} \left[e^{\beta z^2 \frac{\sin\theta}{\theta}} - 1 - \beta z^2 \frac{\sin\theta}{\theta} \right] (1 - z) \cos\theta d\theta\, dz,$$

$\beta = 4\tau^2 x^2$, $\tau = \frac{L}{Vg}$ is the signal transmission time in the waveguide; x — is the effective value of angular deviation of the multichannel signal, which is equivalent to $\frac{\Delta\omega}{\sqrt{2}}$ for the test signal.

Although now the expression for G_1^2 has become more complex because of the addition of new terms, all of them are determined by the same functions $F_n(\beta)$ as in work [1], but with new values of the argument dependent on M. The functions $F_n(\beta)$ have been reproduced here in Fig. 3 from data in [1], and may be used directly for calculations by Formula (8).

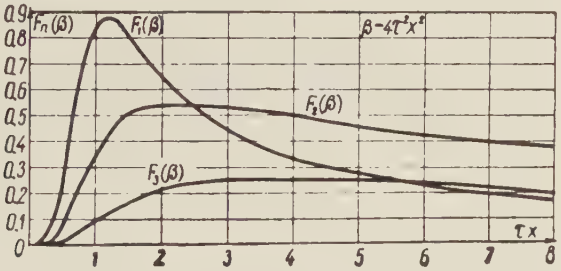

Figure 3

The accuracy of the calculations carried out by means of Formula (8) can be determined from the expression

$$\Delta^0/_0 = \frac{1}{M} \frac{4{,}17}{\{G_1^2\}} \left\{ \frac{M-1}{M} r^2 (r_0^2 + r_M^2) K_{1M} \left[\beta \frac{d}{d\beta_M} F_1(\beta_M) - 4\alpha L F_1(\beta_M) \right] + \right.$$
$$\left. + \frac{M-2}{M} r^4 K'_{1M} \left[\beta \frac{d}{d\beta'_M} F_1(\beta'_M) - 4\alpha L F_1(\beta_M) \right] \right\}. \qquad (9)$$

Here $\{G_1^2\}$ denotes the quantity within brackets of formula (8). Differentiating with respect to the parameter, we find

$$\frac{d}{d\beta} F_1(\beta) = -F_1(\beta) + \frac{4}{\pi} \int_0^{\infty} e^{-\beta} \left(e^{\beta \frac{\sin\theta}{\theta}} - 1 \right) \frac{\sin\theta}{\theta} \cos\theta\, d\theta. \qquad (10)$$

This function is shown in Figure 4.

The basic result of the precise solution is worth noting. The dependence of the arguments of the functions $F_n(\beta)$ and $K_n(\alpha L)$ on the value of M leads

to an exaggerated evaluation for the degree of influence exerted by these functions on the overall noise level. A particularly significant effect of this factor will be observed in the region of rapid changes in $F_n(\beta)$ of the function β, i.e. when $\tau x \sim 1$. At the same time, as actual calculations will show, the value for noise determined from data in [1] may appear to be of an order higher than that obtained from precise calculations. For large values of τx and M, the difference between formulas (8) and (7) in [1] should level out.

From Figures 1 and 2, it follows that for slightly larger values of M, the wave attenuation in the waveguide has a greater effect on the value for relative noise level than is indicated in [1].

In the case when M is so large that $\frac{\theta_M}{\theta}$ and $\frac{\theta'_M}{\theta}$ approach 1, and β does not lie in the region of rapid changes in $F_n(\beta)$, the formula for noise of nonlinear transitions in the approximation which is used in the work [1] ($M \gg 1$) acquires the form

$$G_1^2 = \left(\frac{\tau\omega_N^2}{4x^2}\right)\left\{[r_0^2 r_M^2 + 0{,}5\, r^2(r_0^2 + r_M^2) + 0{,}415\, r^4]F_1(\beta)K_1 + \right.$$
$$\left. + Mr^2(r_0^2 + r_M^2 + r^2)F_2(\beta)K_2 + M^2 r^4 F_3(\beta)K_2\right\}. \qquad (11)$$

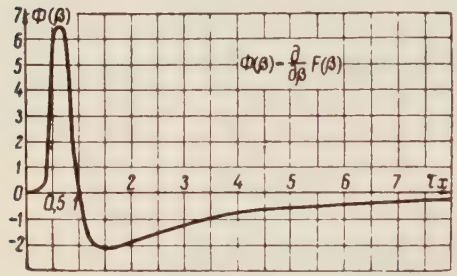

Figure 4

As an example of the application of the obtained results to practical practical purposes, we shall present the results of calculations of noise level at nonlinear transitions of a waveguide transmission line for a typical radio relay line. The magnitude of the noise is taken relative to a power of 1 mw at the mean audio frequency of the highest channel of the multichannel message, and is expressed in picowatts. The scale of the curves takes into account the psophometric (circuit noise) factor, for which the results of calculations by formula (83) [sic] are multiplied by the coefficient $k_n^2 = 0.56$ [2].

The waveguide consists of M sections each of which has a length $l = 4.5$ m. The noise relationships were computed in the function M for various values of the parameters r_0 and r_M, and for simplification, it was considered that the reflections from the waveguide terminations were equal to each other, i.e. $r_0 = r_M$. The magnitude of the reflection from an individual junction was considered to be an independent parameter. Both r_0 and r are expressed in percentages. Figure 5 shows the results of

calculations for the following data: number of channels N = 240; attenuation $\alpha = 2.5 \frac{db}{100\ M}$; x = 550 kc and the angular frequency of the highest channel f_N = 1052 kc.

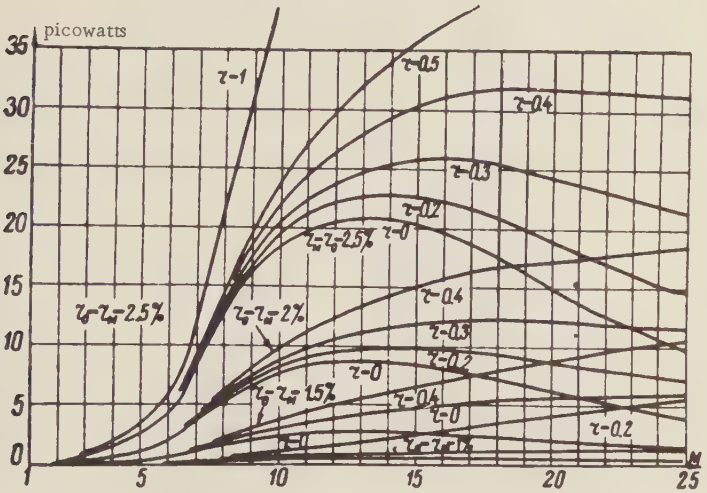

Figure 5

The numerical values for the parameters in Figure 6 are: N = 600; $\beta = 2.5 \frac{db}{100\ m}$; x = 880 kc and f_N = 2540 kc. By analyzing the resulting curves, the following rules may be established. With small reflection factors for the unctions, the curves have clearly indicated noise peaks located near the noise peak for a smooth (continuous) waveguide (r = 0). With an increase in r, the positions of the peaks are displaced in the direction of longer waveguide lengths (larger M).

For small values of reflection factor for the waveguide terminations, the principal role will then be played by the values of reflection factor for the junctions. For small r, the noise level for this calculation will be linear with increase in waveguide length. The greater the value for N, with a constant value for $r_0 = r_M$, the shaper will be the noise peaks.

On the basis of the computed curves, it is possible to determine the conditions under which the noise level in a system will not exceed acceptable limits.

1) The results attained have expanded the possibilities of using the method written up in [1] and previous works, and makes it possible within its framework to analyze sectionalized transmission lines with any number of links. The errors in [1] have been eliminated.

2) The deduced data makes it possible to make an evaluation of the accuracy of the calculations performed.

3) Existing recommendations concerning the computation of noise resulting from nonlinear transitions (see, for example, [4]), require correction.

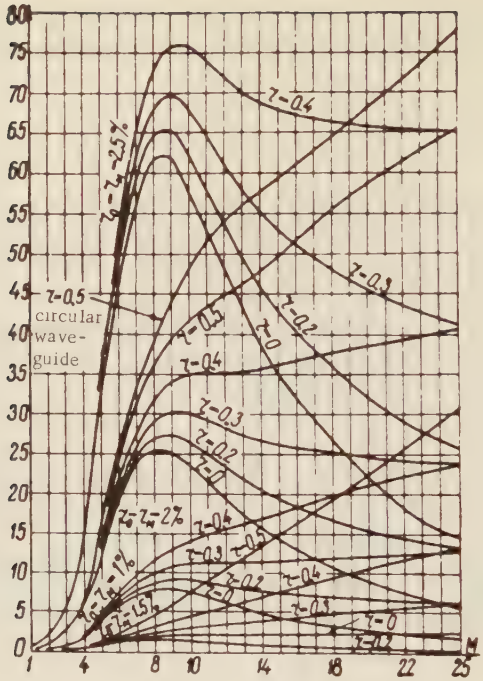

Figure 6

REFERENCES

1. Lewin. The multiple reflections in the long feeders. "Wireless Eng.," 1952, v. 29, No. 246.
2. S.V. Borodich. The Calculation of Noise in the Channels of Radio Relay Lines with Frequency Compression and Frequency Modulation. Elektrosvyaz' No. 1, 1956.
3. A.V. Prosin. Some Calculation Problems in a Multichannel Communications System with Frequency Modulation and Frequency Compression. Radiotekhnika, Electronika, No. 1, 1958.
4. Marko. The calculation of the nonlinear distortion factors and distortion noise for the various types of distortion in multichannel directional FM radio systems. NTZ, 1957, Sept. B. 10, No. 9.
5. I.M. Ryzhik. Tables of Integrals, Summations, Series and Products. GITTL, 1948.

Received September 27, 1960

A SIMPLE ELECTRONIC INSTRUMENT FOR STATISTICAL RESEARCH IN THE FIELD OF RADIO WAVE PROPAGATION

N.S. Stanulov

A description is given of an electronic instrument for the direct determination of the average value of field intensity. An ordinary dc electric meter was used as the indicator of average values. With known distribution of the instantaneous values of the electromagnetic field intensity, the instrument may also be used for determining the corresponding median values.

In the theory of radio wave propagation, the study of ionospheric propagation occupies an important position. Under the conditions of this type of propagation the amplitude of the resulting field at the receiving point changes in a random manner, i.e. fading occurs. The reasons for these oscillations in field intensity are the continuous variations in the electron density of the ionospheric layers, oscillations in their altitude, and interaction between waves which are propagated along many different paths [1, 2]. Quantitatively, the fluctuations in field intensity may be defined by some random function of time E(t). Figure 1 shows a possible form

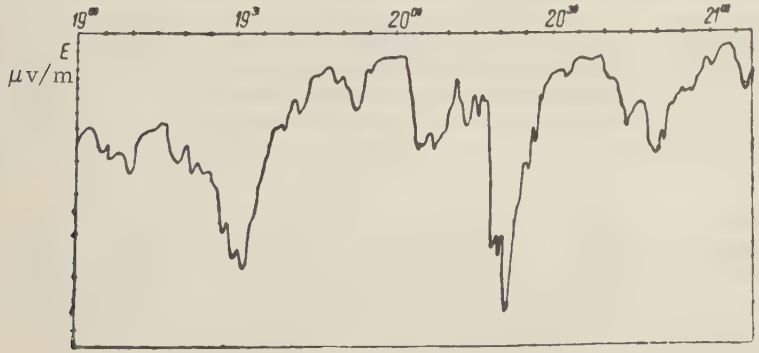

Figure 1

of this function (recorded in the course of a certain interval of time). Characteristic for this type of recording is the fact that each time the recording apparatus is switched on, the function has a different form. This shows that the oscillations in field intensity represent one of several possibilities $E_k(t)$ ($k = 1, 2, 3, \ldots$) of the random function $E(t)$.

For a qualitative and quantitative evaluation of fading in field intensity, we make use of the maxima and minima of the curve $E_k(t)$, the effects of rapid and slow fading as well as interference and absorption fading, etc., and also certain statistical parameters. It should be noted that statistica studies of ionospheric radio wave propagation as the basis for compiling radio forecasts for the requirements of the technical services in communications was confirmed only ten years ago. Among the statistical parameters, we shall denote the average value, with respect to time, of $\bar{E}$ (the fixed component of the process) as practically equal, relative to the average over the total period, to mathematical expectations, and also to the so-called median value E_0, that is, the value of field intensity which exceeds the instantaneous values during 50% of the time of observation. Frequently, the so-called quasi-maximum value is also used. This is the value of field intensity which exceeds the instantaneous values during 5% of the period of observation (some authors take 10% [3]). Through numerous observations it is an established fact that the average value is 35% of the quasi-maximum value [1, 2]. Other authors, by the way, point out that a small quantitative difference exists between the median and average values with respect to time [4]. Actually, with a Rayleigh distribution of the instantaneous values of field intensity, it is easy to establish the relationship between the average and median values as $\bar{E} = 1{\cdot}063\, E_0$ (i.e. the difference between the two values does not exceed 6.3%), while with a Gaussian distribution $\bar{E} = E_0$ [5]. For the so-called m - distribution,[1] with certain exceptions, we also have either the exact equality $\bar{E} = E_0$, or an approximate equality between these values (it goes without saying that our discussion concerns only radio wave propagation beyond the horizon) [6]. This shows that in a very large number of cases of practical, long-distance radio wave communication, the averaging operation gives not only the average value but also, to a first approximation, the median value of the electromagnetic field intensity.

The literature makes reference to instrument-counters which automatically determine the various statistical parameters of a function of form $E_k(t)$, since the direct determination of these parameters by means of oscillograms is very difficult [5]. These instruments record the instantaneous values of intensity for a specified interval of time. They indicate that portion of the interval in which the instantaneous values of intensity exceed a specified level or are confined to known limits. By means of the distribution curves obtained in this manner, the required statistical parameters are read off and calculated. These instruments are relatively

---

[1]The function of probability density of this distribution is determined in the following manner [6]:

$$p(E) = \frac{2m^m E^{2m-1}}{\Gamma(m)\,\Omega^m} e^{-m\frac{E^2}{\Omega}}$$

where $\Gamma(m)$ — is the gamma function, the parameter $m > 1$[2 and $\Omega = \overline{E^2}$.

complex in their design. One version of this type of instrument is given in [7]. An electromechanical counter, connected in the plate circuit of an electron tube, starts to operate when a specified positive potential is applied to the control grid of the tube. Ten such stages (10 tubes) are provided; the value of voltage at which each of these stages begins to function is determined by the voltage which develops across its respective cathode resistor. The counter stages are cut off periodically by means of multivibrators, which makes it possible to make computations for a unit of time.

Let us now proceed to certain theoretical observations. From Figure 1 it is apparent that $E_k(t)$ is a continuous, random function of time which describes the fluctuations in field intensity.[2] It has been established, through numerous statistical data compiled during research on ionospheric radio wave propagation at various wavebands, that the instantaneous values of field intensity obey definite laws, to which we have already referred in references [2, 4, 5, 6]. It is reasonable to assume that these laws do not depend, on the one hand, on the season of the observations, and on the other hand, they maintain their strength independent of the duration and starting point of the observations.[3] This means that the function $E_k(t)$ is a stationary random function. As is known, a random process becomes a stationary [steady-state] one when all conditions creating it do not change in the course of time. Strictly speaking, one can hardly assume the existence of such a process in the course of an unlimited interval of time. However, in practice it is quite satisfactory if these conditions remain constant during the total observation time and the time of the additional interval required for attenuation of the transient process [7].

In stationary processes, on the basis of the Erg hypothesis, the average value over the full range is identical to the average value with respect to time, i.e.

$$\overline{E} = \int_{-\infty}^{+\infty} xp(x)\,dx = \lim_{T\to\infty} \frac{1}{T} \int_{0}^{T} E_x(t)\,dt. \tag{1}$$

Here, $\overline{E}$ is the average value of stationary function $E_k(t)$, p(x) is the function of the probability density of a random, stationary process, T — is the duration of the period of observation.

It can be seen that the determination of the average value of field intensity may be obtained by calculating the integral in the second equality of (1). The proposed instrument is intended for the immediate determination of this value. From this it is possible, of course, to also determine the median value, providing we know (even if approximately) the corresponding distribution of the instantaneous values of field intensity. The literature gives valuable, practical instructions on this problem. For example, data

---

[2] With the condition that the source of the electromagnetic radiation and the receiving apparatus operate during the period of observation, and also with the condition that sudden absorption in the ionosphere does not occur.

[3] Of course, in practice this period is not limited. Thus, for example, a Rayleigh distribution in the meter and decimeter band is observed for a period of not more than 5 — 20 min. [5].

is available concerning the distributions encountered in radio wavebands during a 24-hour period of observation, the distance between the receiving point and the radiation source, etc. [2, 3, 4, 5, 6]. Some of this data is contradictory [8]; in general, a complete investigation is far from realization.

Taking into account the nature of the random process which is of interest to us, a simple electronic instrument was designed, the main component parts of which are a two-stage dc amplifier with a relatively high input resistance and a dc electric meter as the integrating element (Fig. 2). In its present form, our instrument is adapted for connection in the AGC (automatic gain control) of a superheterodyne receiver with long, medium and short wavebands. Naturally, it may also be adapted to other wavelengths.

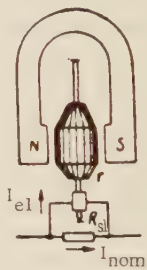

Figure 2

The principal schematic diagram of the instrument is shown in Figure 3.[4] The circuit for the dc amplifier (with a common power supply) is similar to circuits encountered in so-called computing receivers. Under conditions of ionospheric propagation, the negative voltage at the output of the second detector (A) will vary from zero (minimum amplitude of the incoming signal to the receiver) to some negative value (for maximum value of the signal). Thus, the changes in the resulting field intensity picked up by the receiving antenna will be expressed in the instrument through proportional changes in plate current of the second stage of the amplifier (from a certain minimum to a certain maximum value). At the same time, the rotor of the meter, which is connected in series in the plate circuit of this same stage, will rotate in step with the changes in current through its winding. At the end of the observation interval the number

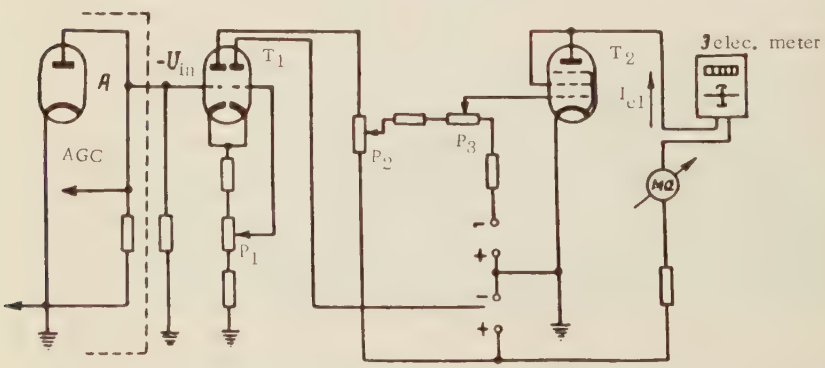

Figure 3

*In connecting the instrument to the receiver, it is necessary to disconnect the lead through which the AGC voltage is applied to the grids of the first tubes of the receiver.

of rotations indicated on the meter will be a measure of the average value of electric current passing through it, i.e. a measure of the average value of field intensity at the receiving point. With potentiometer P_2, the amplification of the signal applied to the second tube may be varied in order to select the most suitable range for the plate current I_{el}. Potentiometer P_3 is used to establish the initial operating point of the second tube (when a signal to the control grid of the first tube has not been applied). In order to decrease drift in the first tube, the well-known Miller circuit is used, which partially compensates for changes in heater voltage. Optimum compensation is achieved by means of potentiometer P_1. The dc voltage supply is provided by a conventional full-wave rectifier (the plate voltage of the right half of the first tube is regulated by means of a gas tube). The instrument is connected to a 220 volt power line through a ferroresonant regulator. To achieve greater stability in relation to drift, the instrument was provided with tubes which had already been in use for some time, and resistors with nominal power ratings twice as large, on the average, as called for in the design. As a result of the stabilization measures referred to above, a satisfactory reduction in drift was achieved — Fig. 4 (initial current through the coil of the electric meter I_{el} = 30 ma; t = 0 at the instant of connection). From the figure it is evident that a preliminary warm-up of the instrument of not less than 1-1/2 hours is desirable.

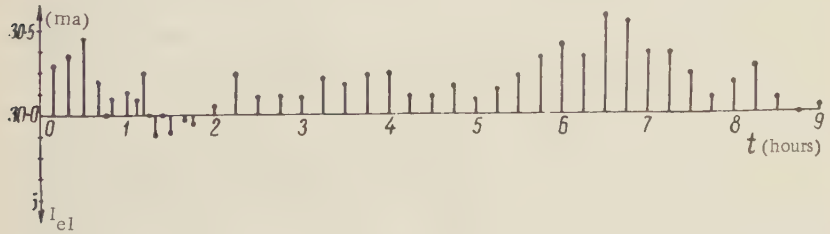

Figure 4

Since the maximum plate current of the second stage is in the order of several tens of milliamperes, whereas the nominal value of current through the electric meter usually amounts to several amperes, then it is expedient to disconnect the shunt mounted in the meter, with the result that the plate current of the second tube will now pass directly through the rotor winding of the meter. Knowing the electrical data of the meter, it is easy to derive the following equation for the current passing through it:

$$I_{el} = \frac{1000}{60} \frac{R_{sh}}{R_{sh}+r} \frac{\kappa'}{U} \frac{n}{T} = \kappa \frac{n}{T}; \quad \left(\kappa = \frac{1000}{60} \frac{R_{sh}}{R_{sh}+r} \frac{\kappa'}{U}\right). \tag{2}$$

Here I_{el} (ma) — is the current through the rotor, R_{sh} (ohms) — is the dc electrical resistance of the meter shunt, r (ohms) — is the dc electrical resistance of the rotor winding, k' (watt-sec/rev) — is the meter constant, U (volts) — is the nominal meter voltage, n (rev) — revolutions of the rotor as recorded on the meter, T (min) — period of observation.

An important characteristic of each meter is its error curve. Figure 5 shows its approximate form. As can be seen, the error is practically constant beginning with a known value of current (this value is about 30 ma in

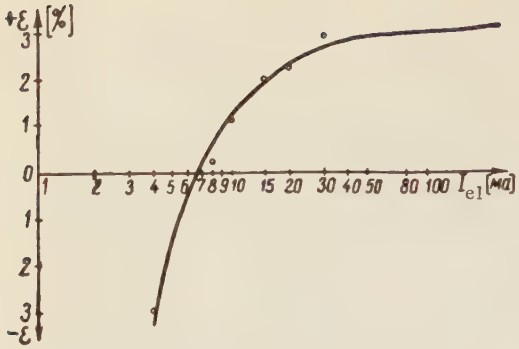

Figure 5

the figure), and it may readily be taken into account in calculating the number of revolutions.

Figures 6 and 7 show two curves of $I_{el} = \varphi(-U_{in})$ for the dc amplifier: for low and high currents. A feature of this amplifier is that it operates with a certain initial plate current (second stage). Thus, the following advantages result: 1) a decrease in the effect of the curvature at the lower part of the plate current — grid bias characteristic of the second tube, and 2) compensation of the inherent error in the meter. The error of the instrument does not exceed 2-3% on the average. It is desirable to determine the number of revolutions to an accuracy of a few revolutions, and T — to an accuracy of seconds [Formula (2) can be modified readily], which practically eliminates errors in the determination of these parameters.

If the number of revolutions and period of observation are known, then from formula (2) it is easy to calculate the average current I_{el}. For convenience, a family of curves of $I_{el} = \varphi_1(n)$ (parameter T) may be plotted; in this case I_{el} may be computed directly from the corresponding T-curve.

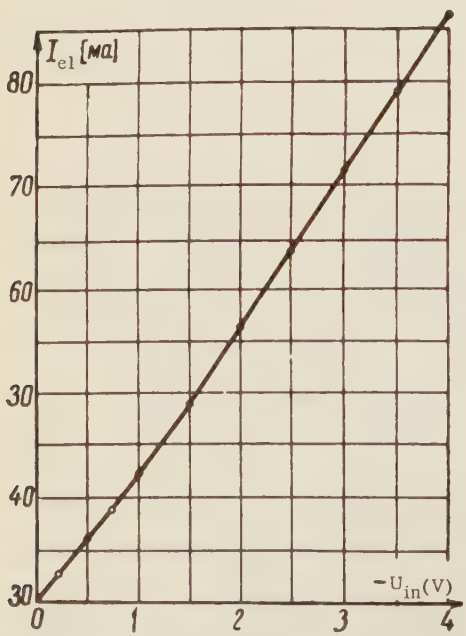

Figure 6

The receiver to which the instrument is connected is calibrated beforehand: the relation $E = \varphi_2(-U_{in})$ is known (E — is the field intensity at the receiving point). Therefore, the unknown average (and correspondingly, the median) value of the observation may be found in the following manner (Figure 8): calculate or read off the current $I_{el} = I_0$, then mark this value (I_0) on the ordinate of I_{el} and finally, follow the procedure indicated by the arrows in Figure 8. As a result, the unknown value E_0 may be read from the second ordinate (E).

In testing the instrument a series of observations were carried out at a frequency of 155 kc — Brashov radio transmitter (distance from receiving point — 380 km). For this purpose, a recorder was connected to the

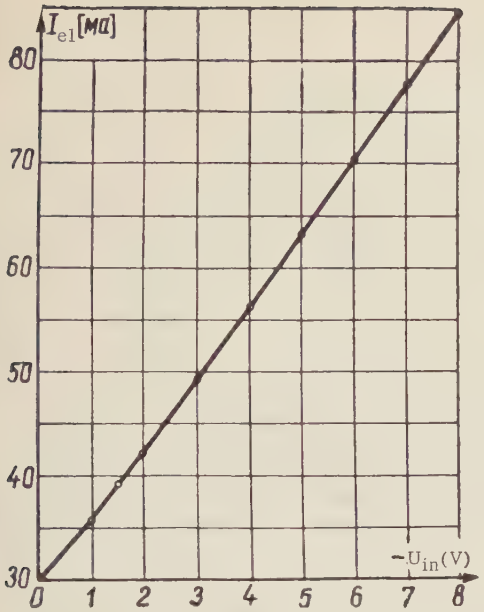

Figure 7

instrument. From the recorded data and usual methods of calculation, the corresponding median values were determined. The latter were compared with the average values indicated by the instrument. During the initial determination of median values, inaccuracies may be permitted since the recordings are frequently quite complex. Besides, it is difficult to reach exact conclusions regarding the law of distribution of the instantaneous values of field intensity for a limited number of observations. Of course, this was not one of the purposes of the trial tests. Nevertheless, on the basis of the values in Table 1 for relative difference between the average ($\bar{E}$) and median values (E_0), it may be stated, generally, that the observed distribution of the instantaneous values of field intensity at this wavelength is of the Gaussian type.

During observation No. 9, this distribution seems to approach the Rayleigh type, and for observations Nos. 8, 10 and 11, it is close to an m-type distribution. The inaccuracies in observations No. 6 and 12 can be explained by insufficient preliminary warmup of the instrument (these were initial observations). The tests, which were carried out on September 7, 1958, show that for different periods of observation, different distributions may be obtained.

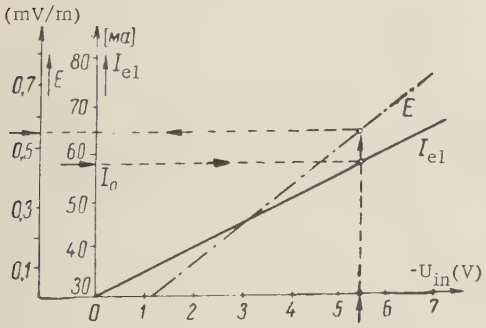

Figure 8

The instrument will operate satisfactorily up to a fading frequency of about 2 cps. As was reported at the MKK conference of 1953 in London, the fading frequency may reach 10 kc. However, this will not preclude the wide application of the described instrument since very rapid fading of this type is, in practice, of less significance in conventional statistical studies. Also, they are not reproduced by the recording inks of recording instruments which are commonly used for surveys on radio wave propagation.

The instrument has good operating qualities. Maintenance is also very simple. It is recommended that the recording apparatus be operated simultaneously with the instrument — to monitor the field, particularly in case

Table 1

Date	No.	Time (Eastern Europe)	$\bar{F}$ (mV/m)	F_0 (mV/m)	$\delta\bar{F}$ [%]
4/IX 1958	1	19^{00}—20^{00}	0.525	0.520	+0.95
•	2	20^{00}—21^{00}	0.650	0.640	+1.54
•	3	21^{00}—22^{00}	0.740	0.740	0
•	4	19^{00}—22^{00}	0.635	0.640	—0.79
6/IX 1958	5	19^{30}—22^{00}	0.810	0.810	0
7/IX 1958	6	20^{45}—21^{15}	1.780	1.900	—6.74
•	7	21^{15}—21^{45}	1.420	1.420	0
•	8	21^{45}—22^{17}	2.230	2.150	+3.59
•	9	21^{15}—22^{17}	1.910	1.800	+5.76
9/IX 1958	10	20^{15}—21^{25}	0.850	0.820	+3.53
10/IX 1958	11	19^{30}—23^{30}	1.040	1.000	+3.84
11/IX 1958	12	18^{00}—18^{30}	0.230	0.256	—11.30
•	13	18^{30}—19^{00}	0.445	0.440	+1.12
•	14	19^{30}—23^{00}	0.980	0.980	0

of ionospheric disturbances, and also for extracting additional useful information. A shortcoming of the instrument is that the determination of the median value (from the average) becomes impossible when the desired signal is lower than the noise level for a period of even less than 50% of the total period of observation, despite the fact that this value does exist in this case.

REFERENCES

1. M. P. Dolukhanov. Radio Wave Propagation. Svyaz'izdat, 1952.
2. Engineering and Technical Manual on Telecommunications, Vol. VIII. Radio Communications. Svyaz'izdat, 1958.
3. Scholz. Die ionospharische Ausbreitungsdampf ung der Hektometer-Wellen (550 - 1600 kHz), "NTZ," 1958. No. 1.
4. Gough. The analysis of field strength records for radio link assessment. "Point to point telecommunications," 1958, No. 6.
5. Grosskopf, Einige Bewerkungen zur Schwendanalyse im m — und dm—Bereich. "NTZ", 1958.
6. The VII Plenary Assembly of MKKP, Warsaw. Documents Nos. 76 and 330, 1956.

7. Betriebslaboratorium für Rundfunk und Fernsehen. Technischer Bericht, No. 234. Ministerium fur Post und Fernmeldewesen. DDR.

Received September 12, 1960

SYNTHESIS OF FILTERS WITH LINEAR PHASE CHARACTERISTICS

A.F. Beletskiy

Several methods for solving the problem of approximating the transfer functions of filters with linear characteristics as well as, in the general case, with given phase (shift) characteristics, are examined. It is assumed that the synthesized filter will be a reactive four-terminal network.

In recent years it has become increasingly necessary in communication engineering to use filters which, in a specific frequency band, have phase shift characteristics approaching linearity in one sense or another. [1]

The current article is devoted to the examination of several of a number of possible methods for synthesizing electric filters with linear phase characteristics by means of their operating parameters. It is assumed that the synthesized filter will take the form of a reactive four-terminal network.

The problem of synthesizing a filter of one of the various types to be discussed below shall be considered solved if the function expression the filter transfer function satisfies the conditions of the problem, as well as conditions for its physical realization. This implies that we shall examine all practicable methods for approximating the transfer function of filters with linear phase characteristics. In order to determine the appropriate circuits and values for the elements comprising the possible variants of these filters, we shall make use of the known methods for the synthesis of reactive four-terminal networks by means of a given transfer function.

---

[1] Henceforth, for the sake of simplicity, filters of this type will be referred to as filters with linear phase characteristics.

The results obtained below may also be broadened to include the synthesis of filters with nonlinear phase characteristics.

PHASE CHARACTERISTICS OF REACTIVE FOUR-TERMINAL NETWORKS

When a reactive four-terminal network is connected between purely resistive loads (Fig. 1), its effective propagation constant g, effective attenuation b, effective phase a and effective transfer function $S(i\omega)$ are related by the following relationship

$$g = b + i\,a = \ln S(i\omega), \tag{1}$$

where

$$S(i\omega) = \frac{\dot{E}}{2\dot{U}_2}\sqrt{\frac{R_2}{R_1}} = \frac{a_0(i\omega)^n + a_1(i\omega)^{n-1} + \ldots + a_n}{(i\omega)^m + b_1(i\omega)^{m-1} + \ldots + b_m}.$$

Let us recall [1, 2] the properties of the function

$$S(p) = \frac{a_0p^n + a_1p^{n-1} + \ldots + a_n}{p^m + b_1p^{m-1} + \ldots + b_m} = \frac{v(p)}{f(p)}. \tag{2}$$

Figure 1

The Hurwitz polynomial v(p) appears in its numerator, i.e. a polynomial, with real coefficients, all roots of which are found to be in the left hand p plane.

The denominator of the function is, in the general case, an even or odd polynomial f(p), all coefficients of which are also real. It should be noted that, in particular cases, the polynomials v(p) and f(p) in Eq. (2) may have a common multiplier $\psi(p)$. The latter, on the basis of the properties of the polynomial v(p), is the Hurwitz polynomial. Under these conditions the polynomial f(p) will be neither an odd nor an even one. However, it may always be reduced to one of these, without disturbing the properties of the function S(p), by multiplying its numerator and denominator by the Hurwitz polynomial $\psi(p)$.

Finally, with a change in p along the imaginary axis, i.e. with $p = i\omega$

$$|S(i\omega)| \geqslant 1. \tag{3}$$

The effective phase of a reactive four-terminal network is equal to

$$a = \arg[S(i\omega)] = \arg\left[\frac{v(i\omega)}{f(i\omega)}\right]. \tag{4}$$

Since $f(i\omega)$ can only be an even or odd polynomial, then it follows from the latter relationship that the effective phase of a four-terminal network will be determined — to an accuracy of the component $r\pi$, if $f(i\omega)$ is an even polynomial, or of the component $(r - 0.5)\pi$, if $f(i\omega)$ is an odd

polynomial — by the argument of the Hurwitz polynomial $v(i\omega)$, i.e. by the argument of the numerator of the polynomial $S(i\omega)$ [3]. Actually, as ω changes, the polynomial $f(i\omega)$ — which has either purely real values when $f(i\omega)$ is an even polynomial, or purely imaginary values when $f(i\omega)$ is an odd polynomial — may change in sign when real roots in odd multiples are present. A change in the sign of the polynomial also leads to a jump in phase by an angle of π radians. It should be noted that for each jump in phase there is a corresponding pole in the transfer function $S(i\omega)$ and a discontinuity in attenuation of the filter.

In accordance with the above statements

$$a = \operatorname{arc\,tg} \frac{1}{i} \frac{v(i\omega) - v(-i\omega)}{v(i\omega) + v(-i\omega)} + r\frac{\pi}{2}. \quad (5)$$

*

It is important to note that the poles of the function S(p) for a four-terminal network of the minimum-phase type may be located only on the imaginary axis of p, i.e. when $p = i\omega$, including the values $\omega = 0$ and $\omega = \infty$. This is a direct result of the even (odd) polynomial f(p) of the denominator in Eq. (2). Therefore, in reactive four-terminal networks of the minimum-phase type, if they are not polynomials or semi-polynomials [2], then jumps in phase are unavoidable.

In conclusion, it should be noted that if we substitute the inequality $|S(i\omega)| > 0$ for the inequality (3), then all of the above statements hold true not only for the effective phase of a reactive four-terminal network but also for phase shift in current, voltage and electromotive force.

POSSIBILITIES OF PRODUCING FILTERS WITH GIVEN PHASE AND ATTENUATION CHARACTERISTICS

In the general case, the number of variable parameters for the transfer function of a reactive four-terminal network, which is a rational function of type (2), does not exceed 1.5 n + 1 for even values of n, and 1.5 n + 0.5 for odd values of n.

For approximating a given relationship between filter phase and frequency, no more than n parameters should be used since the filter phase is determined by the polynomial $v(i\omega)$ of function (2). The given relationship between filter attenuation and frequency may be approximated by using all the variable parameters of this same function. In the latter case, the filter phase characteristic is not controlled, which is typical for standard methods of synthesizing filters on the basis of their operating parameters. In the general case for approximating a given relationship between filter attenuation and frequency, the number of variable parameters used may be equal to the difference between their total number and the number of parameters used for approximating the given relationship between filter phase and frequency.

If the conditions of the problem specify that phase distortions in the filter within the boundaries of its pass band must not exceed a certain permissible value, then these requirements may always be satisfied by using a Hurwitz polynomial v(p) of as low a degree as desired, beginning with n = 1, while the requirements for the relationship between attenuation and frequency may be fulfilled, usually, only by functions of the form

---

*tg = tangent (Transl.)

(2) of relatively high order. Consequently, a problem arises in regard to the determination of the most suitable relationship, between the number of variable parameters used for approximating the given relationships of filter phase and attenuation, which will result in a minimum number of elements in the given or selected filter structure. A similar problem arises in the general case when the given phase relationship of the filter within the boundaries of its passband is nonlinear.

In the above-indicated general treatment, the problem of systhesizing filters on the basis of the given requirements for their phase and attenuation characteristics is seldom solved analytically, with the exception, of course, of its simplest variants.

However, it is always possible to select a Hurwitz polynomial v(p) of sufficiently high degree so that the requirements in the relationship between phase and frequency of the filter in its passband will be satisfied.

By further selecting a corresponding polynomial f(p), the degree of which must not exceed the degree of the polynomial v(p), it is then possible to fulfill the requirements for the relationship between filter attenuation and frequency. At the same time, the filter phase characteristic, which was either found or selected in the initial stages, will remain unchanged.

The solution of the relationship between filter attenuation and frequency is a function of frequency of the form

$$b = \frac{1}{2} \ln \frac{v(i\omega)\, v(-i\omega)}{f(i\omega)\, f(-i\omega)} = \ln \frac{\sqrt{v(i\omega)\, v(-i\omega)}}{|f(i\omega)|} . \tag{6}$$

The resulting solution will not be an optimal one in the general case for reasons indicated above. A numerical determination of the loss in the number of filter elements is not possible, mostly because of the absence of an optimal solution of the problem. However, this loss will seldom be a significant factor if sufficiently rigid requirements are set for accuracy in reproducing the given relationship between phase and frequency.

The given phase-frequency characteristic may be approximated by again using a Hurwitz polynomial of the form

$$v(p) = v_0^{2q}(p). \tag{7}$$

Corresponding to this polynomial, we have

$$S(i\omega) = \frac{v_0^{2q}(i\omega)}{f(i\omega)} = \frac{[v_0(i\omega)\, v_0(-i\omega)]^q}{f(i\omega)} \left[\frac{v_0(i\omega)}{v_0(-i\omega)}\right]^q . \tag{8}$$

The product

$$V_0(\omega^2) = v_0(i\omega)\, v_0(-i\omega)$$

is, obviously, an even polynomial with real coefficients, where

$$V_0(\omega^2) > 0$$

for any real values of ω.

A transfer function of the form (8) will have a corresponding phase characteristic

$$a = 2q \operatorname{arc\,tg} \frac{1}{i} \frac{v_0(i\omega) - v_0(-i\omega)}{v_0(i\omega) + v_0(-i\omega)} + r\frac{\pi}{2}, \tag{9}$$

which differs from the phase characteristic of a network composed of uniform phase circuits only by the component $r\frac{\pi}{2}$.

The attenuation factor in this case may be determined from the function

$$b = \ln \frac{V_0^q(\omega^2)}{|f(i\omega)|}. \tag{10}$$

Here, $f(i\omega)$ represents the modulus of an even or odd polynomial, all coefficients of which are real.[2]

LOW FREQUENCY FILTERS WITH LINEAR PHASE CHARACTERISTICS AND WITH ISOEXTREME ATTENUATION CHARACTERISTICS IN THE ATTENUATION BAND

Let us solve the problem of synthesizing a low frequency filter in which:

a) the transfer function is expressed by a function of form (2);

b) in the frequency band $0 \leqslant \omega \leqslant \omega_{0c}$, either the deviation of the phase-frequency relationship from linearity, or the deviation in delay time, from a certain fixed value, does not exceed a value which is considered permissible;

c) the attenuation for $\omega = 0$ is equal to zero;

d) in the frequency band $\omega \geqslant \omega_{0b}$, the smallest attenuation values will occur when the remaining equal conditions are the maximum possible.

Proceeding to a solution of the problem, let us select a Hurwitz polynomial $v(p)$ of degree $n = 2l$, the phase characteristic of which satisfies condition (b) of the problem.

As a polynomial of this type we may use, for example, a Bessel polynomial [4, 5, 6] of a corresponding degree.

Then, in accordance with (6), the attenuation of the synthesized filter will be determined by the function

$$F(\omega^2) = \frac{f(i\omega)}{\sqrt{v(i\omega)\,v(-i\omega)}} = \frac{\beta_0\omega^{2r} + \beta_1\omega^{2r-2} + \ldots + 1}{\sqrt{\alpha_0\omega^{4r} + \alpha_1\omega^{4r-2} + \ldots + 1}}. \tag{11}$$

In this expression, the degree of the polynomial

$$f(i\omega) = \beta_0\omega^{2r} + \beta_1\omega^{2r-2} + \ldots + 1 \tag{12}$$

is taken as high as possible, which corresponds to the maximum possible number in the selected polynomial

$$V(\omega^2) = \alpha_0\omega^{4r} + \alpha_1\omega^{4r-2} + \ldots + 1 \tag{13}$$

---

[2] Filters with linear phase characteristics which correspond to the particular case when $q = 1$ are examined in reference [3].

of variable parameters which are used in approximating the attentuation characteristic of the filter. In addition, expression (11) is standardized so that condition (c) of the problem under examination will be satisfied.

It is also necessary that in the interval $\omega \geqslant \omega_{0b}$, the maximum deviation of function (11) from zero will be as small as possible.

Using methods employed in the theory of highest approximation of a function [2], we find that

$$F(\omega^2) = \frac{\cos \sum_{r=1}^{l} \arccos \dfrac{\omega^2 - \omega_{0b}^2 - \sqrt{(\omega_{0b}^2 + \rho_r^2 - \sigma_r^2)^2 + 4\rho_r^2\sigma_r^2}}{\sqrt{(\omega^2 + \rho_r^2 - \alpha_r^2)^2 + 4\rho_r^2\sigma_r^2}}}{\cos \sum_{r=1}^{l} \arccos \dfrac{-\omega_{0b}^2 - \sqrt{(\omega_{0b}^2 + \rho_r^2 - \sigma_r^2)^2 + 4\rho_r^2\sigma_r^2}}{\rho_r^2 + \sigma_r^2}}. \tag{14}$$

Here $(-\rho_r + i\sigma_r)$ are the roots of the polynomial v(p) with a positive imaginary component.

All null points of function (14) lie inside the interval of its least deviation from zero $\omega_{0b} \leqslant \omega \leqslant \infty$. Consequently, all discontinuities in the filter attenuation

$$b = -\ln |F(\omega^2)| \tag{15}$$

lie in the attenuation band of the filter, which condition is satisfied by a four-terminal network of a minimum-phase type. The total number of discontinuities in filter attenuation will be equal to the degree of the polynomial f(iω) with respect to the variable ω^2, i.e. equal to l.

From the latter relationships it follows that within the limits of the filter attenuation band

$$b > b_0 = \operatorname{ch} \sum_{r=1}^{l} \operatorname{Arch} \frac{\omega_{0b}^2 + \sqrt{(\omega_{0b}^2 + \rho_r^2 - \sigma_r^2)^2 + 4\rho_r^2\sigma_r^2}}{\rho_r^2 + \sigma_r^2}. \tag{16}$$

Here, the value of the guaranteed filter attenuation in its attenuation band b_0 corresponds to the sign of equality. This lowest value of filter attenuation passes at $l + 1$ frequencies, including the frequencies $\omega = \omega_{ob}$ and $\omega = \infty$.

In the frequency band $0 \leqslant \omega \leqslant \omega_{0b}$, the filter attenuation will increase monotonously from the value $b = 0$ to $b = b_0$, providing the polynomial v(p) is a Bessel polynomial. A similar type of change in filter attenuation within the limits of the indicated band is also characteristic for a number of other types of Hurwitz polynomials.

Figure 2 shows the dependence of filter attenuation and delay time on frequency, which was calculated by the method presented above for the particular case when $n = 6$ and $\omega_{0b} = 5$. In the example, a Bessel polynomial of sixth degree is used for the polynomial v(p).

For each given type of Hurwitz polynomial, it is possible to calculate the relationship between the guaranteed filter attenuation b_0 and the degree n of the polynomial, and the value of the limiting frequency of the guaranteed attenuation band ω_{0b}. This relationship, which was calculated by A.T. Lebedev using Bessel polynomials, is shown in Figure 3. The

---

*ch = cosh (Transl.)

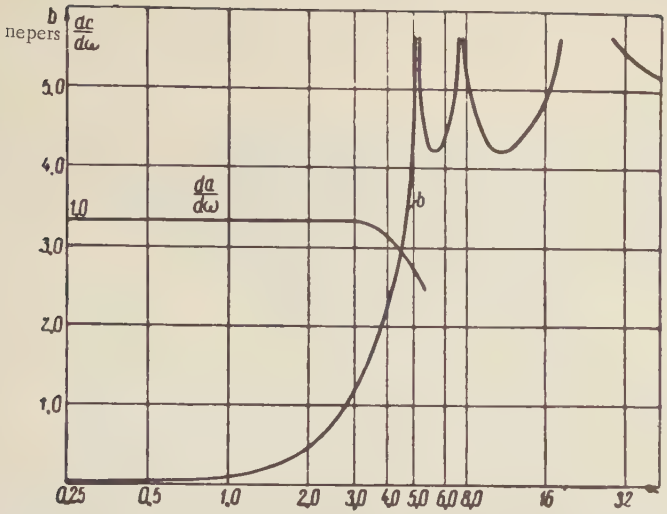

Figure 2

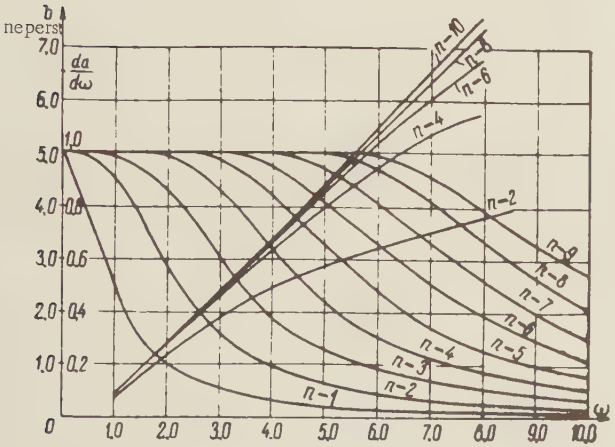

Figure 3

phase characteristics of filters in this case do not differ, with respect to the above considerations, from those expressed in Bessel polynomials. The corresponding relationship between delay time and frequency is shown in the same figure.

GRAPHICAL METHOD FOR CONSTRUCTING THE ATTENUATION CHARACTERISTICS OF FILTERS WITH GIVEN PHASE CHARACTERISTICS

Function (6) may be transformed into the form

$$b = \ln \frac{\sqrt{v(i\omega)\,v(-i\omega)}}{\left|\prod_{r=1}^{m} \omega_r^2\right|} + \sum_{r=1}^{m} \ln \frac{\left|\frac{\omega_r}{\omega}\right|}{\left|\frac{\omega}{\omega_r} - \frac{\omega_r}{\omega}\right|}. \qquad (17)$$

If ω_r are real numbers, then the relationship between frequency and any one of the components within the summation mark of the latter expression may be constructed on a logarithmic frequency scale by means of parallel transformation, using the same pattern in each case. The shape of the pattern is determined from the relationship

$$b_r = -(u + \ln 2 \operatorname{sh} |u|), \qquad (18)$$

where

$$u = \ln \left| \frac{\omega}{\omega_r} \right|.$$

The pattern is shown in Figure 4. the first component of (17) is determined, to an accuracy of the fixed component, by the polynomial $v(i\omega)$ which is initially selected in accordance with the requirements of the filter phase characteristic. The dependence of this component on frequency may be shown to the same scale as in (18).

By using the described pattern and changing the number and location of the attenuation discontinuity of the filter, it is then possible to fulfill the requirements of its attenuation characteristic in the stop band. In the pass band the attenuation characteristic for low-frequency filters will be similar to that shown in Figure 2.

Naturally, the described pattern is suitable for the construction of attenuation characteristics of band-pass filters as well as of low-frequency filters. In order to increase the attenuation of such filters in the low frequency region, it is permissible to insert the attenuation discontinuities

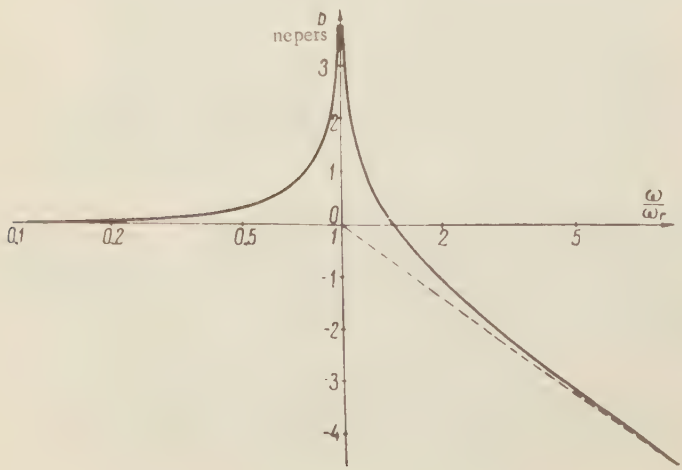

Figure 4

for ω 0. On a logarithmic frequency scale, for each such attenuation discontinuity of the filter there will be a corresponding straight line with a slope of 0.69 nepers per octave.

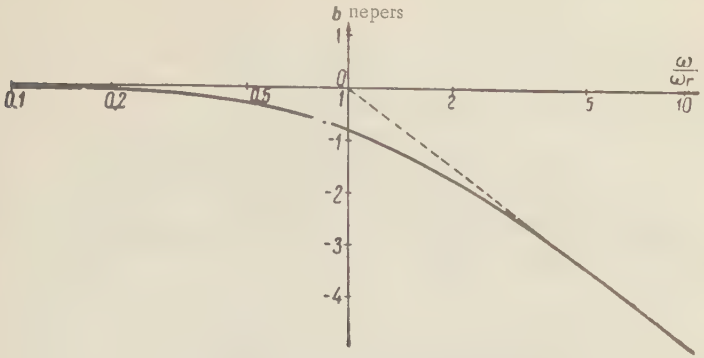

Figure 5

Amplitude distortions within the limits of the pass band of a low-frequency filter may be reduced if we permit the existence of imaginary roots in the plynomial f(iω). In this case, it is necessary to use a pattern in which

$$b_r = -(u + \ln 2 \operatorname{ch} u). \tag{19}$$

This pattern is shown in Figure 5.

CORRECTION OF FREQUENCY ATTENUATION CHARACTERISTICS OF FILTERS WITH LINEAR PHASE CHARACTERISTICS

In a number of cases, the attenuation characteristics for filters of the type examined above prove to be unsuitable because of significant amplitude distortions in the pass band.

In such cases, some of the variable parameters in the polynomial f(iω) of a function of the type given in (6) must be used to control the attenuation characteristics in the pass band. The latter causes, as a rule, the appearance in the plynomial f(iω) of roots outside of the real axis of the variable ω, and correspondingly, a transition to structures of the non-minimal phase type.

As yet, a rigorous solution of the problem, by methods employing the theory of highest approximation of the functions, has not been attained for the case of filters with linear phase characteristics and with isoextreme attenuation characteristics both in the stop band and in the pass band.

The attempt to use, in this case, solutions which are not optimal in a Chebyshev sense will, as calculations show, result in filters with an unrealistically high number of elements.

The simplest of all, for our purposes, is to equalize the attenuation characteristics of the filter in its pass band with the aid of these same functions of form (6). The values of their variable parameters may be determined most conveniently by the interpolation method. Then the transfer function of the filter with an equalized attenuation characteristic will be equal to the product of the transmission constants of the equalizer

network and of the original filter, which has an unequalized attenuation-frequency relationship in the pass band.

As an example, the solid lines in Figure 6 represent the attenuation

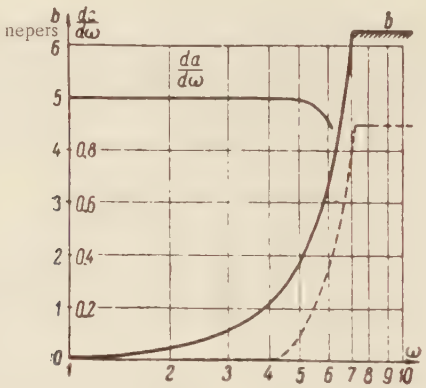

Figure 6

characteristic and delay time of a filter calculated by the above methods for the particular case when N = 8 and $\omega_{0b} = 7$. On the same graph, the dotted line represents the attenuation characteristic of the filter after its correction by means of the function

$$b_k = \ln \left| \frac{v_7\left(\frac{i\omega}{1,2}\right)}{a_0\omega^4 + a_1\omega^2 + a_2} \right|,$$

where $v_7(\frac{i\omega}{1,2})$ is a Bessel polynomial of seventh degree. The latter introduces practically no phase distortions in the given frequency band $0 \leqslant \omega \leqslant 5.2$.

REFERENCES

1. V.A. Taft. Principles of a Method for Calculating Linear Electrical Circuits by Their Given Frequency Characteristics. Izdat. AN SSSR, 1954.
2. A.F. Beletskiy. Theoretical Principles in Electric Wire Communications. Chapter III — Synthesis of Reactive Four-Terminal Networks and Electric Filters. Svaz'izdat, 1959.
3. Bennett. Synthesis of electric filters with arbitrary phase characteristics. "Convention Record of the IRE," part 5, 1953.
4. Frink Krall. A new class of orthogonal polynomials. The Bessel polynomials., Trans. of the American Math Soc., January, 1949, vol. 65, No. 1.
5. Thomson. Networks with maximaly — flat delay. Wireless Engineer, Oct. 1952, vol. 29, No. 349.
6. Storch. Synthesis of constant — time — delay ladder networks using Bessel polynomials. Proc. IRE, November, 1954, vol. 42, No. 11.

Received August 22, 1960

STRUCTURAL STABILITY OF A LINEAR FOUR-TERMINAL NETWORK

V.Z. Nayderov and Yu. L. Simonov

The basis for a method of increasing the stability of a linear four-terminal network by correcting its internal feedback is presented. A structure for the four-terminal network which is stable for any load on its terminals is shown to be attainable. [1]

One of the causes for operating instability in linear amplifiers is internal feedback in the amplifying element of the circuit (electron tube, transistor, etc.). In designing amplifiers, this feedback must be taken into account, or else its effect must be compensated for by additional external feedback (various neutralizing circuits).

The proof of one of the theorems on the stability of an active four-terminal network is given below.

Using a transistorized tuned amplifier as an example, a method for increasing the stability of linear amplifiers, based on the use of the proven theorem, is examined.

STABILITY OF A LINEAR FOUR-TERMINAL NETWORK

Theorem. A non-autonomous, active, linear four-terminal in which the transfer function is determined by the expression[2]

$$\frac{\dot{U}_2}{\dot{U}_1} = -\frac{Y_{21}}{Y_L + Y_{22}}, \qquad (1)$$

---

[1] Regarding the problem of stability of linear four-terminal networks, the editors propose to review the results of discussion on the article by A.A. Kulikovskiy (Elektrosvyaz' No. 12, 1959).

[2] This condition signifies that the phase shift between U_2 and U_1 equals 180°, if we ignore the additional phase shift introduced by the passive elements of the four-terminal network.

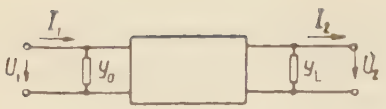

Figure 1

will be absolutely stable for any passive loads on its input and output terminals (Y_0 and Y_L) proviing it is stable when the input and output terminals are shortcircuited, and if the product of the characteristic conductances $Y_{12}Y_{21}$ are real numbers.

The physical processes in a non-autonomous linear four-terminal network (Figure 1) which satisfies condition (1) and which is loaded at the input and output terminals by the conductances Y_0 and Y_L, respectively, may be described by the following system of equations, written in matrix form

$$\begin{bmatrix} Y_{11} + Y_0 & Y_{12} \\ -Y_{21} & -(Y_{22} + Y_L) \end{bmatrix} \begin{bmatrix} \dot{U}_1 \\ \dot{U}_2 \end{bmatrix} = \begin{bmatrix} \dot{I}_1 \\ \dot{I}_2 \end{bmatrix}.$$

Here, $Y_{11} \ldots Y_{22}$ are the characteristic conductances of the four-terminal network.

In reference [1], it was shown that a four-terminal network will be absolutely stable if its amplitude-phase characteristic

$$\dot{\beta}\dot{K} = \frac{Y_{12}Y_{21}}{(Y_{11} + Y_0)(Y_{22} + Y_L)} = a + \mathrm{i}\, b \qquad (2)$$

does not encompass the point $\dot{\beta}\dot{K} = 1$.

Assuming:

$$Y_{11} + Y_0 = g_{11} + \mathrm{i}\, b_{11},\ -Y_{12} = g_{12} + \mathrm{i}\, b_{12},\ Y_{21} = g_{21} + \mathrm{i}\, b_{21},$$
$$Y_{22} + Y_L = g_{22} + \mathrm{i}\, b_{22},$$

considering that

$Y_{12}Y_{21} = \mathrm{Re}\,(Y_{12}Y_{21}) = -(g_{12}g_{21} - b_{12}b_{21})$, and separating the real and imaginary parts in (2), we obtain the following expression for a and b:

$$a = \frac{g_{21}|Y_{12}|^2(b_{11}b_{22} - g_{11}g_{22})}{g_{12}|Y_{11}Y_{22}|^2},$$
$$b = -\frac{g_{21}|Y_{12}|^2(b_{11}g_{22} + b_{22}g_{11})}{g_{12}|Y_{11}Y_{22}|^2}. \qquad (3)$$

The requirement for stability is met when $a < 1$ for $b \quad 0$; accordingly,

$$b_{11} = -b_{22}\frac{g_{11}}{g_{22}}. \qquad (4)$$

Substituting (4) in (3), we obtain

$$a = -\frac{g_{11}g_{21}}{g_{12}g_{22}}\left|\frac{Y_{12}}{Y_{11}}\right|^2. \qquad (5)$$

The right part of this equation is negative for any real values inserted in its terms; consequently, $a < 0$. The $\dot{\beta}\dot{K}$ diagram excludes not only the point $\dot{\beta}\dot{K} \quad 1$, but also the point $\dot{\beta}\dot{K} \quad 0$. The four-terminal network will be

stable with a sufficiently large stability margin for any values of Y_0 and Y_L.

In the particular case of a transistorized tuned amplifier, the proof of the theorem may be carried out on the basis of the stability conditions obtained in reference [4],

$$\frac{R_{0e}^2 [X_e (Y_{12}Y_{21})]^2}{(g_{22} R_{0e} + n_{out}^2)[|Y_{12}Y_{21}| + \mathrm{Re}(Y_{12}Y_{21})]} - 2g_{11}R_{0e} < 2n_{in}^2(1 - k_y).$$

Assuming in this inequality, in accordance with the theorem, that $X_e(Y_{12}Y_{21}) = 0$, it is easy to see that the tuned amplifier will be stable for any values of n_{in}, n_{out} and R_{0e}.

The proven characteristic may be used to increase the stability of linear amplifiers, for example, transistorized tuned amplifiers.

INCREASING THE STABILITY OF A TRANSISTORIZED SELECTIVE AMPLIFIER WITH A COMMON-EMITTER CIRCUIT CONNECTION

The characteristic conductances of a transistor in a common-emitter circuit are expressed most frequently in the following form [2]:

$$\begin{aligned} Y_{11} &= \frac{1}{r_{11}} + i\omega C_{11}, \\ -Y_{12} &= \frac{1}{r_{12}} + i\omega C_{12} = \frac{1}{r_{12}}(1 + i\omega\tau_{12}), \\ Y_{21} &= \frac{1}{r_{21} + i\omega L_{21}} = \frac{1}{r_{21}(1 + i\omega\tau_{21})}, \\ Y_{22} &= \frac{1}{r_{22}} + i\omega C_{22}, \end{aligned} \qquad (6)$$

where

$$\tau_{12} = r_{12}C_{12}, \quad \tau_{21} = \frac{L_{21}}{r_{21}}.$$

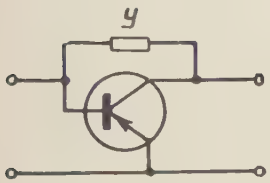

Figure 2

It is not difficult to show that, in this case, the condition $Y_{12}Y_{21} = \mathrm{Re}(Y_{12}Y_{21})$ takes the form

$$\tau_{12} = \tau_{21}. \qquad (7)$$

In order to achieve this, an additional passive conductance Y is connected to the transistor (Figure 2).

The matrix for this combination will be

$$[y] = \begin{bmatrix} Y_{11e} & Y_{12e} \\ -Y_{21e} & -Y_{22e} \end{bmatrix} = \begin{bmatrix} Y_{11} + Y & Y_{12} - Y \\ -Y_{21} + Y & -Y_{22} - Y \end{bmatrix}. \qquad (8)$$

The matrix elements in (8) may be written in a form analogous to (6):

$$Y_{11e} = Y_{11} + Y = \frac{1}{r_{11e}} + i\omega C_{11e}$$

$$-Y_{12e}=-Y_{12}+Y=\frac{1}{r_{12e}}+i\omega C_{12e}=\frac{1}{r_{12e}}(1+i\omega\tau_{12e})$$

$$Y_{21e}=Y_{21}-Y=\frac{1}{r_{21e}+i\omega L_{21e}}=\frac{1}{r_{21e}(1+i\omega\tau_{21e})},$$

$$Y_{22e}=Y_{22}+Y=\frac{1}{r_{22e}}+i\omega C_{22e} \qquad (9)$$

where

$$\tau_{12e}=r_{12e}C_{12e},\ \tau_{21e}=\frac{L_{21e}}{r_{21e}}.$$

For an equivalent four-terminal network, expression (7) may be rewritten in the following form:

$$\tau_{12e}=\tau_{21e}. \qquad (10)$$

Table 1 shows the relationships connecting the components of the characteristic conductances Y_{12e} and Y_{21e}, respectively, with the components of the conductances Y_{12} and Y_{21} for various forms of the conductance Y.

Table 1

	$Y=\frac{1}{R}$	$Y=\frac{1}{i\omega L}$	$Y=i\omega C$
r_{12e}	$\frac{r_{12}R}{r_{12}+R}$	r_{12}	r_{12}
τ_{12e}	$\frac{r_{12}C_{12}R}{r_{12}+R}$	$r_{12}\left(C_{12}-\frac{1}{\omega^2 L}\right)$	$r_{12}(C_{12}+C)$
r_{21e}	$r_{21}\left[1+\frac{1-\frac{r_{21}}{R}-\omega^2\tau_{21}^2\left(1+\frac{r_{21}}{R}\right)}{\frac{R}{r_{21}}+\frac{r_{21}}{R}-2+\frac{r_{21}}{R}\omega^2\tau_{21}^2}\right]$	$\frac{r_{21}}{\left(\frac{r_{21}}{\omega L}\right)^2+\left(\frac{r_{21}\tau_{21}}{L}-1\right)^2}$	$\frac{r_{21}}{(1+\omega^2 r_{21}\tau_{21}C)^2+\omega^2 r_{21}^2 C^2}$
τ_{21e}	$\frac{r_{21}}{1-\frac{r_{21}}{R}(1+\omega^2\tau_{21}^2)}$	$\tau_{21}-\frac{r_{21}}{\omega^2 L}(1+\omega^2\tau_{21}^2)$	$\tau_{21}+r_{21}C(1+\omega^2\tau_{21}^2)$

By substituting the values τ_{22e} and τ_{21e} from the table into (10), it is easy to obtain the following expressions which connect R, L and C with the parameters of the triode frequency:

$$R=\frac{1+C_{12}\frac{r_{21}}{\tau_{21}}(1+\omega^2\tau_{21}^2)}{\frac{\tau_{12}}{\tau_{21}}-1}r_{12}\quad(\text{for }\tau_{12}>\tau_{21}),$$

$$L = \frac{1 - \frac{r_{21}}{r_{12}}(1 + \omega^2 \tau_{21}^2)}{\omega^2\left(C_{12} + C_L - \frac{\tau_{21}}{r_{12}}\right)}, \quad (\text{for } \tau_{12} > \tau_{21}),$$

$$C = C_{12}\frac{\frac{\tau_{21}}{\tau_{12}} - 1}{1 - \frac{r_{21}}{r_{12}}(1 + \omega^2 \tau_{21}^2)} \quad (\text{for } \tau_{21} > \tau_{12}), \tag{11}$$

where C_L — is the self-capacitance of the inductance L.

Calculations show that in the frequency band where it is usually necessary to pay particular attention to increasing the stability of selective amplifiers, the following inequalities must be adequately fulfilled:

$$C_{12}\frac{r_{21}}{\tau_{21}}(1 + \omega^2 \tau_{21}^2) \ll 1, \quad \frac{r_{21}}{r_{12}}(1 + \omega^2 \tau_{21}^2) \ll 1. \tag{12}$$

then

$$R = \frac{\tau_{21}}{C_{12} - \frac{\tau_{21}}{r_{12}}}, \quad L = \frac{1}{\omega^2\left(C_{12} + C_L - \frac{\tau_{21}}{r_{12}}\right)}, \quad C = C_{12}\left(\frac{\tau_{21}}{\tau_{12}} - 1\right). \tag{13}$$

As is obvious from (8) and (9), when a resistance R is used as the element for increasing the stability, the triode output resistance R_{out} may decrease considerably because of the increase in Y_{22e} in comparison with Y_{22}. This leads to an undesirable shunting of the oscillatory loop in the collector circuit. Therefore, an inductance should be used in place of the resistance.

However, from constructive considerations for $\tau_{12} > \tau_{21}$, it is more expedient to use capacitance instead of inductance as the element for increasing the stability. To facilitate this substitution, the amplifier circuit should include a phase-inverting autotransformer or transformer(Fig. 3).

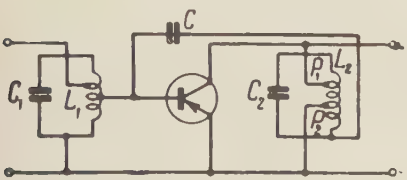

Figure 3

It is not difficult to show that the equivalent characteristic conductances of this circuit may be determined from the following relationships:

$$Y_{12e} = Y_{12} + i\omega \frac{p_2}{p_1} C,$$

$$Y_{21e} = Y_{21} + i\omega \frac{P_2}{P_1} C,$$

where p_1 and p_2 — are the coefficients for the oscillatory circuits connected into the collector and base circuits, respectively.

Determining, from this, the expressions for τ_{12e} and τ_{21e}, as was done in (9), and substituting them in (6), we find the following formula for the capacitance C:

$$C = C_{12}\frac{p_1}{p_2}\frac{1 - \frac{\tau_{21}}{\tau_{12}}}{1 - \frac{r_{21}}{r_{12}}(1 + \omega^2 \tau_{21}^2)}.$$

This formula may be simplified if we disregard the small terms in accordance with (12).

We have

$$C = C_{12}\frac{p_1}{p_2}\left(1 - \frac{\tau_{21}}{\tau_{12}}\right). \tag{14}$$

The circuit of Fig. 3 is analogous to an amplifier circuit with neutralization of the y - type, but the value of the capacitance, determined from (14), is lower than that calculated by formula (11) in reference [3] by the magnitude

$$C_{12}\frac{p_1}{p_2}\frac{\tau_{21}}{\tau_{12}}.$$

Thus, the circuit (Fig. 3) may be used successfully in place of a neutralizing circuit of the y - type in which the neutralizing network is composed of resistors and condensers. A substitution of this type is feasible only with weak coupling between the triode and the input and output oscillatory circuits, or with relatively low Q - factors for these circuits, since such shortcomings as interaction between the tuning circuits have not been completely eliminated.

EXPERIMENTAL RESULTS

The experimental verification of the theorem which was proved above was carried out on a tuned amplifier (Figure 4).

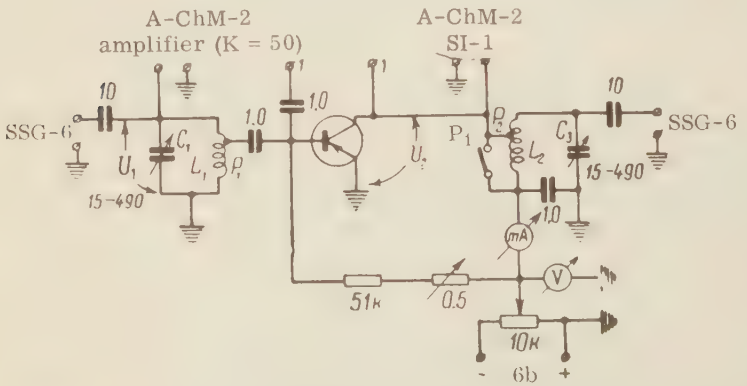

Figure 4

The circuit makes it possible to carry out measurements of: a) the resonance amplification factor by the voltage $K_0 = \frac{U_2}{U_1}$, b) the stability factor $k_y = \frac{U_1}{U_1'}$. (Here U_1 — is the resonant voltage across the L_1C_1 circuit with connection P_1 closed; U_1' — is the maximum resonant voltage across the same circuit with connection P_1 open and a corresponding

detuning of the L_2, C_2 circuit), c) the bandwidth for each of the oscillatory circuits.

The following types of transistors were used in the circuit: P-15 (frequency range 100-300 kc), P-403 and P-405 (frequency range 1-5 Mc).

In all of the measurements, the values for the connection coefficients p_1 and p_2 were selected so that the frequency bands passed by the oscillatory circuits would be approximately equal to each other. The measurement results for k_y and K_0 for the P-15 triode are shown in Figure 5).

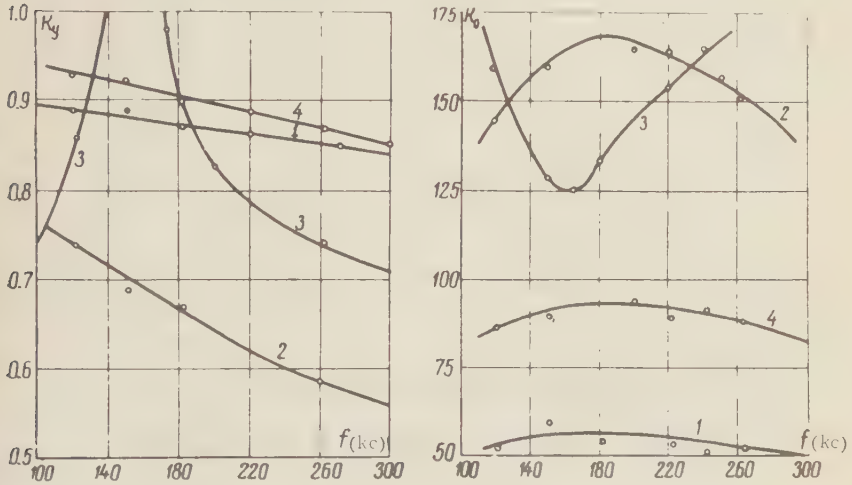

Figure 5

The numeration of the curves corresponds to the cases: 1) Regular amplifier ($p_1 = 0.012$, $p_2 = 0.2$). 2) Regular amplifier ($p_1 = 0.025$, $p_2 = 0.38$). 3) Amplifier with increased stability. An inductance L, calculated by formula (13) for a frequency of 150 kc, was connected across the terminals 1 - 1 ($p_1 = 0.025$, $p_2 = 0.38$, L = 24.6 Mc [sic]). 4) Amplifier with increased stability. A resistance R, calculated by formula (13), was connected across the terminals 1 - 1 ($p_1 = 0.038$, $p_2 = 0.25$, R = 36 kohms).

From an examination of the graphs, it may be concluded that the proposed method for increasing the stability permits a substantial gain in amplification of tuned amplifiers without decreasing the stability margin: in this connection, the use of an inductance L permits an increase in stability in a narrow frequency band, whereas a resistor R serves the same purpose in a wide frequency band. Similar results were obtained with the triodes P-403 and P-405.

REFERENCES

1. G. Bode. Theory of Circuits and Design of Amplifiers with Feedback. IIL [Foreign Literature Press], 1948.
2. K.A. Shul'gin. Equivalent Circuits and a System of Parameters for Semi-conductor Triodes. Gosenergoizdat, 1958.
3. Yu. L. Simonov. Neutralization of Transistorized Tuned Amplifiers. Electrosvyaz' No. 6, 1959.

4. Ye. F. Vorob'yeva. Stability of Tuned Amplifiers with Junction Transistors Connected in Common-Emitter and Common-Base Configurations. Radiotekhnika No. 6, 1959.

Received February 27, 1960

USING TRANSISTORS A QUARTZ MASTER OSCILLATOR

S. L Kunina

A master oscillator using a P-403 transistor and a quartz crystal between collector and base is investigated in the 0.75 to 5 Mc frequency band. The effects of operating conditions and circuit parameters on frequency instability during changes in temperature and line voltage are studied. An engineering method is developed for carrying out calculations on the master oscillator.

INTRODUCTION

In references [1-3], which were devoted to an investigation of crystal oscillators with junction-type semiconductor triodes (PPT), the results of measurements of frequency instability were obtained for circuits with the crystal inserted between collector and base. Expressions were worked out for calculating amplitude and frequency of auto-oscillations at the limits of the self-excitation region. However, none of these references presents a detailed investigation of frequency instability under steady-state conditions, or recommendations in regard to the selection of operating conditions and circuit parameters.

The purpose of our work was to investigate the properties of a transistorized master oscillator, with a crystal connected between collector and

base (Fig. 1), at frequencies of $f \leqslant 0.05\, f_\alpha$[1] (where the inertial effects of the transistor on the operation of the oscillator are small), to study the effects of operating conditions and circuit parameters on frequency instability, and finally, to develop methods for engineering design which take frequency instability into account.

For analogous oscillator circuits using electron tubes, similar problems were solved by V.P. Zhukhovitskay in references [4, 5]. In our work, the analytical method developed in [4, 5] was used, taking into consideration the properties of the static characteristics and high-frequency parameters of the transistor.

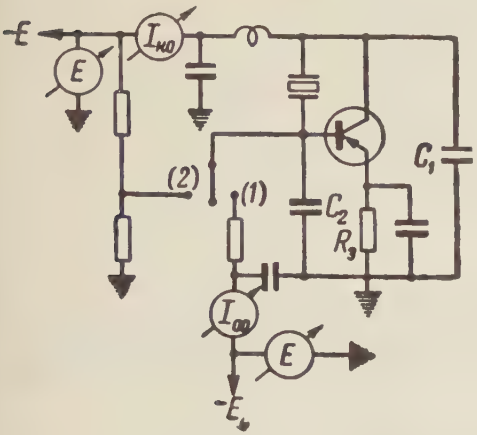

Figure 1

The design relationships were obtained in a system of Y-parameters for a common emitter circuit.

These investigations were carried out with the use of a fragmented-line approximation for the static collector current characteristic, fragmented-parabolic approximation for the base current characteristic [6] and, in addition, the following expressions were used for the relationships between the admittances and parameters of the triode [7]:

$$\dot{Y}_{11} = \dot{S}_0 \approx S_0 + i\omega C_{0e} \quad (1)$$

$$\dot{Y}_{22} \approx i\omega C_{ke} \quad (2)$$

$$\dot{Y}_{21} = \dot{S} = S e^{i\varphi_s}. \quad (3)$$

Here, C_{0e} and C_{ke} are the input and output capacitances of the triode, S_0 — the input conductance, S, φ_s — the modulus and phase, respectively, of the collector current characteristic.

We did not obtain an expression for the admittance Y_{12}, nor have we in Eq. (2) taken into account the active component of the output conductance g_{ke}. This is explained by the fact that for $f \leqslant 0.05\, f_\alpha$, under oscillating conditions (with a small load resistance), the effects of Y_{12} and g_{ke} on conditions and frequency of self-oscillations are very small [7].

At frequencies of $f \leqslant 0.05\, f_\alpha$, the phase φ_s of the characteristic is usually small and Eq. (3) may be replaced by the following approximation:

$$\dot{Y}_{21} = \dot{S} \approx S(1 + i\varphi_s). \quad (4)$$

---

[1] f_α — is the frequency at which the modulus of the current transfer factor of the triode in a common-base configuration will drop $\sqrt{2}$ times.

The parameters of the triode C_{ke}, C_{0e}, S_0, S and ω_s depend on frequency, collector voltages E_k, current I_k and temperature t°.

At any frequency (when $f \leq 0.05 f_\alpha$) the expressions (1-4) may be used for analyzing the processes in master oscillators not only at the threshold of self-oscillations, i.e. when the fundamental voltage $U_0 \to 0$, but also for investigating stationary conditions with high amplitudes for U_0 and cutoff of collector current. The difference is only in the method used to determine the transistor parameters. In the first place, at any frequency for each of the values E_k, I_k and t°, the local parameters C_{ke}, C_{0e}, S_0, S, and ω_s may be measured for amplitudes $U_0 \to 0$. However, when investigating stationary conditions, quasi-linear (average) values of the parameters C_{ke1}, C_{0e1}, S_{01}, S_1 and ω_{s1}, may be calculated for each frequency and temperature in relationship to C_{ke}, C_{0e}, S_0, S, ω_s (E_k, I_k) by an approximate method presented in reference [8].

The capacitances C_{ke1} and C_{0e1}, which are connected in parallel with the capacitances C_1 and C_2 of the circuit (Fig. 1), are for convenience considered to be part of C_1 and C_2. Then, in analyzing stationary conditions of the oscillator, it is sufficient to take into account only the following triode conductances:

$$\dot{Y}_{11\,1} = \dot{S}_{01} \approx S_{01}, \tag{5}$$

$$\dot{Y}_{21\,1} = \dot{S}_1 \approx S_1 (1 + i\varphi_{s1}). \tag{6}$$

In accordance with [8], S_1 and S_{01} are also calculated as average plate and grid current transconductances of tube [9]. In using the approximations, the characteristics S_1 and S_{01} are determined from the expressions in [8]:

$$S_1 = S\gamma_1(\theta), \tag{7}$$

$$S_{01} = aU_0\gamma_1^{(2)}(\theta_0). \tag{8}$$

Here, a — is the coefficient of the parabola approximating the base current characteristic; θ, θ_0 — are the angles of cutoff of the collector and base current (usually in semiconductor oscillators $\theta \approx \theta_0$ [6]; $\gamma_1(\theta)$, $\gamma_1^{(1,2)}(\theta)$ — are the resolution factors for a cosinusoidal pulse of the first harmonic with line-fragment and parabolic-fragment approximation of the characteristics. In reference [6] tables are given of the values of $\gamma_1^{(2)}(\theta)$ and $\gamma_0^{(2)}(\theta)$[2] for various θ.

The expression for calculating the phases of the quasi-linear transconductance ω_{s1} was not worked out by us since research shows that for $f \leq 0.05 f_\alpha$ this factor has no influence on oscillator operation. The method for calculating the changes in ω_{s1} due to changes in temperature and supply voltage, which affects frequency instability, will be discussed below.

---

[2] $\gamma_0^{(2)}(\theta)$ — is the resolution factor for a cosinusoidal pulse with reference to a fixed component with parabolic approximation of the characteristics, which is necessary in designing the oscillator base circuits.

DESIGN RELATIONSHIPS IN STATIC CONDITIONS

The design relationships for static conditions were obtained by the method of symbolic reduction of equations, developed by S.I. Yevtyanov [10]. In order that the effect of base current of a suitable oscillator (Fig. 1) is properly considered in these reduced equations, the analogous electron tube oscillator used for calculating grid current in reference [9] should be replaced by a generalized equivalent circuit (Figure 2).

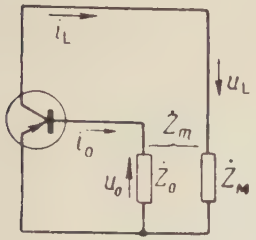

Figure 2

The processes occurring in the circuit of Fig. 2, taking into account the accepted symbols, may be expressed by the following symbolic equations

$$u_0 = \dot{Z}_m \left(i_к - \frac{\dot{Z}_0}{\dot{Z}_m} i_b \right). \tag{9}$$

The impedances $\dot{Z}_m$ and $\dot{Z}_0$ of the circuit in Fig. 2 are related to the impedances of Fig. 1 by the following expressions [11].

$$\dot{Z}_m = -\frac{\dot{Z}_1 Z_2}{\dot{Z}_1 + \dot{Z}_2 + \dot{Z}_{qu}}; \quad \dot{Z}_0 = \frac{\dot{Z}_2 (\dot{Z}_1 + \dot{Z}_{qu})}{\dot{Z}_1 + \dot{Z}_2 + Z_{qu}}. \tag{10}$$

Here

$$\dot{Z}_{qu} = \frac{r_к (1 + i\nu)}{1 + i\tau_0 (1 + i\nu)} - \tag{11}$$

is the impedance of the crystal;

$$\dot{Z}_1 \approx \frac{1}{i\omega_к C_1}; \quad \dot{Z}_2 \approx \frac{1}{i\omega_к C_2} - \tag{12}$$

the reactive part of the circuit (Figure 2).

In Equation (11) and (12), the following symbols are used:

$\nu = 2Q_к \left[\frac{\omega}{\omega_к} - 1 \right]$ — is the generalized detuning of crystal relative to the frequency of its series resonance ω_k [5], ω, ω_k, and Q_k — are, respectively, the frequency of the generated oscillations, the series resonance frequency of the crystal, and the crystal Q - factor; r_k — is the resistance of the dynamic part of the crystal [9]; $\tau_0 = \omega_k r_k C_0$ — is the crystal parameter, taking into account the effect of its static capacitance C_0.

In expression (12) it was considered that the difference between the frequencies of self-oscillations ω and of the quartz ω_k may be neglected.

Substituting (11) and (12) in (10), and then the latter result in (9). we obtain the following reduced equation showing the relationship between the complex amplitudes of the first harmonics of the collector current $\dot{I}_{k1}$ and base current $\dot{I}_{01}$ with the amplitude of the base voltage $\dot{U}_0$.

$$\dot{U}_0 = \frac{R\tau_L}{(\tau_L + \tau_0)(1 + i\nu) - i} \{\dot{I}_{k1}[1 + i\tau_0(1 + i\nu)] + \dot{I}_{01}[1 + i(\tau_0 + \tau_L + \tau_L K_0)(1 + i\nu)]\}. \quad (13)$$

Here $R = \frac{X_1 X_2}{r_k}$ — is the control resistance of the oscillator at a frequency ω_k without considering the capacitance C_0: $\tau_L = \omega_k r_k C_L$ — is the parameter expressing the effect of the circuit-switching capacitance; $C_L = \frac{C_1 C_2}{C_1 + C_2}$ is the total capacitance of the circuit; $K_0 = \frac{C_1}{C_2}$ — is the circuit capacitances.

The expressions for calculating the amplitudes and frequencies of the oscillations under stationary conditions may be obtained from (13) if we adjust both parts of it separately into real and imaginary components. At the same time, it is necessary to take into account, by analogy with a tube oscillator [9], that

$$\frac{\dot{I}_{k1}}{\dot{U}_0} = \dot{S}_1; \quad \frac{\dot{I}_{01}}{\dot{U}_0} = \dot{S}_{01}, \quad (14)$$

where $\dot{S}_1$ and $\dot{S}_{01}$ — are the complex, quasi-linear transconductances of currents in the collector (6) and base (5).

With the above considerations, the following expressions were obtained for calculating the frequency and amplitude of oscillations in a stationary state:

$$\tau_L = \frac{[(1 - \tau_0\nu)^2 + \tau_0^2]B + \{\varphi_{s1}[\nu(1 - \tau_0\nu) - \tau_0] + B\} S_{0L}}{[\nu(1 - \tau_0\nu) - \tau_0]B - \varphi_{s1}}, \quad (15)$$

$$S_1 R_y \left(1 - \varkappa \frac{S_{01}}{S_1}\right) = 1, \quad (16)$$

where $S_{0L} = S_{01} r_k \frac{K_0}{1 + K_0}$ — is the normalized base current curve; $B = 1 + \frac{S_{01}}{S_1}$ — is the coefficient which takes into account the base current

$$R_y = R[(1 - \tau_0\nu)^2 + \tau_0^2] - \quad (17)$$

is the controlling resistance of the oscillator

$$\varkappa = \tau_L(1 + K_0) \frac{\nu(1 - \tau_0\nu) - \tau_0}{(1 - \tau_0\nu)^2 + \tau_0^2} - \quad (18)$$

— is the transmission factor, taking into account the effect of base current on the oscillation amplitude under stationary conditions.

From (15) it may be seen that there are two values of generating frequency ν for each value of circuit capacitance C_L (or τ_L). The investigation of stability in reference [12] shows that under "soft" operating conditions

(operation with self-bias), for each value of C_L (τ_L) there will be created and sustained an oscillation at the lower of the two frequencies v determined from Eq. (15).

A detailed study of (15) and (16) also shows that in master oscillators using PPT (junction transistors), in which the collector current transconductance characteristic S is the order of hundreds of ma/v, stable stationary conditions will be obtained with large circuit capacitances. In addition, the following condition is fulfilled:

$$\tau_L \gg \tau_0;\ \nu \gg \tau_0. \tag{19}$$

Besides, in the frequency band under examination, usually

$$\tau_0 \ll 1 \tag{20}$$

and, in the conditions recommended below, the following relationship is fulfilled

$$\frac{S_{01}}{S_1} \ll 1. \tag{21}$$

Considering (19) - (21), we obtain from (15) - (17) the following approximate expressions for calculating the parameters of circuits under stationary conditions:

$$SR_y = G, \tag{22}$$

$$C_1 = 530\lambda\sqrt{\frac{K_0}{R_y r_k}};\quad C_2 = \frac{C_1}{K_0}, \tag{23}$$

where λ — is the wavelength of the self-oscillations, $G = \frac{1}{\gamma_1(\theta)}$ — is the regenerative factor.

With known parameters for the triode and crystal, the following order of calculations of the oscillator is recommended: select a regenerative factor $G > 1$ and determine from (22) the required value R_y. Next, a value should be assigned to K_0 and the capacitances C_1 and C_2 should be calculated by formula (23). Then it is necessary to select the initial data for determining the operating conditions — collector voltage E_k and the static component of the collector current I_{k0}. This method of calculation is similar to the calculations for the tube oscillator in reference [9] and described in [6].

Information on a rational selection of G, K_0, E_k and I_{k0} are given below on the basis of investigations of frequency instability.

METHODS FOR INVESTIGATING FREQUENCY INSTABILITY

Frequency instability due to temperature variations is caused by changes in the parameters of the transistor, circuit, and crystal, whereas frequency instability due to variations in line voltage is caused by changes in the parameters of the transistor and by the power dissipated in the crystal.

From (15), the following expressions were obtained for calculating the components of frequency instability caused by changes in:

a) output capacitance of the transistor

$$\frac{\Delta f}{f}(C_{ke}) = -\frac{1}{2Q_k r_k C_1^2 \omega_k}\Delta C_{ke1}, \tag{24}$$

b) input capacitance and conductance (base current transconductances)

$$\frac{\Delta f}{f}(C_{0e}) = -\frac{1}{2Q_k r_k C_2^2 \omega_k}\Delta C_{0e1};\quad \frac{\Delta f}{f}(S_0) = \frac{1}{2Q_k \omega_k C_2}\Delta S_{01}, \tag{25}$$

c) phases of collector current transconductance

$$\frac{\Delta f}{f}(\varphi_{s1}) = \frac{1}{2Q_k}\Delta\varphi_{s1}, \tag{26}$$

d) capacitances C_1 and C_2 of the circuit

$$\frac{\Delta f}{f}(C_1) = -\frac{1}{2Q_k r_k C_1 \omega_k}\cdot\frac{\Delta C_1}{C_1};\quad \frac{\Delta f}{f}(C_2) = -\frac{1}{2Q_k r_k C_2 \omega_k}\frac{\Delta C_2}{C_2}, \tag{27}$$

e) static capacitance and resistance of the dynamic branch of the crystal

$$\frac{\Delta f}{f}(C_0) = -\frac{C_0}{2Q_k r_k C_L^2 \omega_k}\frac{\Delta C_0}{C_0};\quad \frac{\Delta f}{f}(r_k) = \frac{\omega_k r_k C_0}{2Q_k}\frac{\Delta r_k}{r_k}. \tag{28}$$

The expression for calculating the instability components caused by changes in power dissipated by the crystal ΔP_{qu} was obtained by the method described in [5] and has the form

$$\frac{\Delta f}{f}(P_{qu}) \approx \frac{TKF_{qu}}{K_{qu}}\frac{I_{k0}^2[g_1(\theta)]^2}{K_0 S_1}\frac{\Delta I_{k0}}{I_{k0}}, \tag{29}$$

where TKF_{qu}, K_{qu} – are the frequency temperature coefficient and the heat emission coefficient of the crystal: according to data in [13] for non-vacuum type crystals $K_{qu} \approx 10^{-2}$ wt/deg; $g_1(\theta)$ – is the form factor for a cosinusoidal pulse with line-segment approximation of the characteristic.

An analysis of the resulting expressions shows that the instability component $\frac{\Delta f}{f}(\varphi_s)$ does not depend on the capacitances C_1 and C_2, and the components

$$\frac{\Delta f}{f}(C_{ke}),\quad \frac{\Delta f}{f}(C_{0e}),\quad \frac{\Delta f}{f}(S_0),\quad \frac{\Delta f}{f}(C_1),\quad \frac{\Delta f}{f}(C_2)$$

decrease as C_1 and C_2 increase.

In agreement with (23), with other conditions equal, the capacitances C_1 and C_2 increase with decrease in R_v, that is, with a decrease in the regeneration factor G (22). In addition, when G decreases, the instability factor $\frac{\Delta f}{f}(P_{qu}$ also decreases (29) since the angle of collector current cutoff increases and, correspondingly, $g_1(\theta)$ drops and S_1 builds up [9], while the ratio $\frac{\Delta I_{k0}}{I_{k0}}$, as investigations show, hardly changes during

variations of G within wide limits. Therefore, during the calculations, it is desirable to select small values for G. However, in view of the dispersion in transistor parameters and also possible fluctuations in line voltage, it is recommended that the selection of G be made in the range G = 2-4.

Recommendations on the selection of K_0, E_k, I_{k0} may be worked out after a preliminary clarification of their effect on the frequency instability arising from changes in temperature and line voltage.

The investigations of instability was carried out by calculation and experiment on an oscillator using a P-403 transistor ($f_\alpha \geqslant 100$ Mc) at frequencies of f = 0.75, 2 and 5 Mc with operation in an undervoltage condition. Preliminary measurements showed that for an overvoltage condition the frequency instability rises sharply.

The experimental oscillator was designed in accordance with the circuit in Fig. 1 Provision was made for two methods of supplying power to the base: from a separate source (1) and from the collector voltage supply (2).

The calculations of the instability components with changes in temperature and supply voltage were carried out by the formulas obtained above. The resultant instability was calculated as the sum of the separate components and verified experimentally.

The current I_{k0} varies with changes in temperature and supply voltage. The increments in current ΔI_{k0} caused by changes in temperature or supply voltage, which are necessary in calculating instability, may be measured by the instrument I_{k0} in the circuit of Fig. 1.

In calculating the instability components under stationary operating conditions, it is necessary to determine ΔC_{ke1}, ΔC_{0e1}, ΔS_{01}, $\Delta \varphi_{s1}$, which depend on changes in temperature or supply voltage and the increments in current ΔI_{k0} created by them, with high amplitudes of voltage U_0 and cutoff of collector current (changes in the quasi-linear parameters of the transistor). The approximate calculation method in [8] does not permit a determination of changes in the quasi-linear parameters for low-level oscillations E_k, I_k and t°. Therefore, the changes in transistor parameters, which are essential in calculating instability, were determined from experimental relationships of C_{ke}, C_{0e}, S_0, φ_s (E_k, I_k, t°), obtained for $U_0 \to 0$ with the assumptions taken in reference [7]. These assumptions lead to the hypothesis that the relationships of C_{ke}, C_{0e}, S_0, φ_s (E_k, I_k, t°), obtained for $U_0 \to 0$ also hold true for high amplitudes if the current at the operating point with $U_0 \to 0$ is replaced by the fixed component of the collector current under stationary conditions. As in [7], experimental verification (Fig. 4, 5) showed that under these assumptions the calculated and experimental results conformed to a sufficient degree.

Fig. 3 shows the experimental relations between C_{ke} (E_k, I_k, t°), and C_{0e}, S_0, φ_s (I_k, t°) for the P-403 triode at f = 2 Mc. The dependence of C_{0e}, S_0, φ_s on E_k was expressed somewhat weakly and, therefore, is not shown in Fig. 3. The measurements of the transistor parameters at frequencies of f = 0.75 Mc and f = 5 Mc show that the nature of the indicated relationships are maintained, although the absolute values of the parameters vary.

At all frequencies, with known variations in temperature or supply voltages, known increments of current ΔI_{k0} and experimental relationships between C_{ke} (E_k, I_k, t°) and C_{oe}, S_0, φ_s (I_k, t°), ΔC_{ke}, ΔC_{0e}, ΔS_0, $\Delta \varphi_s$ were determined and both the component as well as resultant instabilities were calculated.

During the experimental verifications the resultant frequency instability

was measured directly.

In reference [7] it was shown that with no change in E_k and I_{k0} and an increase in the self-bias resistor R_e[3] in the emitter circuit (Figure 1), the

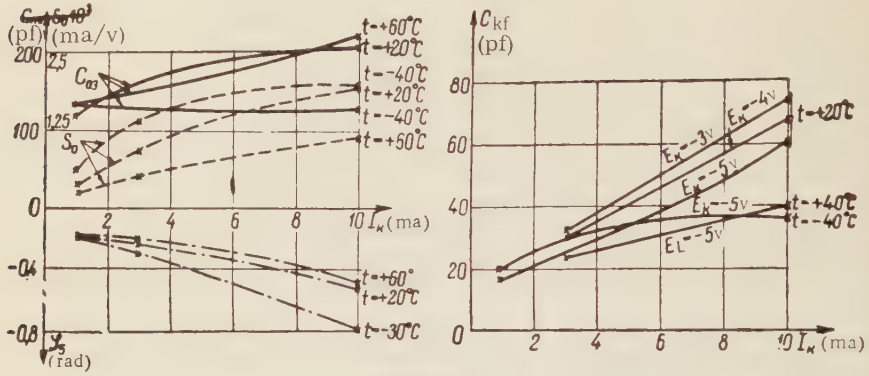

Figure 3

ΔI_{k0} decrease due to a change in the temperature or supply voltage. Thus, with an increase in R_e, the frequency instability due to supply voltage variations will decrease. The temperature instability of frequency in an oscillator with a drift transistor is determined basically by the changes in phase of the transconductance from temperature and the resulting increments in current ΔI_{k0} [7]. To lessen this instability it is not expedient to select a much larger R_e. The difficulty is that with an increase in temperature, I_{k0} starts to rise. In drift transistors, an increase in temperature and current I_{k0} causes a change in phase of the transconductance of opposite sign (Fig. 3). Therefore, by selecting $R_e \approx R_{e\ opt}$ it is possible to attain such increments of current ΔI_{k0} which will assure a reciprocal compensation in frequency drift resulting from temperature variations in the triode parameters.

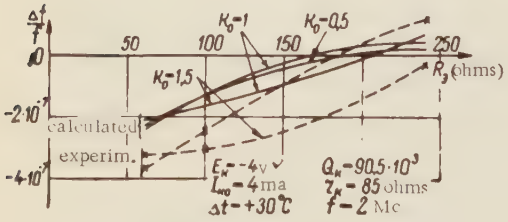

Figure 4

In connection with the above, the effects of R_e, as well as of K_0, E_k and I_{k0}, on frequency instability were studied. For this purpose, at each of the frequencies (0.75, 2 and 5 Mc), during changes in temperature or supply

---

[3]The voltages on the transistor collector and base differ from those of the voltage sources E_0 and E (Figure 1) because of the voltage drops in the resistor R_e from the collector current I_{k0} and base current I_{00}. Therefore, with a change in R_e, the current I_{k0} and E_k will vary. In order to hold I_{k0} and E_k constant with increases in R_e, it is necessary to raise the source voltages E_0 and E accordingly.

voltage, the calculated and experimental dependence on R_e was obtained of the resultant frequency instability $\frac{\Delta f}{f}$ caused by changes in the transistor parameters and power dissipated by the crystal. At the same time, the regenerative factor G was held unchanged; K_0, E_k and I_{k0} were varied. In addition, in order to be able to evaluate the effect of changes in power dissipated in the crystal, calculated relationships between $\frac{\Delta f}{f}$ (P_{qu}) and R_e were obtained under these same conditions. The selection of K_0 with G = const was accomplished by varying the capacitances C_1 and C_2. For each set of values of K_0, E_k and I_{k0}, with a change in R_e, the voltage sources E_0 and E (Fig. 1) were simultaneously regulated in order to obtain, with G, K_0 = const, the relation $\frac{\Delta f}{f}$ (R_e) with unvarying E_k and I_{k0}.

While investigating temperature instability, besides the indicated relationships, additional measurements were obtained of frequency instability caused by changes in temperature of circuit parts and crystal.

FREQUENCY INSTABILITY DUE TO TEMPERATURE CHANGES

At frequencies of f = 0.75, 2 and 5 Mc the variations in $\frac{\Delta f}{f}$ (P_{qu}) and $\frac{\Delta f}{f}$ as R_e varies were obtained with a variation in transistor temperatures of +30° C (from +23° C to +53° C) G = 4 for various values of K_0, E_k and I_{k0}. At all frequencies the component $\frac{\Delta f}{f}$ (P_{qu}) proved to be less than the resultant instability ($\frac{\Delta f}{f}$) and it may be considered that the latter is determined mainly by changes in the transistor parameters.

As an example, Fig. 4 shows the calculated and experimental relationships of $\frac{\Delta f}{f}$ (R_e) obtained with f = 2 Mc, E_k = 4v, I_{k0} = 4 ma and various values of K_0.

Fig. 4 shows a sufficiently close adherence of the calculated and experimental relationships. This confirms the correctness of carrying out the calculations with the indicated assumptions.

It may be seen from Fig. 4 that for all values of K_0 it is possible to select $R_e = R_{e\,opt}$ which results in the frequency being independent of temperature, i.e., a reciprocal compensation takes place of frequency deift due to changes in the transistor parameters [7]. The resistance $R_{e\,opt}$ may be selected experimentally.

The value of $R_{e\,opt}$ is only slightly dependent on K_0. When $R_e > R_{e\,opt}$ the temperature instability of frequency is not large.

Tests show that the values of $R_{e\,opt}$ remain practically unchanged when E_k varies from 3 - 5 v, but are dependent on the current I_{k0}. In varying I_{k0} from 2 - 6 ma, a separate $R_e = R_{e\,opt}$ could be selected for each setting.

The investigations at f = 0.75 Mc and f = 5 Mc also confirmed the above results.

The calculations and measurements show that with fluctuations in temperature of $\pm 1°$ C, the change in triode parameters (for $R_e > R_{e\,opt}$) cause frequency instability of the order of one part in 10^{-8}, change in

capacitance of the circuit of 10^{-9}, change in capacitance C_0 and resistance r_k of 10^{-10}, and the TKF_{qu} of 10^{-6}. These results coincide with data from experimental investigations in reference [3] and show that temperature instability of frequency is determined basically by the TKF_{qu} (the temperature coefficient of frequency of the crystal). In order to decrease it, the first step is to arrange thermostatic control of the crystal. Taking into consideration the small dimensions of the transistor and circuit parts, and the low level of power dissipated in them, it may be recommended that the whole oscillator be thermostatically controlled.

FREQUENCY INSTABILITY DUE TO CHANGES IN SUPPLY VOLTAGE

We have already investigated frequency instability during voltage variations on the collector E_k, the base E_0 and source E in networks with common supply to the collector and base (Fig. 1, position 2).

Investigations at frequencies of f = 0.75, 2 and 5 Mc showed that with G = 4, various E_k, I_{k0}, $R_e \geqslant R_{e\ opt}$ and K_0 = 0.5 - 1.5, the change of one collector voltage by ±20% causes a frequency deviation due to the triode parameters of $\frac{\Delta f}{f} < 10^{-8}$, and due to the power dissipated in the crystal of $\frac{\Delta f}{f}(P_{qu}) < 10^{-9}$.

There is considerably stronger dependence of frequency on voltage of the base E_0 or of the source E, with a common supply, in which case the frequency instability from E_0 and E are of the same order. This is explained by the fact that with a change in E, in a common supply circuit, the voltages on the collector E_k and base of the triode also change. The frequency stability is determined mainly by changes in the latter since its effect on frequency is greater than that of E_k. Therefore, the results of the investigation of instability due to E_0 relate in the same degree to the common supply circuit.

Figure 5 shows the calculated and experimental dependence of $\frac{\Delta f}{f}(R_e)$ and the calculated dependence of $\frac{\Delta f}{f}(P_{qu})$ on R_e obtained for various K_0

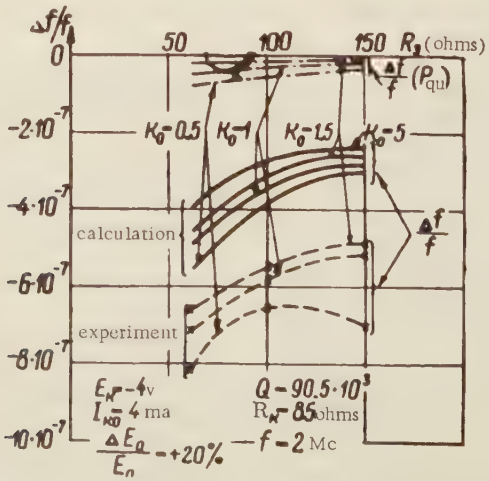

Figure 5

with f = 2 Mc, I_{k0} = 4 ma, E_k = -4 v and a variation in E_0 (or E) of +20%. The figure shows a sufficiently close concurrence of the calculated and experimental relationships and also, as in Fig. 4, confirms the correctness of the instability calculations on the basis of indicated assumptions.

Figure 5 shows that frequency instability is determined basically by changes in the transistor parameters. Variations in power dissipated in the crystal are seen to be considerably less important. As R_e increases, $\frac{\Delta f}{f}$ and $\frac{\Delta f}{f}(P_{qu})$ decrease. However, for large values of R_e ($R_e \geqslant 100$ ohms), a further increase does not result in an appreciable gain in stability. Since the values of $R_e = R_{e\ opt}$ are obtained on the basis of fairly broad conditions of temperature compensation (Fig. 4), then it is quite permissible to select $R_e > R_{e\ opt}$ in order to increase stability during changes in E_0 (or E),

Figure 5 shows that instability of frequency due to E_0 decreases with a rise in K_0. The reason for this is that, with other conditions equal, with an increase in K_0 the instability components $\frac{\Delta f}{f}(C_{ke})$, $\frac{\Delta f}{f}(P_{qu})$ fall, and $\frac{\Delta f}{f}(C_{0e})$ and $\frac{\Delta f}{f}(S_0)$ increase. Only the component $\frac{\Delta f}{f}(\varphi_s)$ is independentof K_0. Calculations show that with $K_0 > 1$ the frequency instability is determined mainly by the components $\frac{\Delta f}{f}(\varphi_s)$, $\frac{\Delta f}{f}(C_{0e})$, $\frac{\Delta f}{f}(S_0)$ ($\frac{\Delta f}{f}(C_{ke})$ and $\frac{\Delta f}{f}(P_{qu})$ are small). Since the first one is independent of K_0 on the resultant frequency instability is determined by the advantages in the relationships between the components $\frac{\Delta f}{f}(C_{0e})$ and $\frac{\Delta f}{f}(S_0)$. Taking into consideration the signs in the expressions for calculating these components in (25) and (26), and also the fact that with an increase in E_0 (or E) the current I_{k0} rises, and in accordance with Fig. 3 we have $\Delta C_{0e} > 0$, $\Delta S_0 > 0$, we may conclude that $\frac{\Delta f}{f}(C_{0e})$ and $\frac{\Delta f}{f}(S_0)$ cause frequency drift of opposite sign. Consequently, there must exist a $K_0 = K_{0\ opt}$ at which the frequency instability will be a minimum. As an illustration of the above, Fig. 6 shows the calculated relationships of $\frac{\Delta f}{f}(K_0)$ obtained at f = 2 Mc, G = 4, I_{k0} = 4 ma, E_k = -4v, E_0 varied ±20% and two values of R_e. The figure shows that for both values of R_e the frequency instability was at a minimum with $K_{0\ opt}$ = 8-10. The selection of $K_{0\ opt}$ is not critical. With K_0 = 1 - 1.5, the frequency instability is not more than 20-30% that

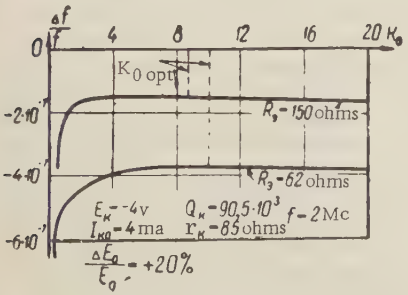

Figure 6

obtained with $K_0 = K_{0\,opt}$. An increase in K_0 above $K_0 = 1 - 1.5$ does not produce an appreciable gain in frequency stability. It is brought about through the selection of G and I_{k0}, that is with a given $U_0 \left(U_0 = \frac{I_{k0}}{S \gamma_0(\theta)} [6] \right)$ to a decrease in amplitude of the collector voltage $U_k = \frac{U_0}{|K|}$, where $|K| = \frac{1}{\sqrt{1 + \frac{x_2^2}{R_y^2}}}$ is the modulus of the feedback coefficient. The oscillator power developed by the transistor is also decreased. Therefore, it is quite satisfactory to select $K_0 = 1 - 1.5$.

With $R_e > R_{e\,opt}$ and $K_0 = 1 - 1.5$, the frequency instability during changes in E_0 (or E) of $\pm 20\%$ is of the order of one in 10^{-7}.

Investigations of instability for various values of E_k, I_{k0} with f = 2 Mc and at other frequencies (0.75 and 5 Mc) also confirmed the above results and showed that at these frequencies, also, it was permissible to select $R_e > R_{e\,opt}$ and $K_0 = 1 - 1.5$. In order to increase frequency stability it is desirable to supply power to the base circuit from a highly stable source.

The investigations also showed that frequency instability due to E_0 (or E) is nearly independent of the selection of E_k and I_{k0} if, for each value of E_k and I_{k0}, we select $R_e > R_{e\,opt}$ and $K_0 = 1 - 1.5$. Therefore, the recommendations on selection of E_k and I_{k0} values concur with those made in [7]. This means that for the P-403 triode, the selected values should be I_{k0} = 2-6 ma and E_k = 3-5 v.

CONCLUSION

A method was developed for the engineering design of a transistorized master oscillator with a crystal connected between the collector and base, for frequencies of $f \leqslant 0.05\, f_\alpha$. This method may be used for the design of master oscillators with any type transistor.

Certain design recommendations may be considered general in nature for all types of transistors. In order to attain high frequency stability in master oscillators of any type transistor, it is advisable to select undervoltage operating conditions, to have a regeneration factor G = 2-4, to arrange the self-bias from the emitter current (or combined) and to provide a highly stable power supply for the base circuit. Depending on the type of triode, the recommendations may differ as to the selection of E_k, I_{k0}, K_0 and R_e.

For master oscillators using the P-403 transistor, the following values are considered suitable: E_k = 3-5 v, I_{k0} = 2-6 ma, $K_0 = 1 - 1.5$ and $R_e > R_{e\,opt}$. These same recommendations apply to the P-402 triode.

It should be noted that for master oscillators using the diffusion-type triodes P-13 - P-15, in order to achieve high frequency stability it is desirable to select E_k - 8-10 v, I_{k0} = 5-8 ma and as large a value as possible for R_e. The latter requirement is based on the fact that it is impossible in these triodes to compensate for frequency drift when the triode parameters change with temperature [7], and in order to raise the temperature stability it is desirable to decrease the increment in current I_{k0} which is produced by the change in temperature. It is also recommended orientationally that for these transistors $K_0 \approx 0.3 - 0.5$. For a more exact solution of the problem of selecting values of K_0, it is necessary to calculate the dependence of frequency instability on K_0, with given values of E_k, I_{k0} and R_e, and then to select a value of K_0 which results in low instability.

In conclusion, I wish to express my thanks to N.K. Bekasov for his

participation in the experiments.

REFERENCES

1. Strutt Schaffenhauser. Experimentell und theoretische Untersuchung eines Frequenzstabilisirten Transistor Oszillator fur 8 Mggz. "Archiv der Elektrotechnischen Übertragung," 1957, No. 11.
2. Ludloff Awender. Über Transistorszillatoren mit Quarzsteuerung. "Elektronische Rundschau," 1958, No. 3.
3. B.A. Timofeyev. Transistorized Oscillator with Increased Frequency Stability. Transistor Electronics in Instrument Production. Oborongiz, 1959.
4. V.P. Zhukhovitskaya. On the Design and Comparison of Crystal-Controlled Master Oscillators, NDBS. "Radiotekhnika i Elektronika," No. 1, 1959.
5. V.P. Zhukhovitskaya. Design and Comparison of Crystal-Controlled Master Oscillators. Candidates Dissertation, MEI, 1959.
6. S.L. Kunina. Design of Low-Frequency Master Oscillators Using Junction Transistors. "IVUZ — Radiotekhnika," No. 3, 1958.
7. S.L. Kunina. Frequency Instability of Master Oscillators Using a P-403 Transistor. "Elektrosvaz'," No. 7, 1960.
8. B. Ye. Petrov. Equivalent Circuit of a Junction Transistor for High Sinusoidal Voltages. Semiconductor Instruments and Their Applications (No. 4). "Sovetskoe Radio," 1960.
9. S.I. Yevtyanov. Radio Transmitting Apparatus. Svyaz'izdat, 1950.
10. S.I. Yevtyanov. The Relationship Between Symbolic and Reduced Equations. "Radiotekhnika," No. 1, 1946.
11. S.L. Kunina. Investigation of Crystal Oscillators Taking Grid Current into Account. "Trudy MEI," No. XXI, "Radiotekhnika," 1956.
12. S.I. Yevtyanov. Theory of Crystal-Controlled Master Oscillators. "Radiotekhnika," No. 1, 5, 1949.
13. M. Ye. Zhabotinskiy, P. Ye. Zil'berman. Relationship Between Frequency of Crystal Oscillators and Power Dissipated in the Crystal. "Radiotekhnika i Elektronika," No. 2, 1958.

Received May 10, 1960

ON THE FORMATION OF TELEPHONE DISTRICTS UNDER CONDITIONS OF UNEQUAL DENSITY

I. M. Zhdanov

In working out prospective plans for the development of city telephone networks, the layout of the telephone districts is carried out on the basis of the principle of equal-capacity districts. A brief explanation of this problem is given and a new principle is proposed for the layout of telephone district s — the principle of equality of the total length of the subscribers' lines. By means of an example, the possibility of decreasing the cost of line construction is illustrated. Along with this, attention is also given to the necessity for exposing and calculating inequalities in district telephone densities, and through an example, the effect of inequalities on the length of the subscribers' lines, and on the degree of accuracy achieved in determining this length, is shown.

INTRODUCTION

In the prospective planning of district telephone networks many difficult tasks arise, the correct solutions of which may lead to a considerable saving in costs and materials, since the volume of work on district telephone networks amounts to many millions of rubles.

Among these tasks, by no means the least, concerns the determination of the correct principle for the layout of the telephone districts, and solving the problem of the effect of, and calculations for, the inequalities in distribution densities of subscribers in the districts. The correct solution of these problems can bring about essential economies in resources.

In recent times, during the preparation of the general layout for the telephone systems of Moscow (1953) and Leningrad (1960), and also in publications [1], the principle of equal-capacity districts (equal capacity for district ATS [automatic or dial telephone stations or exchanges]), as the basis for laying out telephone districts, has had considerable application. This principle, without having adequate basis, is put forth as the basic principle both for the equal distribution of subscribers (where its correctness is not disputed), as well as for unequal district densities, which can lead to an increase in material outlays, particularly where the variation in density is large.

As a rule, the subscriber densities in districts in the central part of a city's territory are higher than in the peripheral areas and reaches a ratio of 30:1, as can be seen from the general layout of the Leningrad telephone system.

With such significant inequalities, the use of the principle of equal-capacity districts leads to a considerable rise in construction costs.

The present article intends to throw light upon another principle for laying out telephone districts, with an without taking into account the inequalities in density, and to give a comparative evaluation. Along with this, some results will be presented of preliminary investigations on the problem of the effect and calculation of inequalities.

Everything, together with the preceding, will be directed toward maximum clarification of the problem of district layout and to anticipate all possible essential deviations which may be permitted in laying out the telephone districts.

PRINCIPLE FOR LAYING OUT TELEPHONE DISTRICTS

As is known, the basic quantity in determining the number of districts, and for laying them out within the territory of a city of area S, is the optimal capacity of the district ATS — C_0.

The number of stations or districts — n for an equal subscriber density within a district σ (Figure 1) is determined from

$$n = \frac{S\sigma}{C_0}, \tag{1}$$

where σ — is the territorial density in T/ha [telephones per hectare].

In the particular case when S = 7200 ha, σ = 25 T/ha and C_0 = 10,000 subscribers, we have

$$n = \frac{7200 \cdot 25}{10,000} = 18.$$

The capacity of the total network will be

$$N = S\sigma = 7200 \cdot 25 = 180,000$$

subscribers.

In order to have the shortest total length L_a of subscriber lines for all districts, the 18 district ATS should be distributed in accordance with Figure 2, which shows districts of equal area and capacity, with equal and minimal average values for the lengths of the subscriber lines — l_i, that is, the following equalities are preserved [2]:

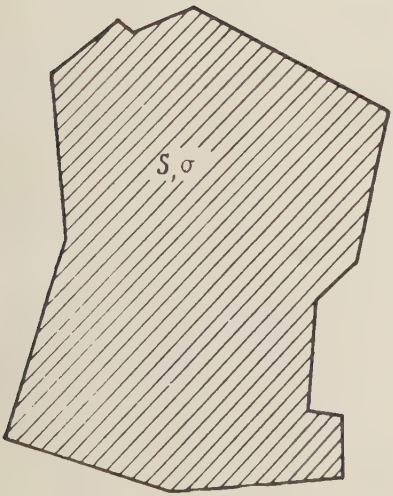

Figure 1

$$S_1 = S_2 = S_3 = \ldots = S_n, \tag{2}$$

$$C_1 = C_2 = C_3 = \ldots = C_n, \tag{3}$$

$$C_1 l_1 = C_2 l_2 = C_3 l_3 = \ldots = C_n l_n, \tag{4}$$

where S_1, S_2, S_3, etc. — are the areas of the territorial districts; C_1, C_2, C_3, etc. — are the capacities of the districts; and l_1, l_2, l_3, etc. — are the average lengths of the subscriber lines in the districts.

Consequently, in laying out the telephone regions, we may be guided by the following principles corresponding to expressions (2), (3), and (4):

a) equality of district territories, or equal-sized districts (2),

b) equality of district capacities, or equal-capacity districts (3),

c) equality of total length of subscriber lines in the districts (4).

In the case of equal density, all three principles are equally correct.

But in practice, we already have cases of unequal distribution of density.

Figure 3 shows one such density distribution where the average density σ_1, corresponds to the central area S, and the average value σ_2, to the

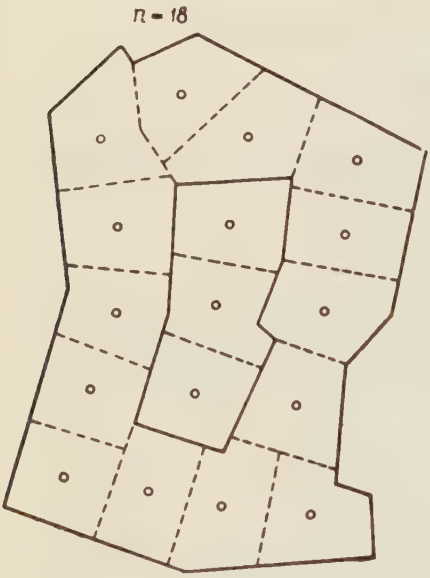

Figure 2

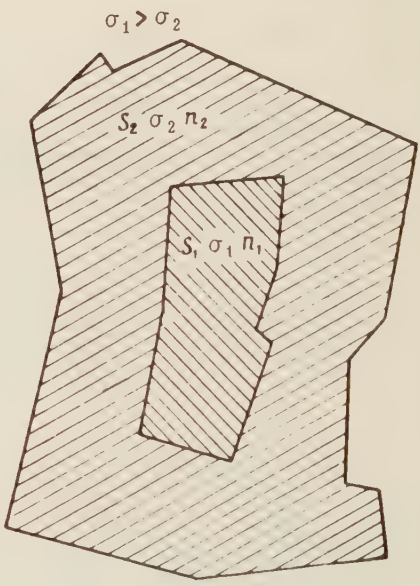

Figure 3

peripheral part with a total area S_2, in which case $\sigma_1 > \sigma_2$ (Figure 3 shows these areas in different crosshatching).

In reference [2] by this author, it was shown that in this case only one third of the principles is applicable — the equality of total length of subscriber lines. The remaining two principles will lead to a longer total length of subscriber lines L_a.

In preserving the third principle under the new conditions, Eq. (4) may be transformed into the form

$$S_1\sigma_1F_1\sqrt{S_1} = S_2\sigma_2F_2\sqrt{S_2} = S_3\sigma_3F_3\sqrt{S_3} = S_n\sigma_nF_n\sqrt{S_n}, \qquad (5)$$

where, in place of C_1, C_2, C_3, etc. we have substituted $S_1\sigma_1$, $S_2\sigma_2$, $S_3\sigma_3$, etc, and in place of l_1, l_2, l_3, etc. we have taken

$F_1\sqrt{S_1}$, $F_2\sqrt{S_2}$, $F_3\sqrt{S_3}$ etc.

Here, σ_1, σ_2, σ_3 — are the subscriber densities in the districts; S_1, S_2, S_3 — are the areas of the district territories, and F_1, F_2, F_3, etc. — are the coefficients which characterize the subscriber distribution in the districts, the location of the ATS in the districts, the shape of the territory and the direction of the main cable layouts. The value of the coefficient F for a uniform distribution of subscribers in the districts, with the ATS located in the center of a square district territory, and with the lines laid along two mutually-perpendicular directions, will be, as is known, 0.5 — and accordingly, $l = 0.5\sqrt{S}$ or $l = 0.5$ a where a is one side of the square. The value of F for other rectangular territories, or approximations of them, may be found in the literature [3].

As can be seen, Equation (5) contains the value σ_i which characterizes the densities by districts.

Consequently, in using the third principle and its corresponding equation (5), inequalities in district densities are taken into account, as a result of which this principle will give a shorter total length of subscriber lines L_a.

This is confirmed by the example below.

Let us assume that 18 districts (n = 18) are laid out in a fixed territory S with uniform distribution of densities in accordance with Fig. 3 where the central area S_1, has a density σ_1 which is greater than the density σ_2.

Laying out the telephone districts on the basis of the first principle — equality of district territories (2), we will have a distribution in accordance with Figure 2. The equality of district capacity (3) gives a distribution as in Figure 4 and for the third principle — equality in the total lengths of subscriber lines — we have the distribution of Figure 5.

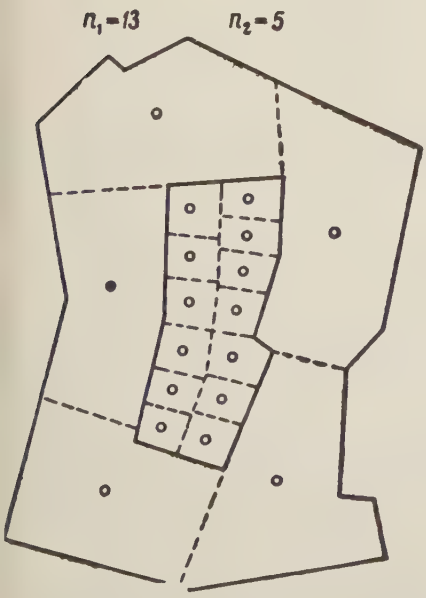

Figure 4

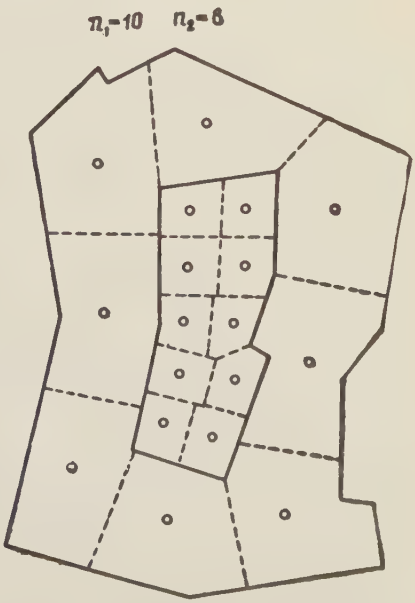

Figure 5

Table 1

No.	Principle for laying out the telephone districts	Total length of subscribers lines, km	Increase in length of subscribers' lines in comparison with the third principle	
			km	%
1	Principle of equal-sized district territories (Figure 2).	175,440	37,160	27
2	Principle of equal-capacity districts (Figure 4).	148,920	10,640	8
3	Principle of equality of total length of subscribers' lines (Figure 5)	138,280	—	—

Data calculated with $S = 12,000$; $S_1 = \frac{1}{6} S$; $S_2 = \frac{5}{6} S$; $F = 0.5$; $\sigma_1 = 48$ t/ha; $\sigma_2 = 4$ t/ha.

In Table 1, in all three cases the values for the total length of the subscribers lines L_a were calculated by the formulas:

a) for the 1st principle

$$L_{a1} = (S_1\sigma_1 + S_2\sigma_2) F \sqrt{\frac{S}{n}}, \tag{6}$$

b) for the 2nd and 3rd principles

$$L_{a2,3} = S_1\sigma_1 F \sqrt{\frac{S_1}{n_1}} + S_2\sigma_2 F \sqrt{\frac{S_2}{n_2}}. \tag{7}$$

The footnote indicates the initial data taken for calculations by the above formulas.

The results of the calculations completely affirm the correctness of the expressed statement on the advantages of the 3rd principle of laying out telephone districts as the one which gives the shortest total length of subscribers' lines L_a.

The divergence in the values of L_a was essentially 27% for the 1st principle, 8% for the 2nd principle, which must be taken into account, particularly when it is considered that each percent of saving in cable expenditures for subscribers' lines may add up to a considerable sum.

This divergence may be increased still further if the difference in the values for densities of the districts is increased. In our example, the density ratio was taken as $\frac{\sigma_1}{\sigma_2} = \frac{48}{4} = 12$, while in practice it may be higher than this. In regard to expenditures for station equipment, since the number of stations (districts) remained unchanged and the capacity of the entire network also remained constant, there is no basis for assuming that there will be any essential change in this factor for the three principles examined.

From all of the above, we may draw the conclusion that for conditions of unequal distribution of subscribers' densities by districts, when laying out the latter it is necessary to be guided by the third principle — equality

of total length of subscribers' lines.

The principle of equal-capacity districts which was used in the general layouts for Moscow and Leningrad, as we can see from the above, does not give a correct solution of the problem. It inevitably leads to an increase in line expenditures, the amount of which will become larger as the divergence in the subscribers' densities in the districts increases.

As regards the principle of equal-sized districts, being suitable only for conditions of equal distribution of subscribers with unequal densities in the districts, it may result in an even more substantial increase in cable expenditures for subscribers' lines than the 2nd principle.

ON THE EFFECT AND CALCULATION OF INEQUALITIES IN DISTRIBUTION OF SUBSCRIBERS IN CITY TERRITORIES

The inequalities in subscriber distribution in a city territory are two-fold: on the one hand, there is inequality of density (for average values) in the districts, which was examined above, and on the other, there is an unequal spacing of subscribers within the district.

The first type of inequality, when using the 3rd principle for the Layout of telephone districts, is taken into account in (5) by the values of σ_1, σ_2, σ_3, while the second type of inequality is also taken into account in (5) through the values of F_1, F_2, F_3 . . .

For example, for a concentrated distribution of subscribers in a square territory (Fig. 7) it is necessary to take a lower value for a uniform distribution (Fig. 6).

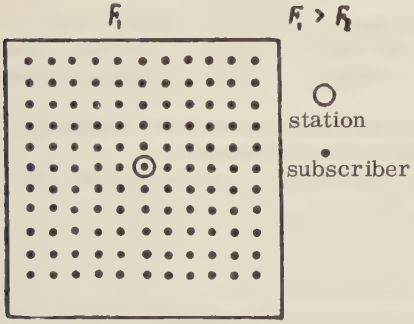

Figure 6

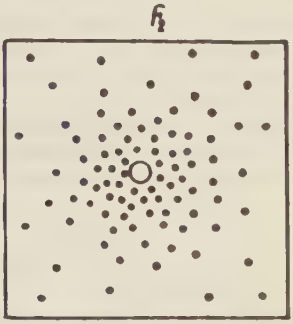

Figure 7

The investigations carried out by P.P. Yushkov [4], N.Ye. [sic] Bukhman [5] and also by the author of the present article [3, 6] (sic - 2, 3) shows that the change in the value of F arising from different distributions of subscribers inside a district will be relatively small, for example, up to 50% in comparison with F, either as an increase or decrease, will not result in any essential changes in total length of subscribers' lines L_a, inequality in subscriber distribution inside a district may be disregarded, i.e. a uniform distribution may be assumed.

Thus, it is necessary to take into account the inequality of densities of the districts which, as was shown in the previous example, may cause substantial changes in the value of L_a.

In order to judge the relative importance of this inequality, another

example will be examined.

Let us assume that a city territory with an area S is square-shaped (Fig. 8) and has N subscribers. Not knowing the actual distribution of subscribers within the territories of city S, we shall, for the sake of a simple and approximate solution of the problem, assume a uniform distribution with an average density value of σ_{av} = 60 T/ha = 6000 T/sq km and have laid out 24 telephone districts (n = 24) in accordance with the pattern in Fig. 9.

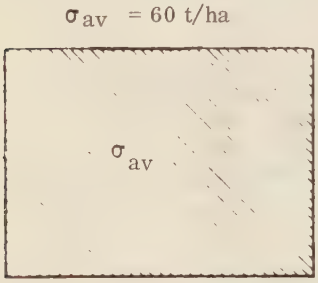

Figure 8

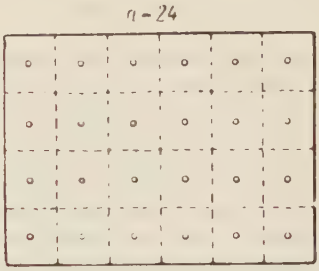

Figure 9

In such a distribution we have, calculating L_a by formula (6)

$$L_{a1} = 612.2 S \sqrt{S} \text{ km}.$$

Further, for a more precise definition of subscriber distribution, let us consider that their densities in sections S_1 and S_2 are not the same (Fig. 10). Let us take, for example, a density of σ_1 = 10 t/ha for S_1 and σ_2 = 110 t/ha for S_2.

Under such conditions the layout of the same 24 districts resulting from (5) should be carried out in accordance with Figure 11.

Calculating the total length of the subscribers' lines by formula (7) gives

$$L_{a2} = 525.8 S \sqrt{S}.$$

Continuing further a more precise and clearer definition of the inequality, we shall assume, for example, that in section S_2 (Fig. 10) there is also inequality in subscriber distribition in accordance with Fig. 12 where together with the average value σ_2, we also have the different values σ_2' and σ_3.

The calculation of L_a in this case by formula

$$L_{a3} = S_1 \sigma_1 F \sqrt{\frac{S_1}{n_1}} + S_2' \sigma_2' F \sqrt{\frac{S_2'}{n_2}} + S_3 \sigma_3 F \sqrt{\frac{S_3}{n_3}} \qquad (8)$$

gives us a value of

$$L_{a3} = 480.9 S \sqrt{S}.$$

Further definition of this inequality (Figure 14) leads to a new distribution of these same 24 districts (Figure 15). Calculating L_{a4} according to the formula

$$L_{a4}=S_1\sigma_1 F\sqrt{\frac{S_1}{n_1}}+S_2'\sigma_2' F\sqrt{\frac{S_2'}{n_2'}}+S_3'\sigma_3'\sqrt{\frac{S_3'}{n_3'}}+S_4\sigma_4 F\sqrt{\frac{S_4}{n_4}} \qquad (9)$$

gives, in this case, an even smaller value $L_{a4} = 477.2\ S\sqrt{S}$.

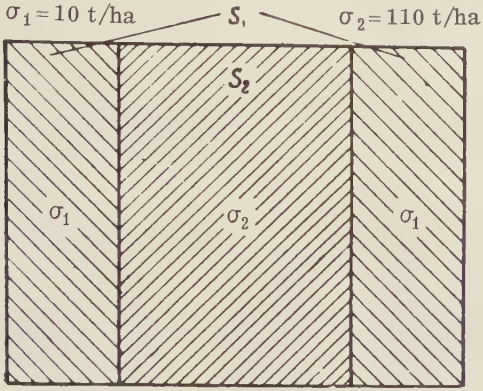

Figure 10

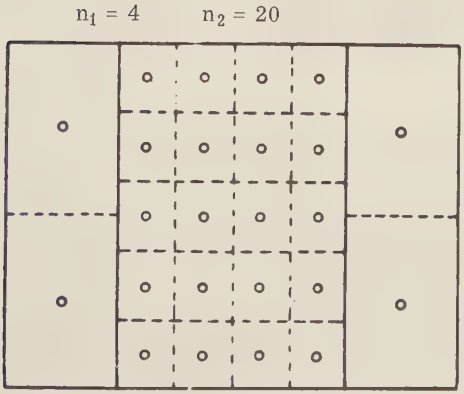

Figure 11

The above example shows graphically how the value of L_a depends on the degree of definition of the inequality in subscriber density by districts.

The more precisely the inequality is defined, the higher is the degree of accuracy in the calculations, and also the more correct can be the selection of the best possible variation for the layout and distribution of the

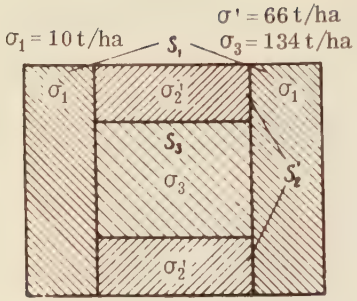

Figure 12

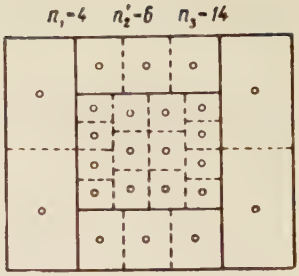

Figure 13

districts. In our case, the most suitable variant is the one shown in Figure 15. However, to simplify the problem and speed up its solution, the degree of

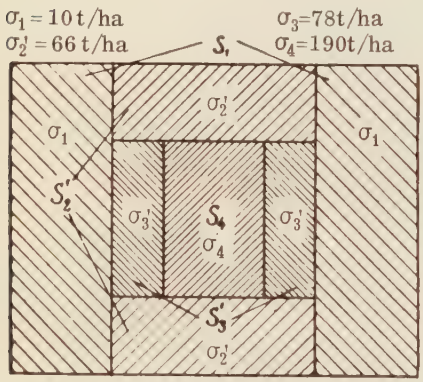

Figure 14

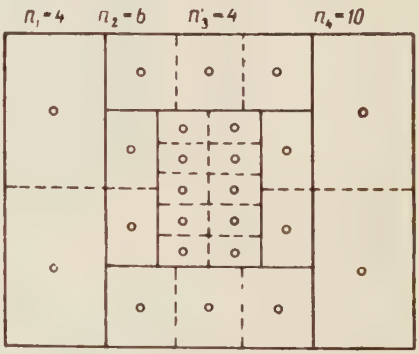

Figure 15

precise definition of the inequality may be limited if further definition does not result in a substantial change in La.

In our example it is sufficient to take three gradations of density (σ_1, σ_2, σ_3), without resorting to further definition of subscriber distribution. Such a limitation in accuracy of calculations will give an error for L_a not greater than 10%.

A braoder and deeper investigation of this problem by the author showed that the same limitation of three gradations may be applied to many other cases. When this solution must be carried out with greater accuracy, it is necessary to increase the number of density gradations K to the number of districts n, and only with k = n can we be assured of a minimum L_a.

The above examples enable us to set forth the following. Resorting to the most rational principle for laying out the telephone districts — the principle of equality of the total lengths of the subscribers' lines when laying out and organizing the telephone districts for a specific network capacity and a specific number of district ATS — we shall obtain a total length of subscribers' lines L_a which will be shorter for unequal densities in the districts than in the case of a uniform distribution. This can be seen graphically in the distributions of Figures 9 and 15.

This difference will be quite substantial when the subscribers are concentrated in the central part of the city territory, in which case, aside from a decrease in total length of subscribers' lines, there will also be a decrease in connecting lines due to an increase in density of the ATS spacing in the central part.

Accordingly, inequality in density distribution in the districts creates more suitable conditions for a district layout of the telephone network than does a uniform distribution or equal values for the densities. However, this advantage may be attained only by observing the following conditions:

a) equality in total lengths of the subscribers' lines for the laid-out telephone districts,

b) sufficiently-detailed definition of the inequality in densities by districts, or by larger areas containing several districts.

In practice, the calculation of the inequality and laying out the telephone districts in accordance with established norms of line construction costs, for subscribers' lines, may be carried out in the same manner as is done in the general layouts "Genskhema" except that the principle of equality of total lengths of subscribers' lines is used instead of the principle of equal-capacity districts.

CONCLUSION

The limitations of this article do not permit a more detailed examination of this problem and thus, to deal more thoroughly with the theoretical aspects. The latter was covered to some extent by the author in reference [2], to which particular attention is called.

But even in the present article it is obvious how important it is to have the right approach to the solution of the problem of laying out telephone districts, taking into account the inequality of subscriber distribution.

On the basis of the examples given and conclusions reached for each particular problem, we come to the following general conclusion.

The principle of equality of total lengths of subscriber lines is the best one, and with fixed costs for station equipment, will result in minimum expenditures for subscriber-line cables.

The opposing principle used in practice, that of equal-capacity districts, can compete with the proposed principle only in the case of equal densities in the districts, and even then is permissible only for very insignificant deviations in densities.

With density ratios of 1:10 and higher, the presently-accepted principle, as was shown in the example, will lead to significant increases om cable expenditures of the order of 8% and higher, depending on the degree of deviation in district densities.

Nonuniform distribution of densities, particularly with concentration of density in the central part of a city territory, creates the most favorable conditions for laying out of a telephone system, more so than a uniform distribution.

This advantage may be realized with sufficient nonuniformity in the district densities. The above situation should prevail in each district separately. In some cases, when a high degree of accuracy in the determination of L_a is not required, an average value of density may be used for a group of districts, keeping in mind that the approximation of the most desirable solution depends on the density gradations, the number of which must not be less than three. (With three gradations, the error will not exceed approximately 10%).

The basic quantity in laying out districts, as is known, is the optimum capacity, on the basis of which the number of districts is determined, and which also determines the layout for the telephone districts in accordance with the principle used for laying out the districts. The optimum value for capacity with different densities in the districts need not remain fixed, and will increase as the district densities increase, and vice versa.

The principle of equal-capacity districts makes possible an equal-capacity arrangement of district ATS, which is occasionally pointed to as an advantage of this method.

From our viewpoint, such an advantage (if it may be considered an advantage at all does not sufficiently compensate for the increase in cable costs which of necessity results in comparison with the recommended principle of equality in total lengths of subscribers' lines.

REFERENCES

1. D.F. Fat'kin. Graphical Method for Determining the Most Advantageous Capacities and Locations of Newly-Opened Municipal Telephone Stations. "Vestnik Svazi," No. 2, 1954.
2. I.M. Zhdanov. Layout for Municipal Telephone Networks. "Manual of Scientific Articles on Wire Communications, Acad. Sci.," No. 5, 1956.
3. I.M. Zhdanov. On Calculations of Average Length of a Subscriber Line. "Symposium of the LEIS," No. III, 1948.
4. P.P. Yushkov. Determination of Average Value of a Subscriber Line. "Scientific and Technical Collection " [Nauchno-Tekhnicheskiy sbornik], No. 4, 5, 1930.
5. Ye. N. Bukhman. Elements of Design for Line Construction of Municiple Telephone Networks. "Elektrosvyaz'," No. 8, 10, 1940.

Received May 3, 1960

TRANSMISSION PARAMETERS AND EFFECTS OF TYPE TG CABLES IN A FREQUENCY RANGE TO 600 KC

A.D. Ruga and Ye. V. Kostyanets

The transmission parameters and effects of using Type TG cables in a frequency spectrum to 600 kc are presented. Conclusions are reached regarding the possibility and advisability of hf (high frequency) multiplexing of circuits in existing interoffice connecting cab es of GTS [City Telephone Networks].

INTRODUCTION

The intense development of city telephone networks (GTS) is tied in with considerable capital investment and large outlays of such short-supply metals as lead and copper. One of the most effective methods for utilizing city cables is that of high-frequency multiplexing of the trunk-line circuits.

At the present time the GTS trunk lines are designed for MKS cables with multiplexing of their circuits by means of type KRR-30/60 equipment. A large, as yet unused, reserve is available through the multiplexing of the existing type TG cables of GTS. Investigations carried out in 1957-1958 by the TsNIIS [Central Scientific Research Institute of Communications?] on type TG cable in the high-frequency spectrum, and also the investigations of NIITS [Scientific Research Institute of Telephone Networks?] in recent years, show the feasibility of multiplexing in circuits using the existing type TG cables, and data is also available abroad regarding the development of hf equipment for multiplexing GTS cables [1, 2, 3] which confirms the fact that sufficiently-low cost equipment may be produced for this purpose.

The present article contains basic results achieved by NIITS of the Ministry of Communications in their investigations on the parameters of GTS cables of type TG in the frequency range to 600 kc.

TRANSMISSION PARAMETERS AND EFFECTS OF TG CABLES

In city trunk lines TG cables of various diameters and differently-designed conductor insulation are in use.

Formerly, the industry produced, for the most part, cables with a paper-air insulation, type "Trubochka" [little tube], chiefly in diameters

0.5, but also 0.6, 0.7 and 0.8 mm. Cables with a conductor diameter of 0.4 mm were produced with insulation of type "Treugol'nik" [triangle].

At the present time, cables of 0.5 mm conductor diameter are produced with paper-composition insulation.

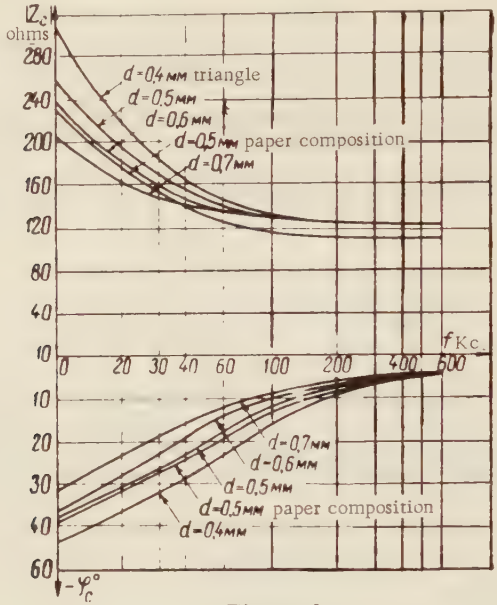

Figure 1

Figures 1, 2 and 3 show data on the transmission parameters of circuits using these cables in factory lengths which represent the average values of the index of characteristic impedance [Z_c] and its angle φ_c, and also the attenuation constant β and phase-shift constant α.

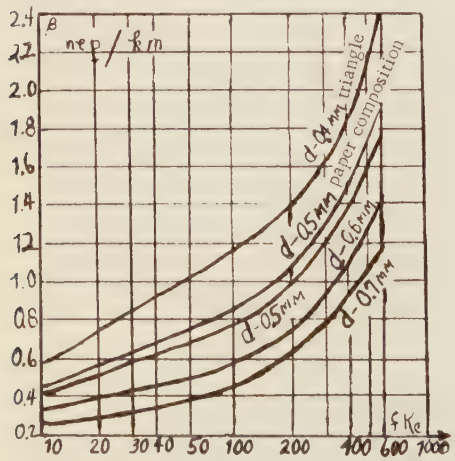

Figure 2

An analysis of measured data showed that the capacitance of circuits with paper-composition insulation exceeds that of circuits with type "Trubochka" insulation by 11.2%. This explains their relatively high kilometer attenuation (on the average, 0.1 - 0.2 nepers/km).

Separate circuits using the same cable in different factory lengths vary somewhat in attenuation, which

Table 1

Table 1

Parameters \ Value	Impedance ohms/km	Effective capacitance mμf/km	Frequency 500 kc |z_c|, ohms	Frequency 500 kc β, nep/km	Type of insulation
Minimum	164	41	85	1.5	Paper composition
Average	172	46	110	1.73	
Maximum	180	60	125	1.9	
Minimum	162	33	110	1.33	Paper-air (Trubochka)
Average	170	41	122	1.6	
Maximum	190	50	130	1.7	

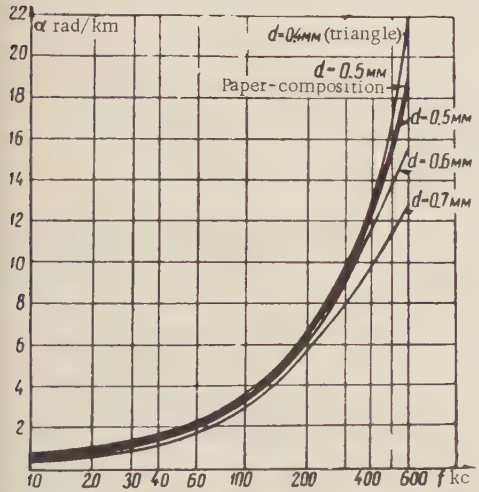

Figure 3

is explained basically by deviations in their effective capacitances. The latter, for cables with a conductor diameter of 0.5 mm, are illustrated in Table 1.

The suitability of a cable circuit for multiplexing is determined to a considerable degree by the extent of shielding at the far end (b_z) and by the near-end crosstalk (B_0).

Investigations of the dependence of b_z and B_0 in factory lengths, on frequency showed that the average value[1] of B_0 in the frequency range from 20-200 kc drops approximately 2.5 nepers and with further increase in frequency to 600 kc, remains nearly constant at a level of approximately 9 nepers (Fig. 4). The dependence of the average value b_z on frequency is similar, decreasing by about 2-2.5 nepers in the frequency range to 300 kc, and then remains practically constant at about 8 nepers with further increase in frequency to 600 kc (Fig. 5).

Figure 6 shows a cross-section of a TG-50 x 2 x 0.5 cable. As can be seen from Fig. 5 and 6, the circuit shielding increases with increasing separation of the pairs from each other. The GTS trunk lines, as a rule,

[1]The values of B_0 and b_z (Figures 4 and 5) were obtained as the result of averaging 33 identical pair combinations measured on several factory lengths.

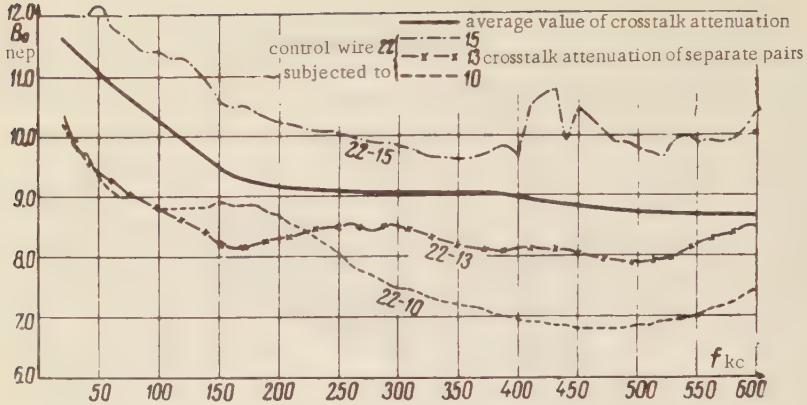

Figure 4

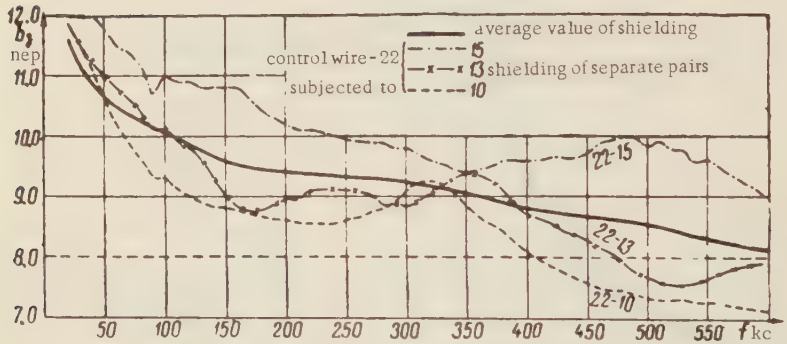

Figure 5

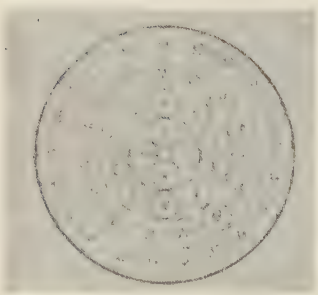

Figure 6

are of the multiple type and contain conductors of different diameters, which make it expedient to characterize them by the operating (effective) parameters b_p and Z_{in}.

The investigations were carried out on trunk lines extending from 1.7 to 10 km. An analysis of the results obtained in measuring the effective attenuation shows that the deviation in attenuation, as with cables in factory lengths, is caused by deviation in

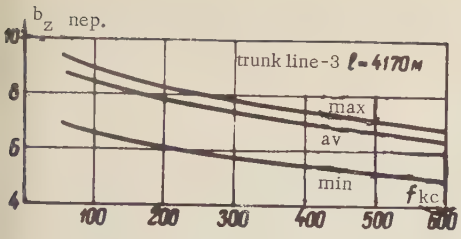

Figure 7

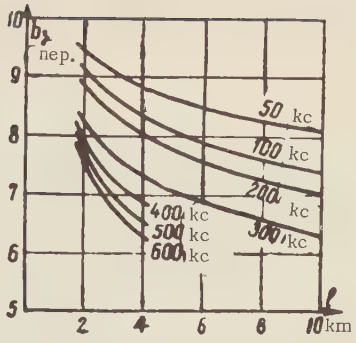

Figure 8

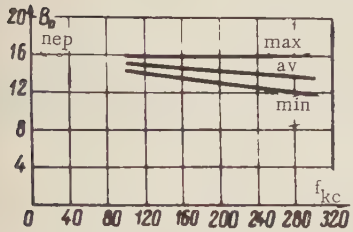

Figure 9

the effective capacitance, and does not exceed 0.25 - 0.3 nepers at 600 kc. The average value of effective attenuation is practically the same as the characteristic attenuation (Fig. 2). The dependence of the scalar input impedance on frequency is of a pulsating nature, and at 600 kc the deviation in the value of $[Z_{in}]$ does not exceed $\pm$ 15 ohms.

An example of the dependence of far-end circuit shielding on frequency is shown in Fig. 7 where the average value is the arithmetical mean of all measured pair combinations in the line, and the minimum and maximum values are the arithmetical means of the measured combinations corresponding to the worst and best cases, respectively, in regard to mutual-shielding of the pairs.

Figure 8 shows curves of average values of circuit shielding at different frequencies.

Figure 9 shows the dependence of near-end crosstalk attentuation on frequency between two inter-exchange trunk-line cables 10 km in length. As can be seen in Fig. 9, the average value of crosstalk attenuation at 300 kc is 14 nepers, which is ample proof of the practicability of using a two-cable system.

DETERMINATION OF NUMBER OF PAIRS SUITABLE FOR MULTIPLEXING AND OPTIMUM MULTIPLEXING SPECTRUM

An analytical prediction of the number of pairs suitable for multiplexing in low-frequency cables is usually carried out as follows [5].

With a total number of pairs in a cable of n, the number of two-pair combinations is equal to

$$N = 1/2\ n\ (n - 1) \qquad (1)$$

If we assume that the number of pairs satisfying the given norms for shielding is equal to k, then, correspondingly, the number of possible two-pair combinations of multiplexed pairs analagous to (1) will be

$$K = 1/2\ k\ (k - 1) \qquad (2)$$

The total number M of two-pair combinations in an n pair cable which

satisfy the shielding norms (blank squares in Fig. 10) will satisfy the relation ship

$$\frac{k}{n} < \frac{M}{N}, \tag{3}$$

which is an indication of the low probability that the percent of suitable pairs will be equal to the percent of suitable combinations. These M - combinations may be arranged in the diagram (Fig. 10) by different methods, the number of which will be

$$C = \left(\frac{N}{M}\right) = \frac{N!}{M!(N-M)!}, \tag{4}$$

where M may have any value from 0 to N.

Assuming that the appearance of all arrangements of favorable combinations are of equal probability, the probability of the appearance of each such picture, which from now on we shall call constellations, may be determined from

$$\frac{1}{C} = \frac{M!(N-M)!}{N!} = W(C). \tag{5}$$

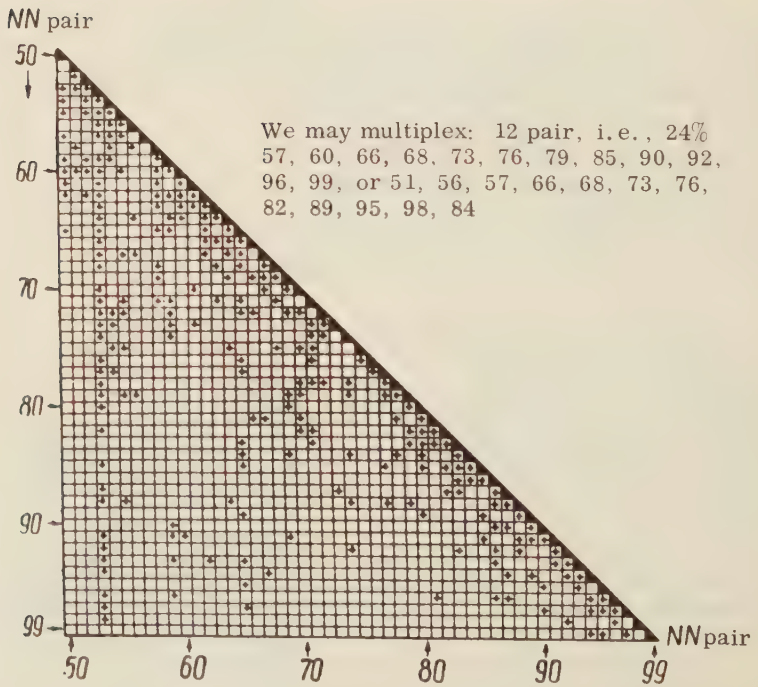

Figure 10

Let C represent a single [individual] constellation, a_{kc} — the number of combinations of k pairs in the given constellation, A_k — average number of combinations of k multiplexed pairs, then

$$A_k = \sum_{C=1}^{C=\binom{N}{M}} a_{kc} W(C) = \frac{M!(N-M)!}{N!} \sum_{C=1}^{\binom{N}{M}} a_{kc}. \tag{6}$$

The sum of the terms of the right hand member — which is the sum of all the suitable combinations of k pairs for all possible constellations — is calculated in the following manner: an individual k pair combination will be s uitable if all of its K combinations lie within the M category, which satisfy the shielding norms independently of the distribution of the remaining (M — K) combinations satisfying the norms. These remaining suitable (M — K) combinations may be arranged in various ways (constellations) on the diagram and their number will be

$$C_{M-K}^{N-K} = \frac{(N-K)!}{(M-K)![(N-K)!-(M-K)!]}. \tag{7}$$

The single k pair combination which we are considering will, therefore, be found in C_{M-K}^{N-K} constellations and this number is the number of components in the summation of Eq. (6).

On the assumption of equal probability of the appearance of all constellations, all combinations of k pairs will also be of equal probability

$$C_k^n = \frac{n!}{k!(n-k)!}. \tag{8}$$

Thus, we finally have

$$A_k = \binom{N}{M}^{-1} \binom{n}{k} \binom{N-K}{M-K}. \tag{9}$$

If M and N $\gg$ K (the case of high frequencies), then

$$\binom{N}{M}^{-1} \binom{N-K}{M-K} \to \frac{M^K}{N^K} = p^K.$$

In this case, expression (9) may be replaced by the approximation

$$B_k = \binom{n}{k} p^K, \tag{10}$$

where $p = \frac{M}{N} 100$ — is the percent of combinations satisfying the shielding norms.

On the basis of (10), a nomograph (Fig. 11) was obtained which permits the determination of the number of k pairs suitable for multiplexing as a function of the percent of suitable pair combinations p in the cable for

various values of n.

It is not difficult to persuade oneself that the value k depends very little on the selection of the value B_k; therefore, the nomograph is calculated for $B_k = 1$. The values of k obtained from the nomograph should be rounded out to the nearest, lowest whole number.

Thus, it is obvious that in determining the number of pairs suitable for multiplexing, it is necessary to establish, experimentally, the value p, which will be different at different frequencies, types of cables and other factors.

As was shown by comparing the experimental and calculated data, the error in an analytical determination of the number of pairs is small in practice, and may become significant (up to 50%) only in the case of cables with a small number of pairs (20-30). In addition, the analytical method does not exclude the necessity of measurements because if, for any particular cable, p is known and k is calculated, then it is still necessary to carry out measurements for determining the actual pairs.

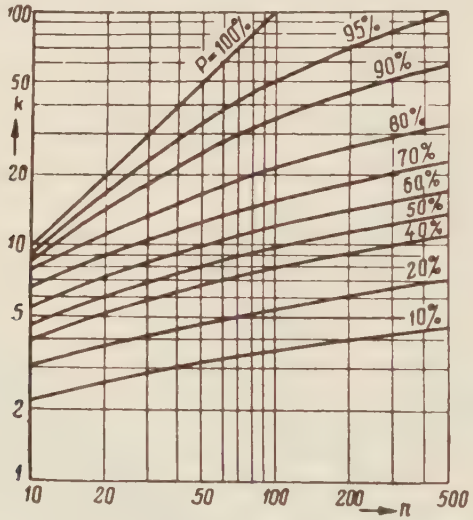

Figure 11

For the same cables in which the transmission parameters and effects were investigated, the number of pairs suitable for multiplexing was also determined.

This determination was made on cables of different capacitance and length, and in each case a 50 pair group was selected arbitrarily for the investigations. The mutual shielding was determined for each pair with respect to each of the others.

Measurements were carried out at frequencies of 60, 100, 200, 300, 400, 500 and 600 kc.

As a result, curves were obtained of the dependence of the average-expected percent of pairs suitable for multiplexing on frequency and shielding norms for a repeater section of the line ($l_{av} = 3.5 - 4$ km, TG-05 cable). The average-expected values of percent of pairs is shown in Fig. 12.

The determination of the number of the circuits to be subjected to

multiplexing is done by selecting them on the basis of the measurements of mutual shielding of each circuit with respect to all the others:

$$M = \frac{N\ 100}{\%}\ .$$

a) in the case when the average-expected number of multiplexed circuits determined from Fig. 12 is substantially above requirements, it is

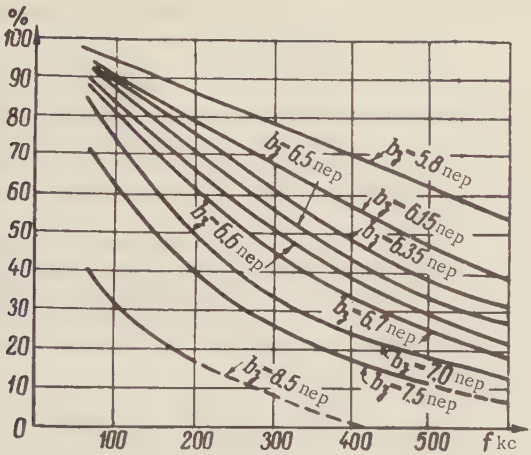

Figure 12

necessary to measure the mutual shielding of M circuits, where N is the number of physical circuits required for multiplexing and the % refers to the average-expected percent of pairs (Fig. 12). These M circuits should be selected with maximum separation between each other within the cross-section of the cable;

b) in the case when the required number of physical circuits approaches the average-expected value, it is necessary to measure mutual shielding of all circuits in the cable.

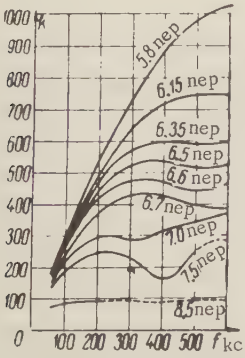

Figure 13

In order to determine the effect of the capacitance of the measured group on the general conclusions regarding the number of pairs suitable for multiplexing, tests were conducted on these pairs for groups of different capacitances from 30 to 100 at 600 kc, which showed that the percent of pairs suitable for multiplexing does not depend on the capacitance of the group.

Increasing the usable frequency range, while increasing the number of channels K (Fig. 13) obtained as a result of the multiplexing of each circuit, causes, at the same time, a decrease in the number of circuits

suitable for multiplexing. In order to express the effect of these factors on the total number of channels obtained with the multiplexing of all suitable circuits in a 50 pair group, the curves in Fig. 13 were constructed as the result of measurements carried out on six 50 pair groups. These curves were constructed with the assumption that each channel occupies a bandwidth of 16.5 kc, which corresponds approximately to the frequency allocation in the KRR 30/60 equipment.

Figure 13 gives an indication of the feasible multiplexing spectrum in relationship to the shielding norms, and shows the dependence of the number of channels on frequency and length of line for a 50 pair group.

CONCLUSIONS

The results of the measurements carried out on factory lengths of type TG cables, and on interoffice trunk lines, showed that:

1. There is considerable deviation in the values of the transmission parameters, which are caused mainly by variations in the values of the effective capacitances.
2. The dependence of the transmission parameters and effects on frequency is of a non-monotonous nature, which can be explained by the presence of a large number of heterogeneities along the length of the line.
3. The magnitude of near-end crosstalk between two cables at f = 300 kc is 13-14 nepers, on the average, which is evidence of the feasibility of using a two-cable high frequency system.
4. Type TG cables contain a certain number of pairs suitable for multiplexing. Thus, for example, at 300 kc and with a shielding requirement of b_z = 7.5 nepers, it will average 27%, but at 600 kc it drops to 7%, and in practice these values are independent of the capacitance of the group in which the suitable pairs are located.
5. At existing prices of the KRR 30/60 equipment, its use in GTS [City Telephone Networks][2] is quite suitable at distances of approximately 12 km [4]. However, taking into consideration the substantial economy in non-ferrous metals resulting from multiplexing, the use of the KRR 30/60 equipment will be justified in a number of cases at shorter distances.
6. In cases where the KRR 30/60 equipment is used for high-frequency multiplexing, the approximate lengths of the repeater sections are shown in Table 2.

Table 2

Diameter of current-carrying conductors	d_0 = 0.4 mm	d_0 = 0.5 mm paper-composition insulation	d_0 = 0.5 mm paper-air insulation Trubochka	d_0 = 0.6 mm	d_0 = 0.7 mm
Lengths of repeater section, km	2.9	3.5	3.8	4.8	5.7

[2] The use of KRR 30/60 equipment with type TG cables is possible only if the compensating network is changed accordingly.

The authors would like to express their gratitude to the workers of the line-cable laboratory of NIITS, MS [Ministry of Communications], USSR who facilitated the carrying out of measurements, and also to M. Ya. Kallera, who reviewed the manuscript and made many valuable suggestions.

REFERENCES

1. "More phones but no additional cables," Elektrical Engineering, 1958, v. 77, No. 12.
2. "Exchange trunk carrier system." Telephony, 1958, v. 155, No. 2.
3. "The K-24 A syncroplex telephone carrier system." ITT Laboratories, a division of ITT Corporation, Palo Alto, California.
4. A. D. Ruga. Some Problems in the Development of High-Frequency Cable with Small-Diameter Conductors for Trunk Lines of City Telephone Networks. "Collection of Scientific Works of NIITS MS USSR," No. 3, 1959.
5. Schouten Boer. On the number of pairs which can be used for carrier working in random — spliced, de-loaded voice-frequency cables: "Philips Telecomm. Review," 1948, v. 19, No. 1.
6. B. Z. Tomchin. Transmission Parameters of Low-Frequency TG Cable in the Frequency Range to 600 kc. "Elektrosvyaz'," No. 4, 1960.

Received October 13, 1960

BIBLIOGRAPHY

1. Communications Systems
2. Radio Relay Lines
3. Cosmic Radio Communications
4. Radio Wave Propagation. Antennas
5. Noise. Prevention of Noise
6. SHF Electronic Instruments
7. Waveguides
8. Television
9. Theory of Circuits
10. Apparatus for Radio and Wire Communications
11. Reliability of Equipment
12. Semiconductor Devices

1. COMMUNICATIONS SYSTEMS

Operating Problems in Communication Techniques. Betriebsfragen der Vermittlungstechnik. Padberg T. "Fernmelde Praxis." 1960, Bd. 37, X, No. 19, S. 761 - 777, ill.

Communications System with Coded Feedback. Metzner, J.J. and Morgan, K.C. "IRE Trans. on Communs. Sys.," 1960 v. CS-8, VI, No. 2, p. 101-113, ill., bibl. 10 NN.

Reliable Communication System with Binary Coding. Reliable Fail—Safe Binary Communication. Metzner, J.J., Morgan K.C. "IRE Wescon Convent, Rec.," 1960. P.5. VII, p. 192-200, bibl. 10 NN.

Comparison of the Efficiency of Some Communications Systems. Sanders. "Foreign Radio Electronics," XII, No. 12, 1960, pp. 52-76, illustrations, bibliography, 6 titles.

Comparison of PSK vs FSK and PSK—AM vs FSK—AM Binary—Coded

PulseCode Modulation Terminal and Repeater Methods, Carbrey, R.L. "Electronic Design," 1960, v. 8, VI, No. 12, p. 52-57, ill., bibl.

PCM System Trends. Sink, R.L. "IRE Wescon Convent. Rec.," 1960, P. 5, VIII, p. 94-100, ill., bibl. 3 NN.

Minimum Signal-to-Noise Ratio at High Frequency in Two-Channel Communication with Identical Program and Amplitude Modulation. Der hochfrequente Mindeststorabstand von zwei mit gleichem Programm amplitudenmodulierten Ubertragungswegen. Freutel, W. und Rautenfeld, F. "Rundfunktechn. Mitt.," 1960. Bd. 4, X, No. 5, S. 181-193, ill., bibl. 40 NN.

Digital Communications. "IRE Trans. on Communs. Sys.," 1960, v. CS—8, VI, No. 2, p. 51.

Digital Techniques in Industrial Radio Communications. Saltzberg, T. "Electronic Design," 1960, v. 8, VI, No. 12, P. 62-65, ill.

Digital Data Transmission by Wire. Fischer Ch. R. "Electronic Design," 1960, v. 8, VI, No. 12, p. 58-61, ill.

Digital Data Fundamentals and the two Level Vestigial Sideband System for Voice Bandwidth Circuits. Hollis, J.L. "IRE Wescon Convent. Rec.," 1960, P. 5. VIII, p. 132-140.

Air-to-Ground Meteoric Scatter Communication System. Hannum, A.J. and oth. "IRE Trans. on Communs. Sys.," 1960, v. CS-8, VI, No. 2, p. 113-133. ill., bibl. 10 NN.

Underground Communications System. "Missiles and Rockets," 1960, v. 7, IX, No. 10, p. 36.

Efficient Transmission of Information in Telephone Communications Networks. Halina, J.W. "IRE Wescon Convent. Rec.," 1960, P. 5, VIII, p. 115-124, ill., bibl. 10 NN

Measured performance of the Sebit-25 Data System Over Wire Line Facilities at 2500 Bits per Second. Hollis, J.L. "IRE Trans. on Communs. Sys.," 1960, v. CS—8, VI, No. 2, p. 134-137, ill.

Introduction to the Theory of Crosstalk. Einfuhrung in die Theorie des Nebensprechens. Steinhardt, K.H. "Nachrichtentechnik," 1960, X, No. 10, S. 435-441, ill., bibl. 18 NN.

An AC Telegraph System and Signal Transmission with the WT-60 Remote Control. Das Wechselstromtelegrafie—und Fernwirkubertragunssystem WT—60. Beyer, R. "Nachrichtentechnik," 1960, X, No. 10, S. 442-445, ill.

"Funk—WT" — A New Transistorized Telegraph System with Channels of Different Band-widths. "Funk-WT," ein neues Telegraphie-Ubertragungssystem in Transistor-Ausfuhrung mit Kanalen verschiedener Bandbreite. Fuchs, E.A. "Nachr-Techn. Zeitshr.," 1960, IX, No. 9, S. 419-423, ill.

2. RADIO RELAY LINES

Transportable Micro-Scatter System Features Trailer-Mounted Antennae. Wilder, J.C. "Electronics and Communs.," 1960, v. 8, VII, No. 8, p. 20-22, 37, ill.

Measurements in Radio Relay Links with Optical Visual Range by the Diversity Antenna Method. Raumdiversity-Messungen an einer Richtfunkstrecke mit optischer Sich. Kuhn, U. "Nachrichtentechnik," 1960, X, No. 10, S. 430-434, ill., bibl. 10 NN.

Supplementary Equipment for the Service Channel of RM-24A Radio Relay Equipment. Litsoyev, N.D. and Starev, V.F. "Avtomatika, Telemekhanika i Svyaz'," XII, No. 12, 1960, pp. 25-26, illustrations.

Remote Control of TV Microwave Equipment. Bullock, J.B. "IRE

Internat. Convent. Rec.," 1960, v. 8, P. 7, 47-54. ill.

3. COSMIC RADIO COMMUNICATIONS

Progress and Problems in World Communication. Green, E. "Electrical Eng-ng," 1960, v. 79, VI, No. 6, p. 494-498, ill.

Digilock Communication System. Sanders, R.W. "IRE Wescon Convent. Rec.," 1960, P. 5. VIII, p. 125-128.

The Telebit System for Space Communication. Taber, J.E. "IRE Wescon Convent. Rec.," 1960, P. 5, VIII, p. 126-149, bibl.

The TRAC(E) System for Communications and Tracking of Cosmic Objects. Brokman and others. "Foreign Radio Electronics," XII, No. 12, 1960, pp. 3-19, illustrations, bibliography, 12 titles.

How Courier Satellite's Ground System Works. "Electronics," 1960, v. 33, VII, No. 30, 38-39.

Communications Satellite "SKOR." Brown and Senn. "Foreign Radio Electronics," XII, No. 12, 1960, pp. 42-50, illustrations.

Beacon Antennas for Project Mercury. Shea, D.F. and oth. "IRE Wescon Convent. Rec.," 1960, P. 1, VIII, p. 149-157, ill., bibl. 2 NN.

Ground Antenna for Cosmic Communications. Layness and others. "Foreign Radio Electronics," XII, No. 12, 1960, pp. 20-33, illustrations, bibliography.

4. RADIO WAVE PROPAGATION ANTENNAS

Problems Associated with Precise Determination of the Index of Refraction of the Earth Atmosphere. Bush, A.M. "IRE Trans. on Instrumentation," 1960, v. I—9, VI, No. 1, p. 23-28, ill., bibl. 11 NN.

Results of Approximate Calculation of Field Intensity of a Space Wave by the Extreme Usable Frequencies. Ergebnisse zur nahrungsweisen Berechnung der Raumwellenfeldstarke aus den Grenzen des Ubertragunsfrequenzbereiches. Beckmann, B. "Nachr.—Techn. Zeitschr.," 1960 X, No. 10, S. 470-472, ill., bibl. 2 NN.

The Measurement of Time — Quadrature Components of a Scattered Field. Garbacz, R.J. and Eberle, J.W. "IRE Wescon Convent. Rec.," 1960, P. 1, VIII, p. 131-138, ill., bibl. 4 NN.

Design of Corner-Reflector Antennas. "Electrical Eng-ng," 1960, v. 79, No. 6, p. 546, ill.

A new Approach to Antenna Beam-Shaping — the "Coke-Bottle" Antenna. Phillips, C.C. "IRE Wescon Convent. Rec.," 1960, P. 1, VIII, p. 74-82, ill.

Design Techniques for a Light Weight High Power Spiral Antenna. Jones, J.P. and oth. "IRE Wescon Convent. Rec.," 1960, P. 1, VIII, p. 107-122, ill., bibl. 32 NN.

Phase Center Distributions of Spiral Antennas. Barbano, N. "IRE Wescon Convent. Rec.," 1960, P. 1, VIII, p. 123-130, ill.

Miniaturized Cavity-Fed Slot Antennas. Brownell, F.P. and Kendall, D.E. "IRE Wescon Convent. Rec.," 1960, P. 1, VIII, p. 158-165, ill., bibl. 4 NN.

Resonant Slots with Independent Control of Amplitude and Phase. Maxum, B.J. "IRE Trans. on Antennas and Propag.," 1960, V. AP-8, VII, No. 4, p. 384-389, ill.

5. NOISE. PREVENTION OF NOISE

Extra-Terrestrial Radio Noise as a Source of Interference in the Frequency Range 30-1000 mc/s. Horner, F. "Proc. IEE," 1960, v. 107, VII, No. 34, P. B, p. 373-376, ill., bibl. 11 NN.

Effect of Vehicular Generated Interference on Double-Sideband and Single-Sideband A.M. Receivers. Backman K.E.H. "IRE Trans. on Vehicular Communs.," 1960, v. VC-9, V, No. 1, p. 98-104.

Circuit for Communication Receivers. Chow, W.F. "IRE Trans. on Vehicular Communs.," 1960, v. VC-9, V, No. 1, p. 1-9, ill., bibl. 4 NN.

Ignition Noise Suppression. "Wire Radio Communs.," 1960, VI, No. 6, p. 27-29, ill.

Shielding of Equipment qnd Communications Cables. Grodnev, I.I. and Sergeychuk, K. Ya. Svyaz'izdat, M., 1960, 316 pp., illustrations, bibliography, 39 titles.

6. SHF ELECTRONIC INSTRUMENTS

Microwave Valves: A Survey of Evolution, Principles of Operation and Basic Characteristics. Dix, C.H. and Willshaw, W.E. "J. Brit. IRE," 1960, v. 20, VIII, No. 8, p. 577-609, ill., bibl. 89 NN.

Investigation of the Operation of Traveling Wave Tubes with Local Attenuation in Linear Conditions. Kats, A.M. "Radiotekhnika i Elektronika," Vol. 5, XII, No. 12, 1960, pp. 1986-1996, illustrations, bibliography, 12 titles.

An Octave-Bandwidth Ultra-Low-Noise Traveling-Wave Amplifier. Kinaman, E.W. and John, G.E. "IRE Wescon Convent. Rec.," 1960, P. 3, VIII, p. 72-76, ill., bibl. 5 NN.

Very High Convergence Electron Guns. Geppert, D.V. "IRE Wescon Convent. Rec.," 1960, P. 3, VIII, p. 77-89, ill.

A Periodically Focused Backward Wave Oscillator. Johnson, C.C. "IRE Wescon Convent. Rec.," 1960, P. 3, VIII, p. 103-108, ill., bibl. 4 NN.

Design and Operation of an S-Band Traveling-Wave Diode Parametric Amplifier. Shafer, C.G. "IRE Wescon Convent. Rec.," 1960, P. 1, VIII, p. 49-54, ill., bibl. 7 NN.

The Noise Figure of Iterative Traveling-Wave Parametric Amplifiers. Bell, C.V. and Wade, G. "IRE Wescon Convent. Rec.," 1960, P. 1, VIII, p. 55-60, ill., bibl. 3 NN.

Coupling of the Slow Space—Charge Wave with Application to the Travelling-Wave Tube. Forster, D.C. "IRE Wescon Convent. Rec.," 1960, P. 3, VIII, p. 90-95, ill., bibl. 6 NN.

Masers for Systems Applications. Senf, H.R. "IRE Wescon Convent. Rec.," 1960, P. 1, VIII, p. 43-48, ill., bibl. 7 NN.

Tunnel-Diode Microwave Oscillators with Milliwatt Power Outputs. Nelson, D.E., Sterzer, F. "IRE Wescon Convent. Rec.," 1960, P. 1, VIII, p. 68-73, ill., bibl. 9 NN.

7. WAVEGUIDES

Circular Waveguides in a Wide-Band Radio Relay System. Rundhohlleiter fur Brietband-Richfunksysteme. Gillitzer, E. and Herz, R. "Frequenz," 1960, Bd. 14, X, No. 10, S. 347-357, ill., bibl. 4 NN.

Half-Round Inductive Obstacles in Rectangular Waveguide. Kerns, D.M.

"J. Res. of NBS," Sec. B-Mathematics and Mathemat. Phys., 1960, v. 64B, VI, No. 2, p. 113-130, bibl. 14 NN.

Reversible and Non-Reversible Phase Inverters in Rectangular Waveguides. Reziproke und nichtreziproke Phasenschieber im Rechteckhohlleiter. Pivit E. "Frequenz," 1960, Bd. 14, XI, No. 11, S. 369-378. ill., bibl. 10 NN.

On the Problem of Excitation of Higher-Mode Waves in Waveguide Junctions. Zur Anregung hoherer Wellentypen in Hohlleiterubergangen. Schnetzler, K. "Arch. ele t. Ubertragung," 1960, Bd. 14, X, No. 10, S. 425-431, ill., bibl. 4 NN.

Excitation of Higher-Mode Waves at the Coupling Point of Two Circular Waveguides. Die Anregung von Wellentypen hoherer Ordnung durch die Grundwelle an einer Versatzstelle zweier runder Hohlleiter. Schnetzler, K. "Arch. elekt. Ubertragung," 1960, Bd. 14, X, No. 10, S. 421-424, ill., bibl. 4 NN.

Coaxial Attenuators with Low Image Attenuation Constant Regulated by a Magnetic Field. Ein magnetisch regelbares koaxiales Dampfungsglied mit kleiner Grunddampfung. Deutsch, J. und Offner, M. "Frequenz," 1960, Bd. 14, X, No. 10. S. 344-347, ill., bibl. 6 NN.

8. TELEVISION

Problems Relating to the Transmission of Television Signals through Underwater Trans-Atlantic Cables. Problemes poses par la transmission des signaux de television par cable transatlantique sous-marin. Halsey, R.J. et Rendall, H.R. "Electronique," 1960, VII-VIII. No. 164-165, p. 23-28, ill.

Technique of Transmitting Television Signals Through Cables in the FRG [German Postal Service?] Die Technik der Fernsehubertragung auf Kabeln bei der Deutschen Bundespost. Hoffmann, R. "Fernmelde praxis," 1960, Bd. 37, VIII, No. 15, S. 635-640, ill., bibl. 11 NN.

Apparatus for Automatic Reservation of Synchro Generators. Leonov, V.A. "Tekhn. Kino i Televideniya," XII, No. 12, 1960, pp. 68-70, illustrations.

Television Studio—Quality Sweep Linearity with High Efficiency. Torsch, C.E. "IRE Trans. on Broadcast and Telev. Receivers.," 1960, v. BTR-6, VII, No. 2, p. 57-61, ill., bibl. 46 NN.

A New Wide Angle Deflection System and Picture Tube. Bisbing, P.E. and oth. "IRE Trans. on Broadcast and Telev. Receivers," 1960, v. BTR-6, VII, No. 2, 15-19, ill.

Scan Magnification in TV Picture Tubes. Dolon, P.J. and Niklas, W.F. "IRE Trans. on Broadcast and Telev. Receivers," 1960, v. BTR-6, VII, No. 2, p. 20, 29, ill., bibl. 14 NN.

The Use of Phase Equalizers to Improve the Transient Response of a Television Transmitting System. MacDonald, J.K. "IRE Trans. on Broadcasting," 1960, v. BC-6, IX, No. 3, p. 12-20, ill., bibl. 8 NN.

Some Design Aspects of Automatic Gain Control for Television Receivers. Anrooy, P.H.V. "IRE Trans. on Broadcast and Telev. Receivers," 1960, v. BTR-6, VII, No. 2, p. 46-56, ill, bibl. 7 NN.

A Mobile Television Camera and Recording Vehicle. Harris, A. "J. Brit. IRE," 1960, v. 20, VII, No. 7, p. 553-559, ill.

Frequency Modulation System for a Magnetic-Tape Television Signal Recording Vehicle, Vorob'yev, V.F. "Tekhn. Kino i Televideniya," XII, No. 12, 1960, pp. 1-12, ill., bibl., 8 titles.

9. THEORY OF CIRCUITS

On Synthesis with Minimum Number of Contacts. Blokh, A.Sh. "Dokl. AN BSSR," Vol. 4, XI, No. 11, 1960, pp. 447-449, ill., bibl., 1 title.

Series Connection of Non-Reversible Four-Terminal Networks. Die Kettenschaltung nichtumkehrbarer Vierpole. Herzog, W. "Nachr.—Techn. Zeitschr.," 1960, X, No. 10, S. 477-478, ill., bibl. 5 NN.

Replacement of n Different Nonsymmetrical Four-Terminal Networks with Identical Input and Output Impedances by an Equivalent Four-Terminal Network.

On the Use of an Active Filter for Measuring the Frequency Spectrum of Pulses. Uber die Verwendbarkeit aktiver Filter zur Messung der Frequenzspektra von Impulsen. Jungmeister, H.G. "Arch. elekt. Ubertragung," 1960, Bd. 14, X, S. 432-434, ill., bibl. 4 NN.

10. APPARATUS FOR RADIO AND WIRE COMMUNICATIONS

The Appearance of Frequency Pulling in Electron Tube Transmitters. Zieherscheinungen bei Rohrensendern. Spiess S. "Nachrichtentechnik," 1960, X, No. 10, S. 452-456, ill.

Development of a Highly-Stable Short-Wave Decade Master Oscillator for the 1.5-30 Mc Frequency Band. Die Entwicklung einer hochkonstanten dekadischen Kurzwellensteuerstufe fue den Bereich 1.5 - 30 MHz. Valdorf, H. und Klinger, R. "Frequenz," 1960, Bd. 14, X, No. 10, S. 335-343, ill. bibl. 3 NN.

Maximum Band-width Utilization Demodulator. Gatfield, A.G. "IRE Trans. on Communs. Sys.," 1960, v. CS-8, VI, No. 2, p. 83-86, ill.

Transistorized FM and TV Limiter Design and Performance. Gray, C.R. and Lawson, T.C. "IRE Trans. on Broadcast and Telev. Receivers," 1960, v. BTR-6, VII, No. 2, p. 10-14, ill.

Transistorized Receiver with Medium and Microwave Bands. Ein Volltransistorempfanger mit Mittel-und Ultrakurzwellelteil. Rinderle, H. "Fernmelde Praxis," 1960, Bd. 37, X, No. 20, S. 801-824, ill.

Design of an AM/FM Transistorized Receiver. Abbe H.V. "IRE Trans on Broadcast and Telev. Receivers," 1960, v. BTR-6, VII, No. 2, p. 72-78, ill.

The Application of Semiconductors in a 860 mc Radio Receiver. Schimpf, L.C. "IRE Trans. on Vehicular Communs.," 1960, v. VC-9, V, No. 1, p. 33-37, ill.

High Input Impedance Transistor Circuits. Levine, L. "Electronics," 1960, v, 33, IX, No. 36, p. 50-52, ill., bibl. 8 NN.

Analytical Design of Transistor Push-Pull Amplifiers. Riggs, R.H. "Electr nics," 1960, v. 33, VI, No. 24, p. 60-62, ill., bibl. 5 NN.

Simplified Squelch Circuit Uses back Biased Diode. "Electronic Design," 1960, v. 8, VI, No. 12, p. 148-149, ill.

Calculation of Parameters of a Low-Frequency Transistorized Mixer Stage by the Circuit Subbstitution Method. Berechnung der Mischvorgange in Transistorstufen bei niedrigen Frequenzer auf Grund des Ersatzschaltbildes. Vogel, J.S. und Strutt, M.D. "Arch. elekt. Ubertragung," 1960, Bd. 14, X, No. 10, S. 435-440, ill., bibl. 8 NN.

Tunnel-Diode Converter with Low Noise Level. Chang and others. "Foreign Radio Electronics," XII, No. 12, 1960, pp. 106-113, ill., bibl., 4 titles.

The Paralleling of Filters through Resistive Pads. Szentirmai, G. "TMC Technical, J.," 1960, v. 8, VII, No. 4, p. 157-164, ill.

Repeaters for Canada — New Zealand Cable Designed for 20 Year Life Span. Chard, H.J. "Electronics and Communs.," 1960, v. 8, VIII, No. 8, p. 23-25, ill.

Converted Terminating Circuit for Carrier Telephony. Eine Wandlungsfahige Endschaltung fur Tragerfrequenz-Fernsprechkriese. Auer, W. und Bendel, H. "Frequenz," 1960, Bd. 14, XI, No. 11, S. 386-392, ill., bibl. 7 NN.

Transistorized Multiplexing Equipment for a Long-Distance Telephone Communications System. Kanalumsetzer mit Transistoren fur Trager-frequenz-Fernsprech-Systeme. Bode, K. "Nachr.—Techn. Zeitschr.," 1960, X, No. 10, S. 465-469, ill., bibl. 6 NN.

Electronic Telephone Switchboard for 240 subscribers. Eine vollelektronische Fernsprech-Vermittlungseinrichtung fur 240 Teilnehmer. "Nachr.-Techn. Zeitschr.," 1960, X, No. 10, S. 479-482, ill., bibl. 2 NN.

A Diode Matrix Commutator with Transistor Trans. Flip-Flop Switching. Robinette, S.L. "IRE Trans. on Instrumentation," 1960, v. I-9, VI, No. 1, p. 40-42, ill., bibl.

Coaxially-Designed Relay with Contacts in a Protective Gas Atmosphere for Long-Distance Communications Systems. Schutzgaskontakte in Koaxialrelais fur den Nachrichten-Weitverkehr. "Frequenz," 1960, Bd. 14, XI, No. 11, S. 392-394, 398, ill.

Reactor Controlled Current Regulator. Fraser, H.J. "Electr nics," 1960, v. 33, IX, No. 36, p. 56, ill.

Power Output and Efficiency of Thermionic Converters. Saldi, I.T. "IRE Wescon Convent. Rec.," 1960, P. 3, VIII, p. 3-12, ill.

11. RELIABILITY OF EQUIPMENT

Statistical Pitfalls for the Reliability Engineer. Beckhart, C.H. "Conf. Proc. 4th Nat. Convent. Military Electronics," 1960, VI, Washington, p. 117-119.

Reliability Analysis. Loewe, R.T. "IRE Trans. on Reliability and Quality Control," 1960, v. RQC-9, IX, No. 2, p. 6-10.

Availability — A System Function. Bielka, R.P. IRE Trans. on Reliability and Quality Control," 1960, v. RQC-9, IX, No. 2, p. 38-42.

Finding a Figure of Merit for Maintainability. "Space Aeronautics," 1960, v. 34, VII, No. 1, p. 135-136, 138, ill.

Serviciability: Complement to Reliability. Wilcox, R.H. and Wanner, V.R. "Conf. Proc. 4th Nat. Convent. Military Electronics," 1960, VI, Washington, p. 98-102, ill., bibl. 11 NN.

Failure Testing in Preventive Maintenance. Greenberg, H. "Operations Res.," 1960, v. 8, V-VI, No. 3, p. 406-407.

Aspects of Reliability in Transistorized Home Radios. Corning, J.J. "IRE Trans. on Reliability and Quality Control," 1960, v. RQC-9, IX, No. 2, p. 23-28.

The Reliability of Transistors in Battery-Portable Radio Receivers. Cohen, R.M. "IRE Trans. on Reliability and Quality Control," 1960, v. RQC-9, IX, No. 2, p. 11-16.

12. SEMICONDUCTOR DEVICES

Glass Ambient Semiconductor Devices. Carman, J.N. "IRE Wescon Convent. Res.," 1960, P. 3, VIII, p. 27-28, ill.

Quality Assurance Procedures for Power Transistors. Schaffner, J.S.

"IRE Wescon Convent. Rec.," 1960, P. 3, VIII, p. 29-33, ill.

High Power at 1,000 mc Using Semiconductor Devices. Luettgenau, G. and oth. "IRE Wescon Convent. Rec.," 1960, P. 3, VIII, p. 13-26, ill., bibl. 20 NN.

PNPN Switches Diodes and Triodes. Goldey, J.M. "Control Eng-ng.," 1960, v. 7, X. No. 10, p. 101-104, ill., bibl. 11 NN.

Base Turn-Off of PNPN Switches. Van Ligten, R.H. and Navon, D. "IRE Wescon Convent. Rec.," 1960, P. 3, VIII, p. 49-52, ill., bibl. 2 NN.

The New Semiconductor Device "Al'katron." Nouvel element semi-conducteur "Alcatron." "Mesures et Controle Ind.," 1960, IV, No. 275, p. 362, ill.

TELECOMMUNICATIONS

1961

A.S. Popov Technical Society of Radio Engineering and Telecommunications
Svyaz'izdat, Moscow

EDITORIAL BOARD

A. Ch. Pukhal'skiy, Editor

B.F. Anosovich
S.V. Borodich
N.I. Chistyakov
A.D. Fortushenko
P.T. Gobets
I. Ye. Golubtsov
V.A. Kuz'min
G.A. Levin
Ye. V. Markhay
Ye. S. Medvedev
Ye. A. Rizkin
P.V. Shmakov
V.M. Shteyn
N.N. Shumskaya
V.I. Siforov
B.P. Terent'yev
G.S. Tsykin
N.B. Zeliger
E.V. Zelyakh

The English Edition of Telecommunications is mailed to subscribers within 18 weeks after the publication of the original Russian issue.

Russian Electronic Journals published by the
American Institute of Electrical Engineers
Translated by Royer and Roger, Inc.

	Subscription rates			
	Individuals		Libraries	
	$	£	$	£
Telecommunications	14.25	5	28.50	10
Radio Eng. and Electronic Physics	28.50	10	57.00	20
Radio Engineering	14.25	5	28.50	10

Royer and Roger translates and produces
the following Russian scientific journals:

Biophysics
Entomological Review
Geochemistry
Geodesy and Cartography
Izvestiya, Academy of Sciences of the USSR, Geologic Series
Pavlov Journal of Higher Nervous Activity
Problems of Oncology
Radio Engineering
Radio Eng. and Electronic Physics
Refractories
Sechenov Physiological Journal of the USSR
Soil Science
Telecommunications

Comments and inquires regarding *Telecommunications* and other translation journals should be sent to:

International Division
Royer and Roger, Inc.

1000 Vermont Avenue, N.W.
Washington 5, D.C.

41 East 28th Street
New York 16, New York

TELECOMMUNICATIONS
ЭЛЕКТРОСВЯЗЬ

NUMBER 4 1961

CONTENTS

Page

Ya. Z. Tsypkin: Analysis of Open-Loop Systems with Pulse Amplitude Modulation 1

N. L. Teplov: Noiseproofness in Integral Reception of Signals Under the Influence of Fluctuating and Sinusoidal Noise 8

Yu. A. Yerukhimovich: Calculation of Non-Linear Distortion in Waveguide Transmission Lines 20

N. S. Stanulov: A Simple Electronic Instrument for Statistical Research in the Field of Radio Wave Propagation 31

A. F. Beletskiy: Synthesis of Filters with Linear Phase Characteristics 39

V. Z. Nayderov and Yu. L. Simonov: Structural Stability of a Linear Four-Terminal Network 49

S. L. Kunina: A Quartz Master Oscillator Using Transistors 56

I. M. Zhdanov: On the Formation of Telephone Districts Under Conditions of Unequal Density 70

A. D. Ruga and Ye. V. Kostyanets: Transmission Parameters and Effects of Type TG Cables in a Frequency Range to 600 kc 81

Bibliography 91